MODELLING OIL RETENTION, PRESSURE DROP, AND HEAT TRANSFER OF REFRIGERANT-OIL MIXTURES IN A MICROCHANNEL CONDENSER

By

ELLYN HARGES

Bachelor of Science in Mechanical Engineering

Oklahoma State University

Stillwater, Oklahoma

2014

Submitted to the Faculty of the
Graduate College of the
Oklahoma State University
in partial fulfillment of
the requirements for
the Degree of
MASTER OF SCIENCE
December, 2016

MODELLING OILRETENTION, PRESSURE DROP,

AND HEAT TRANSFER OF REFRIGERANT-OIL

MIXTURES IN A MICROCHANNEL CONDENSER

Thesis Approved:

Dr. Lorenzo Cremaschi

Thesis Adviser

Dr. Christian Bach

Dr. Daniel Fisher

ACKNOWLEDGEMENTS

First, I would like to thank my husband, Will Harges, who has been so patient and supportive as I have been working to complete my master's degree. I would also like to thank my parents, who have always encouraged me in education as well as in every other area of life. I would like to thank Dr. Cremaschi, who taught me how to conduct research and helped me through this project. Thank you Dr. Bach, who over the past year has provided me with a lot of help and insight. Lastly, I would like to thank Andrea Bigi and Ardi Yatim, without whose help this project would not have been able to be completed.

Name: ELLYN HARGES

Date of Degree: DECEMBER, 2016

Title of Study: MODELLING OILRETENTION, PRESSURE DROP, AND HEAT TRANSFER OF REFRIGERANT-OIL MIXTURES IN A MICROCHANNEL CONDENSER

Major Field: MECHANICAL ENGINEERING

Abstract:

Microchannel heat exchangers have improved heat transfer capabilities as well as reduced charge when compared to conventional fin and tube heat exchangers. These characteristics led to their increasing application in residential heating and air conditioning systems. Models that can quickly and accurately predict their behavior are necessary for system design and optimization purposes. This research presents a discretized microchannel heat exchanger model which extends beyond pure heat transfer modelling to include pressure drop, charge, and oil retention modelling.

This project takes an already existing microchannel condenser model, evaluates its strengths and weaknesses using experimental data, improves it, and uses it to investigate modelling of oil retention in microchannel condensers. It was found that the oil retention model presented in this thesis underpredicts experimental oil retention data from Yatim et al. (2016). The oil retention model only takes into account oil that is carried through the condenser with the refrigerant, so it was determined that there must also be oil trapped somewhere in the condenser. It was also determined that this trapped oil cannot solely reside as a film on the inside of the microchannel tubes; if this were the case, pressure drop would greatly increase, an occurrence which was not observed in the experiments or the simulation results. Since a significant amount of oil cannot reside in the microchannel tubes, the most likely place for the oil to be is in the inlet header. The refrigerant in this component is always superheated, and so cannot carry the oil through the condenser as well as if it were part liquid. Based on analyses performed in this research, the assumption that the trapped oil all resides in the inlet header is good for some flow conditions, but not all. Future work in oil retention modelling should focus on how mass flux, saturation temperature, refrigerant-oil miscibility, and degree of superheat affect the oil that is trapped in the condenser.

TABLE OF CONTENTS

Chapter Page

I. INTRODUCTION 1

1.1 Background 1
1.2 Research Objectives 4

II. LITERATURE REVIEW 6

2.1 Review of Predictive Tools for Air-Cooled Microchannel Condensers 6
2.2 Review of Modelling the Effects of Oil on Heat Transfer and Pressure Drop in Heat Exchangers 13
2.3 Review of Predictive Methods for Oil Retention in Heat Exchangers 14

III. MODEL DEVELOPMENT 18

3.1 Method of Solution 18
3.2 Air-Side Heat Transfer 21
3.3 Air-Side Pressure Drop 23
3.4 Fluid Properties 23
3.5 Refrigerant-Side Heat Transfer 25
3.6 Refrigerant-Side Pressure Drop 26
3.6.1 Two-Phase Frictional Pressure Drop 26
3.6.2 Single-Phase Frictional Pressure Drop 28
3.6.3 Gravitational Pressure Drop 28
3.6.4 Momentum Pressure Drop 29
3.6.5 Header Pressure Drop 29
3.7 Oil Retention 30
3.7.1 Oil Retention Mass Calculations 31
3.7.2 Oil Retention in the Inlet Header 33

Chapter Page

IV. MODEL VALIDATION: CAPACITY AND PRESSURE DROP 35

4.1 Refrigerant-Side Heat Transfer 35
4.1.1 Validation with Data from Hoehne and Hrnjak (2004) 35
4.1.2 Validation with Data from Yatim et al. (2016) 36
4.2 Refrigerant-Side Pressure Drop 39
4.2.1 Validation with Original Pressure Drop Correlation 39
4.2.2 Literature Search for Better Frictional Pressure Drop Correlations 43
4.2.3 Validation with Top Three Frictional Pressure Drop Correlations from Literature 48
4.2.4 Hydraulic Diameter Sensitivity Analysis 59
4.2.5 Pressure Drop Predictions for the Final Version of the Model 63

V. RESULTS AND DISCUSSION FOR THE OIL RETENTION MODEL 65

5.1 Oil Retention Model Predictions 65
5.2 Oil Difference Fills Inlet Header 68
5.3 Oil Film in Inlet Header and Tubes 70
5.3.1 Constant Oil Film around Inlet Header and Superheated Tube Segments 71
5.3.2 Oil Film Added to Match Pressure Drop 74
5.3.3 Sensitivity of Oil Retention Predictions to Changing Refrigerant Mass .75
5.4 Oil Difference Fills Inlet Header and Inlet Tube 80

VI. CONCLUSIONS AND RECOMMENDATIONS 88

6.1 Summary and Conclusions 88
6.1.1 Heat Transfer Model 89
6.1.2 Pressure Drop Model 90
6.1.3 Oil Retention Model 92
6.2 Recommendations for Future Work 94

REFERENCES 96

APPENDIX 101

LIST OF TABLES

Table Page

2.1 Summary of reviewed microchannel condenser models 12
4.1 Summary of experimental data from Yatim et al. (2016).....37
4.2 Sensitivity analysis of frictional pressure drop to change in refrigerant properties.....43
4.3 Summary of literature search for applicable pressure drop correlations 44
4.4 Values of MAE and bias for R134a data from Zhang and Webb (2001) 50
4.5 Values of MAE and bias for R134a data from Cavallini et al. (2005) 52
4.6 Values of MAE and bias for R134a, 350 kg/m^2-s data from Revellin and Thome (2007).....53
4.7 Values of MAE and bias for R134a, 1000 kg/m^2-s data from Revellin and Thome (2007).....54
4.8 Values of MAE and bias for all R134a literature data.....55
4.9 Values of MAE and bias of R410A data from Cavallini et al. (2005).....56
4.10 Values of MAE and bias for R410A data from Wang et al. (2005) 57
4.11 Values of MAE and bias for all R410A literature data.....58
4.12 Values of MAE and bias for R134a data at various hydraulic diameters.....62
4.13 Values of MAE and bias for R410A data at various hydraulic diameters.....62
5.1 Results of hydraulic diameter reduction analysis 74
5.2 Results of the mass factor analysis when oil mass fraction is 4.0%.....76
5.3 Results of the mass approximation analysis for R410A with low degree of superheat and an oil mass fraction of 0.98% 78
5.4 Results of the mass approximation analysis for R410A with low degree of superheat and an oil mass fraction of 4.0% 78
5.5 Results of the void fraction sensitivity analysis for R410A with low degree of superheat and an oil mass fraction of 0.98% 79
5.6 Results of the void fraction sensitivity analysis for R410A with low degree of superheat and an oil mass fraction of 4.0% 80
A.1 Papers of interest from search for overall microchannel condenser data for R134a or R410A 102

LIST OF FIGURES

Figure Page

3.1 Schematic of the type of microchannel condenser the model was designed to solve with indication of segments used for discretization 19
3.2 Flowchart of the simulation process for the microchannel condenser model 22
4.1 Predicted capacity vs. measured capacity for propane data from Hoehne and Hrnjak (2004) 36
4.2 Predicted capacity vs. measured capacity for R410A data from Yatim et al. (2016) 38
4.3 Predicted capacity vs. measured capacity for R134a data from Yatim et al. (2016) 38
4.4 Predicted pressure drop vs. measured pressure drop for R410A data without oil from Yatim et al. (2016) 40
4.5 Predicted pressure drop vs. measured pressure drop for R134a data without oil from Yatim et al. (2016) 41
4.6 Predicted pressure drop vs. measured pressure drop for propane data from Hoehne and Hrnjak (2004) 42
4.7 Comparison of the three chosen frictional pressure drop correlations with R134a data from Zhang and Webb (2001) 50
4.8 Comparison of the three chosen frictional pressure drop correlations with R134a data from Cavallini et al. (2005) 51
4.9 Comparison of the three chosen frictional pressure drop correlations with R134a, 350 kg/m^2-s data from Revellin and Thome (2007) 53
4.10 Comparison of the three chosen frictional pressure drop correlations with R134a, 1000 kg/m^2-s data from Revellin and Thome (2007) 54
4.11 Comparison of the three chosen frictional pressure drop correlations with R410A data from Cavallini et al. (2005) 56
4.12 Comparison of the three chosen frictional pressure drop correlations with R410A data from Wang et al. (2001) 57
4.13 Predicted vs. measured pressure drop for R134a data without oil using the Kim and Mudawar (2012) correlation 60
4.14 Predicted vs. measured pressure drop for R410A data without oil using the Kim and Mudawar (2012) correlation 60
4.15 Predicted vs. measured pressure drop for R134a data without oil at various values of hydraulic diameter 61
4.16 Predicted vs. measured pressure drop for R410A data without oil at various values of hydraulic diameter 62

Figure Page

4.17 Predicted vs. measured pressure drop for all R134a data using the final version of the model....64
4.18 Predicted vs. measured pressure drop for all R410A data using the final version of the model....64
5.1 Predicted vs. measured oil retention for R410A with low degree of superheat....66
5.2 Predicted vs. measured oil retention for R410A with high degree of superheat....66
5.3 Predicted vs. measured oil retention for R134a....67
5.4 Percentage of inlet header that must be filled with oil for R410A with low degree of superheat....69
5.5 Percentage of inlet header that must be filled with oil for R410A with high degree of superheat....69
5.6 Percentage of inlet header that must be filled with oil for R134a....70
5.7 Predicted vs. measured oil retention for R410A with low degree of superheat, δ/D = 0.125....72
5.8 Predicted vs. measured oil retention for R410A with high degree of superheat, δ/D = 0.037....72
5.9 Predicted vs. measured oil retention for R134a, δ/D = 0.047....73
5.10 Percentage of inlet header and inlet tube that must be filled with oil for R410A with low degree of superheat....82
5.11 Percentage of inlet header and inlet tube that must be filled with oil for R410A with high degree of superheat....83
5.12 Percentage of inlet header and inlet tube that must be filled with oil for R134a....77
5.13 δ/D vs. oil mass fraction for R410A with low degree of superheat....84
5.14 δ/D vs. oil mass fraction for R410A with high degree of superheat....85
5.15 δ/D vs. oil mass fraction for R134a....85
A.1 Predicted vs. experimental capacity for R410A data without oil from Yatim et al. (2016)....101
A.2 Predicted vs. experimental capacity for R134a data without oil from Yatim et al. (2016)....101

NOMENCLATURE

A	Area [m^2]
c	Specific heat [kJ/kg-K]
D_h	Hydrualic diameter [mm]
D_m	Major diameter [mm]
F_l	Fin length [mm]
F_p	Fin pitch [mm]
G	Mass flux [kg/s]
g	Gravitational acceleration [m/s^2]
Ga	Galieo number [-]
h	Heat transfer coefficient [W/m^2-K] and enthalpy [kJ/kg]
j	Colburn j factor [-]
k	Thermal conductivity [W/m-K]
K	Entrance and exit loss coefficients [-]
L	Length [m]
L_l	Louver length [mm]
L_p	Louver pitch [mm]
m	Mass [kg]
NTU	Number of transfer units [-]
Nu	Nusselt number [-]
Nu_B	Nusselt number for free convection [-]
Nu_F	Nusselt number for forced convection [-]
P	Pressure [kPa]
ΔP	Pressure drop [kP]
Ph	Phase change number [-]

Pr	Prandtl number [-]
Q	Heat transfer [kW]
R	Resistance [K/W]
Re	Reynolds number [-]
Su	Suratman number [-]
t	Tube thickness [mm]
T	Temperature [K]
T_d	Tube depth [mm]
T_h	T_p-D_m [mm]
T_p	Tube pitch [mm]
U	Overall heat transfer coefficient [W/m^2-K]
V	Volume [m^3]
v	Specific volume [m^3/kg]
W	Molecular mass [kg/kmol]
X_{tt}	Martinelli parameter [-]

Greek Symbols

α	Void fraction [-]
δ_f	Fin thickness [mm]
ε	Effectiveness [-]
η	Fin efficiency [-]
θ	Louver angle [degrees]
μ	Viscosity [kg/m-s]
ρ	Density [kg/m^3]
σ	Surface tension and area ratio [-]
ψ	Mole fraction [-]
ω	Oil mass fraction [%]

Subscripts

bub	Bubble point
F	Frictional
f	Liquid
g	Vapor
i	Inside
L	Liquid
liq	Liquid
Lp	Louver pitch
LO	Liquid only
LV	Latent heat
M	Momentum
m	Mean
o	Outside
ref	Refrigerant
sat	Saturation
seg	Segment
V	Vapor
vap	Vapor

CHAPTER I

INTRODUCTION

1.1 Background

Microchannel condensers are becoming increasingly popular for use in heat pump systems designed for residential and automotive heating and air conditioning. There are several reasons for this. One is that microchannel heat exchangers have larger heat transfer surface areas than conventionally-sized heat exchangers due to their multi-port tube design, so heat transfer is enhanced. Another is that since they have smaller internal volumes and thus smaller refrigerant charges, environmental impact due to possible refrigerant leakage is reduced. They are also smaller than conventional heat exchangers, allowing package size to be reduced while still maintaining capacity. Because of these and other benefits, microchannel condensers are becoming more and more widely used.

Since microchannel condensers are now an important part of heating and cooling systems, it is important for designers to understand how they behave in many different situations. There have been many experimental studies, especially within the last few decades, performed with microchannel single tubes and entire condensers that investigate heat transfer and pressure drop behavior for various geometries, working fluids, and test conditions. Many researchers have also been working to identify or develop correlations for heat transfer coefficient and friction factor that are accurate for microchannels. Gravitational forces greatly impact the flow in

conventionally-sized channels (D_h larger than about 3 mm), while shear and surface tension forces dominate for flow in microchannels (Awad et al., 2015). Because of the difference in flow mechanisms between large and small channels, one would expect that the same correlations would not be applicable for both. But surprisingly, according to the results of an analysis performed by Kim and Mudawar (2014 a, b), sometimes correlations developed for conventionally-sized channels perform just as well or better for microchannels than those developed specifically for microchannels. To the author's best knowledge, there is not yet one set of heat transfer coefficient and friction factor correlations that is universally recognized as best for microchannels.

The next step researchers have taken in predicting microchannel condenser behavior is to model, or simulate, the heat exchanger as a whole using computer software. This goes beyond simply selecting appropriate correlations for heat transfer and pressure drop; these models attempt to predict everything that occurs in the condenser. This includes, but is not limited to, predicting changes in property values, void fraction, and Reynolds number at each point as the program advances through the condenser. The desired output of these types of models is generally the overall capacity and pressure drop for the heat exchanger. These models are far from trivial to create as geometry and flow patterns are much more complex than for a single tube. Complicated header geometry must now be taken into account when computing pressure drop, and possible flow maldistribution due to momentum and gravitational effects must be considered since the fluid is split between many tubes as it leaves the headers. Additionally, most of the models available are specifically for air-cooled condensers, with the calculations for flow and heat transfer of the cooling air as it passes between the tubes adding another level of complexity. Several overall heat exchanger models have been developed within the last twenty-five years, with one of the earliest presented by Ragazzi and Pedersen (1991), but few models have been created specifically for microchannel condensers.

There is another aspect of performance of heat exchangers that as of yet most modelers do not take into account: that of oil which is circulating and/or trapped in the heat exchanger. All heat pump systems contain a compressor to circulate the working fluid, and these compressors must be lubricated with refrigeration oil in order to function properly. Most of this oil remains in the compressor, but some amount of oil does manage to escape the compressor and travel through the system. Some of this oil mixes with the working fluid and circulates with it through the system, and some becomes trapped and is retained in various system components, including the condenser. There are two primary reasons why it is important to be able to model the effects of circulating oil on the performance of microchannel condensers as well as the amount of oil that is retained in these condensers. First, if the presence of circulating oil changes the capacity and pressure drop of the condenser, the whole system will not perform as expected. This could lead to a lower than necessary efficiency of the heat pump system, or even to a heat pump system with insufficient capacity for the chosen application. If the oil effects can be modeled correctly, however, gains and losses in capacity and pressure drop can be anticipated, and the system will work as expected from the design. Second, if the amount of oil in the condenser at steady state is unknown, the amount of oil that has left the compressor is also unknown. This could present problem as the compressor requires a certain amount of lubrication to operate properly, and low lubricant levels could cause damage to the equipment. If the amount of oil in the condenser can be predicted, however, as well as the amounts of oil in the other components, then the system can be charged with the correct amount of oil.

From the explanation above, it can be determined that a tool is needed that is able to predict microchannel condenser heat transfer and pressure drop performance while taking oil effects into account. In his master's thesis, Shenghan Jin (2012) proposed such a tool. This tool performs relatively well in predicting overall heat transfer and oil retention for an automotive microchannel condenser, but it cannot predict overall pressure drop. To the author's knowledge,

there is only one other tool available (Liu, 2015) that was designed to predict behavior for microchannel condensers when there is oil in circulation, and this tool does not include any calculations for mass of oil retained. Because of this, there is still need for a model that can accurately predict all aspects of overall microchannel condenser performance when there is oil present in the system.

1.2 Research Objectives

The current research is based on an air-to-refrigerant heat pump model already in existence. This model is a simulation tool presented by Ip Seng Iu (2007) in his PhD thesis. It was designed to model an entire heat pump system, but each component of the system can also be modeled separately. It includes a model for a conventionally-sized condenser that calculates its overall heat transfer and pressure drop. The condenser portion of this tool was later updated to predict behavior for a microchannel condenser specifically (Bigi et al., 2014). The correlations used for heat transfer and pressure drop of the condenser were updated, and the effects of oil on heat transfer and pressure drop behavior were added. The goal of the current work is to further update and improve the microchannel condenser component model begun by Iu and Bigi et al. The specific objectives of the current study are as follows:

- To improve the pressure drop prediction for the overall heat exchanger. The model presented in Bigi et al. (2014) predicts overall capacity satisfactorily, but it cannot accurately predict overall pressure drop. This work aims to find and fix the sources of error present in the pressure drop predictions as well as do an extensive investigation into appropriate correlations for pressure drop in microchannels. Based on the results of this investigation, the correlation that is currently implemented in the model will either be replaced or confirmed.

- To perform extensive model validation using data gathered from the literature, with an emphasis on the data presented by Yatim, et al. (2016). This will be done in order to prove that this simulation tool is accurate and applicable in many different situations, and not only for a single data set. This work will focus specifically on validation of the pressure drop portion of the model as this is the part of the model that is currently most in need of improvement.
- To present a model that is able to predict the mass of oil in the condenser that is transported with the refrigerant flow when between 0 and 5% of the circulating fluid fraction is oil and the remaining 95% to 100% is refrigerant. This work will also attempt to identify how and where oil is held up in the condenser if it is not being carried along with the refrigerant. Geometry of the condenser is a large factor in determining the amount of oil trapped, so specific results obtained for this research may not be applicable for other studies. The principles should hold true for many situations, however, so this investigation can provide valuable insight for other researchers calculating oil retention in other types of microchannel condensers.

CHAPTER II

LITERATURE REVIEW

2.1 Review of Predictive Tools for Air-Cooled Microchannel Condensers

Over the years, researchers have developed many simulation tools to predict the performance of heat exchangers, specifically air-cooled heat exchangers. The earliest models were designed for conventional fin and round tube heat exchangers, but as interest in microchannel heat exchangers grew, researchers began to model these as well. One of the first simulation tools developed for microchannel heat exchangers was presented by Yin et al. (2001), and was designed specifically to predict the performance of a CO_2 gas cooler. After this, several other researchers developed microchannel heat exchanger models; some developed models specifically for gas coolers, condensers, or evaporators, but others developed more general models to be used for any type of microchannel heat exchanger application. This section of the literature review covers predictive tools that can be applied to microchannel condensers.

Several years passed after the development of the early gas cooler model by Yin et al. (2001) before models for microchannel condensers began to appear. One of the first of these was created by Park and Hrnjak (2008) to predict the performance of a specific condenser used for residential air conditioning systems they wished to evaluate both experimentally and numerically. Their model employs a finite difference approach, treating each segment as a separate cross-flow heat exchanger analyzed by the effectiveness-NTU method. Refrigerant-side pressure drop was

calculated for all the tubes, but all minor pressure drop losses, including header pressure drop, were neglected. The model was validated against a single experimental data point; simulations were performed once assuming uniform air and refrigerant flow rates, once assuming non-uniform air but uniform refrigerant flow, and once with both non-uniform air and refrigerant flow. The capacity was predicted within a maximum error of 2%, but pressure drop was underpredicted by about 70%.

A simulation tool designed to be used for both microchannel condensers and evaporators was first presented by García-Cascales et al. in 2008. This tool focuses on simulating two-slab heat exchangers and uses an iterative algorithm for when the air inlet corresponds to the second slab (with respect to refrigerant flow) of the heat exchanger. The model was validated with in-house experimental data of two different two-slab microchannel condensers both using R134a as the working fluid. The model predicted capacity within 7% for all cases, but the modeling results for pressure drop were not consistent with experimental measurements.

An update to the model of the previous paragraph was published two years later (García-Cascales et al., 2010). This second paper includes more information about which correlations the model implements for heat transfer, presenting an in-depth investigation into available heat transfer correlations in open literature. It then presents modeling results using three of the best of those correlations. This paper also adds additional model validation; it presents experimental and modeling results of R410A flowing through two single-slab condensers in addition to the validation performed for the previous paper. For the case of single-slab R410A condensers, the capacity appears to be predicted within 5%. No information is given in this paper about how well the model predicts pressure drop for either the single-slab or two-slab condensers.

Shao et al. (2009) presented a model for a serpentine microchannel condenser with propane as the working fluid. This model also uses a finite-volume approach; the condenser is

divided into tubes, which are divided into ports, which are in turn separated into segments. These segments are each analyzed individually. This model is different from the previous proposed models in that it focuses on serpentine condensers rather than the typical configuration, and it takes into account conduction through the tubes and fins between each segment. The model was validated using the authors' own experimental data; most of the simulation points for both capacity and pressure drop were predicted within a 10% error. The authors also performed parametric analyses to investigate how tube and pass configuration as well as airside maldistribution affect the performance of their condenser.

A new model that is capable of predicting the performance of a variable geometry microchannel heat exchanger was presented by Huang et al. (2012). Port type and size, fin type and height, number of tubes per bank, and tube location can all be varied in this model; once sizes and positions are chosen, the tubes and fins are located on a Cartesian grid for analysis. This paper only validates the model for a microchannel CO_2 gas cooler; capacity was predicted within a 5% error, while the majority of pressure drop data was predicted within a 40% error. An updated model was presented two years later (Huang et al., 2014). The major improvements in the new model are the use of a three-stream UA-AMTD method as the primary method of calculating heat transfer rather than a three-stream effectiveness-NTU method, and the addition of a much more extensive model validation. This validation includes predictions for conventional microchannel condenser data and gas cooler data from the literature, as well as data supplied by an industry partner for four variable geometry and four conventional geometry condensers. The model was able to predict most of the capacity data within a 5% error and much of the pressure drop data within a 25% error; there were, however, correction factors applied to the heat transfer and pressure drop correlations when necessary. This model is presented in its entirety in Long Huang's Ph.D. dissertation (2014); in addition, the dissertation also discusses modeling of microchannel heat exchangers under wet, partially wet, and dry conditions while considering

conduction between tubes, optimizing designs of variable geometry microchannel heat exchangers for variable air flow distribution, and a CFD and effectiveness-NTU co-simulation to study maldistribution in microchannel tubes.

In 2013, Martínez-Ballester et al. presented a simulation tool called Fin1Dx3 that is capable of modeling microchannel condensers and gas coolers with any refrigerant flow circuitry (2013a). This tool is based on one they proposed earlier, Fin2d (Martínez-Ballester et al., 2011), which was created to test the impact of classical microchannel heat exchanger modeling assumptions on a microchannel gas cooler. Fin2d simulates a small piece of a gas cooler and does not use any assumptions for fins or heat conduction; in other words, temperature profile and heat conduction are calculated in all directions for fluid, tubes, fins, and air. Fin1Dx3 was developed as a more practical way to model a microchannel heat exchanger as Fin2d is too computationally expensive to use for overall capacity and pressure drop calculations. To decide what to include in the newer model, the authors used the results of the previous model by ignoring heat conduction and temperature profile in places where the old model showed that it was negligible with regards to overall performance. In the Fin1Dx3 model, the heat exchanger is discretized into four types of cells: refrigerant cells, tube cells, fin wall cells, and air cells. The types of cells behave differently, but all exchange heat with their surrounding cells. The number of cells was chosen with the intent of achieving the greatest possible accuracy while maintaining a reasonable computation time. This model is the first microchannel model presented in open literature that does not employ any of the fin efficiency, adiabatic fin tip, or negligible longitudinal heat conduction assumptions. Fin1Dx3 was validated against experimental data for two R410A condensers and one CO_2 gas cooler. It was able to predict capacity for all three heat exchangers within 5%, but it underpredicted pressure drop for all by 50-80%. In a subsequent paper (Martínez-Ballester et al., 2013b), the authors compared the two models and proved that Fin1Dx3

is faster than Fin2d by an order of magnitude and that the degradation in accuracy when using Fin1Dx3 is negligible.

Another model was presented this same year that takes heat conduction through fins into account; it was presented by Ren et al. (2013). They developed a model capable of analyzing microchannel condensers, evaporators, and gas coolers. Their main objectives were to develop a model that could account for heat conduction through fins, could calculate quality and mass distributions among the tubes (evaporator model only), and could analyze any flow circuitry possible for a standard microchannel heat exchanger. The program creates a calculation sequence based on graph theory where the user inputs the flow circuitry information and the program generates a solution method. The condenser model was validated using R410A data from two different literature sources; capacity was predicted within 5% error and pressure drop was predicted within ±10 kPa.

Soon after this, Jin and Hrnjak (2014) presented another model for a microchannel condenser. This model is able to predict the overall capacity of an automotive microchannel condenser, as well as total refrigerant mass and the mass of oil retained in the condenser when there is oil circulating through the system. It is also a finite element model that utilizes the effectiveness-NTU method for its heat transfer solution. The model was validated using the authors' experimental data, and capacity was predicted within a 10% error. The paper does not present information on pressure drop results or validation, but this information can be found in Jin's master's thesis (Jin, 2012). The 2014 paper presents essentially the same information on condenser modeling as does the thesis, but the thesis includes greater detail. In the thesis, pressure drop simulation results are compared with measured pressure drop data, and it is shown that the model cannot predict the pressure drop trend. An update to this work came out earlier this year (Jin and Hrnjak, 2016). This paper goes into more detail about the experimental work used for the validation of the previous paper, as well as makes some small improvements to the condenser

model. One improvement is that the superheated section of the condenser was split into two parts: a single-phase superheated section and a superheated condensing section. In the previous paper these two sections were analyzed as one. This paper also adds another void fraction model for comparison; it now compares results using six different void fraction models rather than five. Despite these improvements, predictions of capacity and charge did not change much.

Yin et al. (2015) presented a finite-volume model for a microchannel condenser that takes into account non-uniform air temperature and velocity, heat conduction through fins, maldistribution of refrigerant among the tubes, and two-slab as well as single-slab heat exchangers. It uses the effectiveness-NTU method to calculate heat transfer, and uses correlations from the literature for heat transfer coefficient and pressure drop. The model was validated with 45 R410A experimental data points gathered in the authors' lab; capacity was predicted within 5%, and pressure drop was predicted within a 15% error for about 84% of the data points. The authors then used their model in several simulation studies; they investigated the effects on overall capacity and pressure drop of non-uniform air velocity, mixed and non-mixed airflow between slabs, fin conduction, refrigerant flow maldistribution between tubes, and ratio of the number of tubes per pass.

Finally, Liu (2015) presented a simplified microchannel condenser model capable of predicting overall capacity and pressure drop when there is oil circulating through the system. Liu applied the effectiveness-NTU method and used standard heat transfer coefficient and friction factor correlations from the literature, but accounted for the presence of oil by using refrigerant-oil mixture properties rather than properties of pure refrigerants. The model was validated against experimental data measured by Liu and predicts condenser behavior satisfactorily. The model captures the trend of the data as the oil circulation ratio was increased from about 1% to 11%, and all pressure drop points were underpredicted by up to 30%.

Table 2.1 provides a simple summary of all the microchannel condenser models reviewed above. As can be seen from the table, only two of the models even consider oil effects, and of the two, only one calculates oil retention. Heat transfer rates, pressure drops, and oil retention volumes are not always satisfactorily predicted by any one of these models. This work aims to fill this gap by developing a physics-based model that is capable of predicting oil retention and the thermal and hydraulic performance of the microchannel condenser when oil is present in the system.

Table 2.1 – Summary of reviewed microchannel condenser models

Model	Accurate Pressure Drop Predictions?	Accurate Heat Transfer Predictions?	Oil Effects Considered?	Oil Retention Predicted?
Park and Hrnjak (2008)	no	✓	no	no
García-Cascales et al. (2008)	no	✓	no	no
García-Cascales et al. (2010)	NA	✓	no	no
Shao et al. (2009)	✓	✓	no	no
Huang et al. (2012)	✓	✓	no	no
Huang et al. (2014)	✓	✓	no	no
Martínez-Ballester et al. (2013a)	no	✓	no	no
Ren et al. (2013)	✓	✓	no	no
Jin (2012), Jin and Hrnjak (2014, 2016)	no	✓	✓	✓
Yin et al. (2015)	✓	✓	no	no
Liu (2015)	✓	✓	✓	no
Ideal requirements for the model of this thesis	✓	✓	✓	✓

2.2 Review of Modeling the Effects of Oil on Heat Transfer and Pressure Drop in Heat Exchangers

Lottin et al. (2003a, b) present a model for an entire compression refrigeration system using a mixture of R410A and lubricant as the working fluid. Part I of their work describes modeling of the compressor and refrigerant-oil mixture properties, and gives results of the system as a whole. Part II describes the modeling of the condenser and evaporator in detail, both of which are plate heat exchangers with a water side and a refrigerant side. Mass transfer thermal resistance terms are included when calculating heat transfer for both heat exchangers because the refrigerant-oil mixture can be treated as a zeotropic mixture. For the condenser, it was found that the refrigerant-side heat transfer coefficient always decreases as the percentage of oil mass in circulation increases; this is also true of the overall heat transfer coefficient for most of the condenser, but the opposite is true near the inlet where quality is very high. For the evaporator, it was found that a small amount of oil in circulation (0.1%) actually improves the refrigerant-side heat transfer coefficient, while larger amounts of circulating oil degrade it. At high qualities near the outlet of the evaporator, however, heat transfer coefficient for all amounts of oil converge to roughly the same value. Lottin et al. calculated that pressure drops in the condenser are negligible for all oil circulation rates, but those in the evaporator increase as the amount of oil in the system increases.

Li and Hrnjak (2013) presented a model for a microchannel evaporator with upward vertical flow and horizontal headers; their main purpose for this model was to investigate oil effects on mass distribution in the heat exchanger, but they also examined the effects that the presence of oil has on heat transfer and pressure drop. They found that heat transfer is degraded when oil concentration is increased from 0% to 5%, and that pressure drop always increases as oil concentration increases. Correlations developed for pure refrigerants were used for both the heat transfer and pressure drop models, but were modified by using refrigerant-oil mixture properties

rather than properties of pure refrigerants. This model was extended and improved in Li and Hrnjak (2015); the new model was validated with experimental data using R134a as the working fluid, and varying the percentage of oil in circulation from 0.1% to 8.3%. This model is able to predict capacity more accurately than conventional refrigerant-oil models, which typically modify mass flow rate by (1-OCR), where OCR is the percentage of oil in circulation. The distribution model presented in Li and Hrnjak (2013) was also extended and applied to a multi-pass microchannel evaporator with vertical headers in Zou et al. (2014). The heat transfer and pressure drop correlations remained the same in this new work. Zou et al. found, using their model, that increased oil in circulation (up to 5%) improves refrigerant distribution in the evaporator, but still always degrades the capacity.

2.3 Review of Predictive Methods for Oil Retention in Heat Exchangers

There is very little to be found in open literature concerning modeling of oil retention in heat exchangers. One of the earliest oil retention models can be found in Lee's (2003) Ph.D. thesis. In this thesis, Lee presents models to predict oil retention in the suction line, microchannel evaporator, and microchannel gas cooler of a carbon dioxide air-conditioning system. Oil retention for the heat exchangers is split into two categories: oil retained in the headers, and oil retained in the microchannel tubes. The evaporator consists of horizontal tubes and vertical headers. Oil retention is assumed to be negligible in the inlet header because the oil is mixed with a large amount of liquid carbon dioxide and the flow direction is down, so it is unlikely that oil will become trapped somewhere in the header. In the outlet header, however, there is carbon dioxide vapor and liquid oil; here oil retention is not negligible because the gas velocity is not great enough to carry all the oil up to the evaporator outlet. Lee calculated the amount of oil trapped in the header by dividing the header into segments, one for each tube, and calculating the mass flow rate in each. If the mass flow rate for a segment was less than the critical mass flow rate needed to carry the oil upward, he assumed the oil would remain in the segment and

completely fill it. For the other segments, an oil film thickness was calculated. Oil retention in the headers of the gas cooler was neglected because the flow direction is downward in both the inlet and outlet headers. The oil retention in the microchannel tubes is calculated using (1-α), where α is the void fraction, and the known charge of the carbon dioxide and oil mass flow rates. Several void fraction models were tested for both the evaporator and the gas cooler, with Hughmark's model performing best for the evaporator, and Premoli's model performing best for the gas cooler. For both heat exchangers, most of the oil retention data is predicted within ± 20%.

The following year, modeling of oil retention in vapor compression systems was presented by Cremaschi (2004) in his Ph.D. thesis. In his thesis, Cremaschi discusses modeling of oil retention in the suction line, liquid line, evaporator, and condenser of a vapor compression system, where the evaporator and condenser are conventionally sized. Similarly to Lee's thesis, Cremaschi calculated oil retention in the heat exchanger tubes using (1-α), the local oil mass fraction, the total volume of the segment in question, and the density of the liquid-oil mixture. He tested several different void fraction models, with Premoli's model agreeing best with experimental data for both the evaporator and condenser. Oil retention in the headers of both the evaporator and condenser were not considered for this model. The model was verified against the Cremaschi's experimental data; this data includes refrigerants R22, R410A, and R134a, which were paired with various lubricating oils. 72 % of the data was predicted within a 29 % error for the evaporator, and for the condenser, 70 % of the data was predicted within a 30 % error.

Crompton et al. (2004) also presented a model for oil retention, but their model was specifically created for refrigerant-oil mixtures flowing adiabatically through a single 9.53 mm outer diameter copper tube. This model is a combination of two other models: the liquid volume fraction model and the viscous film model. The liquid volume fraction model is heavily dependent on the void fraction, oil mass concentration, and liquid density, while the viscous film model is based on the Blasius formula for turbulent flow in smooth tubes and solves for the

thickness of a liquid film by assuming an interfacial shear stress between the liquid and vapor phases. The liquid volume fraction model is used when flow quality is less than 70%, and the viscous film model is adopted when flow quality exceeds 70%. The model is validated against the authors' experimental data; no error percentages are given, but it can be seen that the predictions match the trends of the experimental data for all refrigerant-oil pairs.

He et al. (2004) also present oil retention models for all components of a refrigeration or air conditioning system. Their goal with these models is to subtract the oil retention predicted by each model from the total oil in the system in order to estimate the amount and concentration of oil left in the compressor. The condenser model has three parts: the liquid region, two-phase region, and the superheated region. The model is simple, depending only on the void fraction and liquid density. The evaporator model is very similar, but is only divided into two-phase and superheated regions. Both heat exchanger models use Hughmark's void fraction correlation. The heat exchanger models are not validated individually, but the resulting mass of oil in the compressor was validated against experimental data; the data was over predicted by about 10 %.

In his master's thesis, Jin (2012) presented modeling of a microchannel condenser and a plate evaporator in an automotive air conditioning system, taking lubricant effects and charge into account. For the condenser, an interfacial shear stress model is utilized to calculate oil retained in the inlet tube, while a model developed by Zietlow that is based on gravity and wall shear stress is used for the inlet header. Oil retention is calculated in both the microchannel condenser tubes and the conventional evaporator tubes and headers using void fraction and oil mass concentration. Oil retention was predicted well for the evaporator with most of the data within a 20 % error, but the condenser model could not capture the trend of oil retention mass; it was vastly underpredicted and seems insensitive to the amount of oil in the system. After observing thermal images of the experimental tests, Jin determined that some oil was trapped in the bottom tubes of the condenser; he then modified his model to reflect this by assuming the bottom channels were

always completely filled with liquid. After making this modification, his model could predict most of the oil retention data for the microchannel condenser within a 15 % error. The research was presented again in a more consolidated form later as a journal article (Jin and Hrnjak, 2014).

Jin's research has been updated once more, in Jin and Hrnjak (2016). This most recent paper introduces a new heat transfer process in the condenser: a superheated condensing process. Therefore, there are now four heat transfer zones in the condenser that the model accounts for: a single-phase superheated vapor zone, a superheated condensing zone, a two-phase zone, and a subcooled liquid zone. The model also adds a void fraction model, the Hughmark model, to those that it already evaluates for the condenser. The Hughmark model was found to be best for predicting oil retention in the condenser, though predictions for all void fraction models were improved due to the addition of the superheated condensing heat transfer process. For most of the void fraction models tested, deviation decreased by several percent for calculation of both refrigerant and lubricant charge.

Based on the literature review presented in this chapter, it was concluded that, to the best of the author's knowledge, there was no model in open literature capable of accurately predicting all aspects of microchannel condenser performance, and there are very few models that attempt to handle circulating oil. The research presented in this thesis is an attempt to provide a solution to these gaps. The goal of the research is to present a model that can adequately predict heat transfer, pressure drop, and oil retention for at least one microchannel type condenser.

CHAPTER III

MODEL DEVELOPMENT

The main purpose of the model presented in this chapter is to determine the fluid conditions at every point along the heat transfer path of a microchannel condenser, as well as to determine the overall behavior of the condenser. The primary useful outputs the simulations provide are the refrigerant properties, heat transfer, pressure drop, refrigerant charge, and mass of oil dissolved in the refrigerant both for small segments at any point along the condenser tubes and for the condenser as a whole. This chapter provides a description of the overall method of solution, as well as detailed information about the calculations performed by the model.

3.1 Method of Solution

The model is designed to work for a standard geometry two-pass microchannel condenser as shown in Figure 3.1. It can be seen in this figure that the condenser is divided into elements: the inlet tube, inlet header, microchannel tubes, intermediate header, outlet header, and outlet tube. Pressure drop and oil retention are calculated for all elements, but heat transfer is only calculated from the air to the fins to the refrigerant in the microchannel tubes; heat transfer in all other elements is neglected. As can also be seen, the headers are all vertical and the microchannel tubes are horizontal. The arrows in the schematic indicate the direction of fluid flow through the condenser.

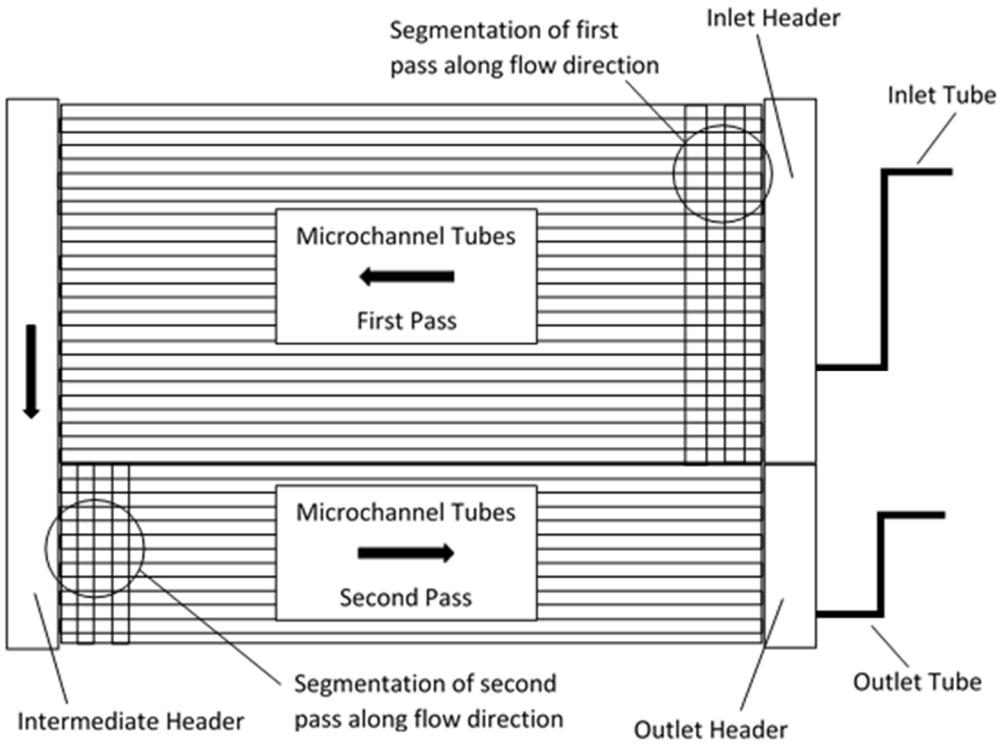

Figure 3.1 – Schematic of the type of microchannel condenser the model was designed to solve with indication of segments used for discretization.

Each simulation is begun by reading inputs from a text file. This input file contains geometry information for the condenser, properties and mass flow rates of the air and refrigerant entering the condenser, type of refrigerant, and oil mass fraction, as well as other information that is used when the larger heat pump code is run. This input file must be updated by the user before each new simulation. The properties used as inputs to fix the entering state of the refrigerant are pressure and enthalpy, while the properties used to fix the state of the entering air are temperature and relative humidity. The next step the program takes is to calculate pressure drop in the inlet tube and inlet header of the condenser. Based on the pressure drop calculated, the new state of the refrigerant can be determined; the properties of this new state are used as inlet properties for the refrigerant as it enters the main body of the condenser. A segment-by-segment approach is used for the calculations in the microchannel tubes of the condenser, where each segment is a control

volume for which mass and energy balances can be solved. The program divides the tubes in each pass into 100 segments along the direction of refrigerant flow and performs identical calculations for each segment, using the outlet properties of a segment as the inlet properties for the next. The first thing the program does when it begins a new tube segment is to calculate the heat transfer coefficient and pressure drop for the air side. Next it calculates the heat transfer coefficient on the refrigerant side, using as an input an initial guess for the temperature of the outer wall of the tube. It then uses both air and refrigerant heat transfer coefficients in the effectiveness-NTU method to calculate the heat transfer for the segment. The primary equations used for this method are given below:

$$UA = \frac{1}{R_{ref} + R_{tube} + R_{air}} = \frac{1}{\frac{1}{h_{ref}A_i} + \frac{t}{k_{tube}A_m} + \frac{1}{\eta h_{air}A_o}} \tag{3.1}$$

$$NTU = \frac{UA}{C_{min}} \quad \text{where } C_{min} = \min(C_{air}, C_{ref}) = C_{air} \tag{3.2}$$

$$\varepsilon = 1 - e^{(-NTU)} \tag{3.3}$$

$$Q_{segment} = \varepsilon C_{min}(T_{ref,in} - T_{air,in}) \tag{3.4}$$

Once the heat transfer for the segment has been calculated, the program uses it to calculate the temperature of the tube outer surface. This temperature is then compared to the original estimate; if the difference is greater than 0.1 ℃, the new estimate is set to be equal to the old estimate plus 0.1 ℃, and the heat transfer calculations are repeated. This process continues until the difference between the estimated and calculated values of surface temperature are less than 0.1 ℃. After the

heat transfer iterations are complete the program calculates the refrigerant-side pressure drop and the outlet properties. It then calculates refrigerant and oil charge for the segment, and prints all segment results to an output file. The outlet properties then become inlet properties for the next segment, and the process repeats itself until the calculations have been performed for all 100 segments. When the segment calculations are finished, pressure drop is calculated for the portion of the intermediate header corresponding to the first pass of the condenser (if the condenser has more than one pass), and overall results for the pass are printed to an output file. This entire process repeats for subsequent passes, with the inputs to the inlet header now being equal to the outputs from the outlet header of the previous pass rather than being read in from a separate file. Figure 3.2 is a flowchart which gives a visual representation of the calculation process that takes place for a single-pass condenser. The process described by the flow chart is performed as many times as there are passes in the condenser under investigation. The following sections in this chapter give details about the solution process and major equations used for subsections of the model.

3.2 Air-Side Heat Transfer

The air-side heat transfer coefficient for a segment is calculated in this model using the j-factor approach. The correlation used for the j-factor comes from Chang and Wang (1997), and is given in Equation (3.5) below:

$$j = {Re_{Lp}}^{-0.49}\left(\frac{\theta}{90}\right)^{0.27}\left(\frac{F_p}{L_p}\right)^{-0.14}\left(\frac{F_l}{L_p}\right)^{-0.29}\left(\frac{T_d}{L_p}\right)^{-0.23}\left(\frac{L_l}{L_p}\right)^{0.68}\left(\frac{T_p}{L_p}\right)^{-0.28}\left(\frac{\delta_f}{L_p}\right)^{-0.05} \tag{3.5}$$

The above correlation is only applicable for a microchannel condenser with louver-fin geometry; for a different type of fin geometry, a different correlation would need to be implemented. After the j-factor is calculated, the heat transfer coefficient of the air is calculated using Equation (3.6) as follows:

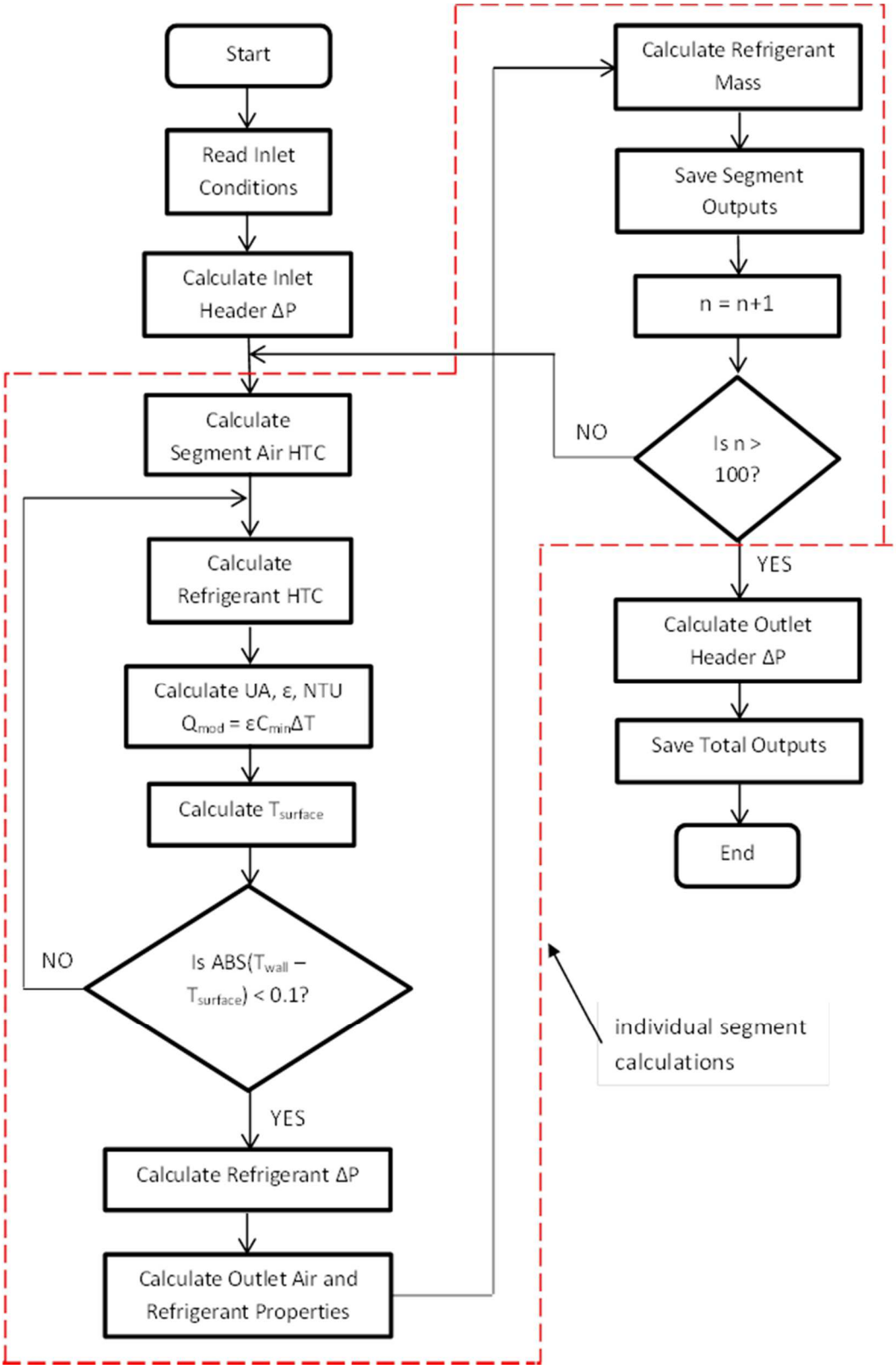

Figure 3.2 - Flowchart of the simulation process for the microchannel condenser model

$$h_{air} = jc_{p,air}G_{max}{Pr_{air}}^{-0.667}, \tag{3.6}$$

where G_{max} is the mass flux of the air calculated using the minimum free flow area.

3.3 Air-Side Pressure Drop

The equation used for air-side pressure drop was taken from McQuiston et. al. (2005), and is given below as Equation (3.7).

$$\Delta P_{air} = \frac{{G_{max}}^2}{2\rho_{in}}\left[(K_i + 1 - \sigma^2) + 2\left(\frac{\rho_{in}}{\rho_{out}} - 1\right) + f\frac{A_{coil}}{A_{min}}\frac{\rho_{in}}{\rho_{avg}} - (1 - \sigma^2 - K_e)\frac{\rho_{in}}{\rho_{out}}\right] \tag{3.7}$$

This equation is applicable for tubes in cross flow, where σ is the ratio of the minimum free flow area to the face area of the condenser, and K_i and K_e are loss coefficients for the air inlet and exit, respectively, which must be obtained from experimental data. The friction factor used in Equation (3.7) comes from Chang et al. (2000) and is calculated as follows:

$$f = f_1 \cdot f_2 \cdot f_3 \tag{3.8}$$

$$f_1 = \begin{cases} 14.39{Re_{Lp}}^{\left(-\frac{0.805F_p}{F_l}\right)}\left(log_e\left(1.0 + \left(\frac{F_p}{L_p}\right)\right)\right)^{0.304}, & Re_{Lp} < 150 \\ 4.97{Re_{Lp}}^{\left(0.6049 - 1.064/\theta^{0.2}\right)}\left(log_e\left(\left(F_t/F_p\right)^{0.5} + 0.9\right)\right)^{-0.527}, & 150 < Re_{Lp} \geq 5000 \end{cases} \tag{3.9}$$

$$f_2 = \begin{cases} \left(log_e\left(\left(F_t/F_p\right)^{0.48} + 0.9\right)\right)^{-1.435}\left(D_h/L_p\right)^{-3.01}\left(log_e\left(0.5Re_{Lp}\right)\right)^{-3.01}, & Re_{Lp} < 150 \\ \left(\left(D_h/L_p\right)log_e\left(0.3Re_{Lp}\right)\right)^{-2.966}\left(F_p/L_l\right)^{-0.7931\left(T_p/T_h\right)}, & 150 < Re_{Lp} \geq 5000 \end{cases} \tag{3.10}$$

$$f_3 = \begin{cases} \left(F_p/L_l\right)^{-0.308}\left(F_d/L_l\right)^{-0.308}\left(e^{-0.1167T_p/D_m}\right)\theta^{0.35}, & Re_{Lp} < 150 \\ \left(T_p/D_m\right)^{-0.0446}log_e\left(1.2 + \left(L_p/F_p\right)^{1.4}\right)^{-3.553}\theta^{-0.477}, & 150 < Re_{Lp} \geq 5000 \end{cases} \tag{3.11}$$

3.4 Fluid Properties

All refrigerant properties used in this model are obtained from REFPROP from NIST. Using REFPROP, three property tables are developed for each pure refrigerant: a saturated table, a superheated table, and a subcooled table. The program interpolates within the appropriate table

when a refrigerant property needs to be calculated. When there is oil in circulation with the refrigerant, however, these pure refrigerant properties must be updated to reflect the presence of oil. These updated properties are then used in all further calculations as if they were pure refrigerant properties. All oil mixture properties except for mixture density, which is calculated using an equation given by the oil manufacturer, are computed using correlations found and compiled by Schwentker (2005) and are given in the equations below.

SATURATION TEMPERATURE

$$T_{sat} = \frac{A(\omega_{local})}{ln\, P_{sat} - B(\omega_{local})}$$

$$A(\omega_{local}) = a_0 + a_1\omega_{local} + a_2\omega_{local}^3 + a_3\omega_{local}^5 + a_2\omega_{local}^7 \qquad (3.12)$$

$$B(\omega_{local}) = b_0 + b_1\omega_{local} + b_2\omega_{local}^3 + b_3\omega_{local}^5 + b_2\omega_{local}^7$$

where $a_0 - a_4$ and $b_0 - b_4$ are empirical coefficients

HEAT RELEASE ENTHALPY CURVE

$$dh = h_{LV} \cdot dx_{mix} + (1 - x_{mix}) \cdot c_{p,mix} \cdot dT_{bub} + x_{mix} \cdot c_{p,ref,vapor} \cdot dT_{bub} \qquad (3.13)$$

SPECIFIC HEAT

$$c_{p,mix} = \omega_{local} c_{p,oil} + (1 - \omega_{local}) c_{p,ref,liq}$$

$$c_{p,oil} = 4.186\left(\frac{0.338 + 0.00045(1.8T[℃] + 32)}{\sqrt{s_g}}\right) \qquad (3.14)$$

$$s_g = \frac{\rho_{oil}}{\rho_{water}}$$

VISCOSITY

$$\ln \mu_{mix} = \xi_{ref,liq} \cdot \ln \mu_{ref,liq} + \xi_{oil} \cdot \ln \mu_{oil} \qquad (3.15)$$

$$\xi_i = \frac{W_i^k \Psi_i}{\sum_j W_j^k \Psi_j}$$

$$\Psi_{oil} = \frac{\omega_{local}(W_{ref}/W_{oil})}{1-\omega_{local}+\omega_{local}(W_{ref}/W_{oil})}$$

SURFACE TENSION

$$\sigma_{mix} = \sigma_{ref,liq} + \left(\sigma_{oil} - \sigma_{ref,liq}\right)\sqrt{\omega_{local}} \quad (3.16)$$

THERMAL CONDUCTIVITY

$$k_{mix} = k_{ref,liq}(1-\omega_{local}) + k_{oil}\omega_{local} - 0.72\left(k_{oil} - k_{ref,liq}\right)(1-\omega_{local})\omega_{local} \quad (3.17)$$

In all the above equations, pure oil properties come from manufacturer data, ω and ω_{local} are the absolute and local oil mass fractions, respectively, calculated as

$$\omega_{local} = \frac{\omega}{1-x_{mix}}, \quad (3.18)$$

where

$$x_{mix} = \frac{x}{1-\omega}, \quad (3.19)$$

and

$$\omega = \frac{\dot{m}_{oil}}{\dot{m}_{total}}. \quad (3.20)$$

3.5 Refrigerant-Side Heat Transfer

Heat transfer coefficient for the refrigerant side is calculated using equations for Nusselt number found in Huang et al. (2010), shown below:

$$Nu = (Nu_F^2 + Nu_B^2)^{0.5} \tag{3.21}$$

$$Nu_F = 0.0152(\Phi_V/X_{tt})Re_L^{0.77}(-0.33 + 0.83Pr_L^{0.8}) \tag{3.22}$$

$$Nu_B = 0.725H(\alpha)\ (Ga_L Pr_L/Ph_L)^{0.25} \tag{3.23}$$

where

$$\Phi_V = 1 + 0.5\{G/[gD\rho_V(\rho_L - \rho_V)]^{0.5}\}^{0.75}X_{tt}^{0.35} \tag{3.24}$$

$$H(\alpha) = \alpha + \{10[(1-\alpha)^{0.1} - 1] + (1.7 \times 10^{-4})Re_{LO}\}\alpha^{0.5}(1-\alpha^{0.5}) \tag{3.25}$$

The void fraction α in the above equations is required in Huang et al. (2010) to be the Smith (1969) correlation, so that correlation is used in this model as well. The heat transfer correlation above was developed using experimental data for mixtures of R410A and oil flowing through tubes with hydraulic diameters of 4.18 mm and 1.6 mm. Because the correlation does not include the diameters used in the testing data set for this research, there is no guarantee that it will be applicable for all data used in this thesis. However, it was developed specifically for refrigerant-oil mixtures, which is not the case for other correlations. Chapter 4 will discuss whether or not this correlation should be used for all the data in this research.

3.6 Refrigerant-Side Pressure Drop

3.6.1 Two-Phase Frictional Pressure Drop

One of the primary objectives of this research is to implement the best possible correlation for the refrigerant-side two-phase frictional pressure drop. The details of how this correlation was chosen are presented in Chapter 4. The correlation implemented is that presented in Kim and Mudawar (2012), and is given below.

$$\left(\frac{dP}{dz}\right)_F = \left(\frac{dP}{dz}\right)_f \varphi_f{}^2$$

where

$$\varphi_f{}^2 = 1 + \frac{C}{X} + \frac{1}{X^2}, \quad X^2 = \frac{(dP/dz)_f}{(dP/dz)_g}$$

$$-\left(\frac{dP}{dz}\right)_f = \frac{2f_f v_f G^2 (1-x)^2}{D_h}, \quad -\left(\frac{dP}{dz}\right)_g = \frac{2f_g v_g G^2 x^2}{D_h}$$

$$f_k = 16 Re_k{}^{-1} \text{ for } Re_k < 2000$$

$$f_k = 0.079 Re_k{}^{-0.25} \text{ for } 2000 \le Re_k < 20{,}000$$

$$f_k = 0.046 Re_k{}^{-0.2} \text{ for } Re_k \ge 20{,}000 \tag{3.26}$$

$$Re_f \frac{G(1-x)D_h}{\mu_f}, \quad Re_g = \frac{GxD_h}{\mu_g}, \quad Re_{fo} = \frac{GD_h}{\mu_f}, \quad Su_{go} = \frac{\rho_g \sigma D_h}{\mu_g{}^2}$$

Liquid	**Vapor**	**C**
Turbulent	Turbulent	$0.39 Re_{fo}{}^{0.03} Su_{go}{}^{0.10} \left(\frac{\rho_f}{\rho_g}\right)^{0.35}$
Turbulent	Laminar	$(8.7 \times 10^{-4}) Re_{fo}{}^{0.17} Su_{go}{}^{0.50} \left(\frac{\rho_f}{\rho_g}\right)^{0.14}$
Laminar	Turbulent	$0.0015 Re^{0.59} Su_{go}{}^{0.19} \left(\frac{\rho_f}{\rho_g}\right)^{0.36}$
Laminar	Laminar	$(3.5 \times 10^{-5}) Re_{fo}{}^{0.44} Su_{go}{}^{0.50} \left(\frac{\rho_f}{\rho_g}\right)^{0.48}$

The above correlation was developed using a database of 7115 frictional pressure drop measurements for both adiabatic and condensing flows. The database includes data for both circular and rectangular horizontal microchannels, several fluids including many measurements of both R410A and R134a, and spans hydraulic diameters from 0.109 mm to 6.20 mm. All data used for the present research is contained within the ranges given above.

3.6.2 Single-Phase Frictional Pressure Drop

For single-phase frictional pressure drop, the program uses Fanning friction factors which are calculated as follows:

Turbulent, Vapor Flow

$$f = \frac{0.046}{Re^{0.2}} \tag{3.27}$$

Turbulent, Liquid Flow

$$f = \frac{0.079}{Re^{0.25}} \tag{3.28}$$

Laminar Flow

$$f = \frac{16}{Re} \tag{3.29}$$

For the case of flow in microchannels, the transition Reynolds number from laminar to turbulent flow is taken to be 1500, the value determined by Harms et al. (1999) for multiple-channel flow. Once the Fanning friction factors have been evaluated, the frictional pressure gradient can be calculated using the equations below:

$$\left(\frac{dP}{dz}\right)_{F,f} = \frac{2f_f G^2 v_f (1-x)^2}{D_h} \tag{3.30}$$

$$\left(\frac{dP}{dz}\right)_{F,g} = \frac{2f_g G^2 v_g x^2}{D_h} \tag{3.31}$$

3.6.3 Gravitational Pressure Drop

Since refrigerant flows horizontally through the microchannel condensers for all data considered in this research, there is no gravitational pressure drop in the microchannel tubes themselves. There is, however, a non-negligible gravitational pressure drop that exists in the vertical headers. The gravitational pressure drop gradient is calculated in this model as:

$$\left(\frac{dP}{dz}\right)_G = \frac{(dz/dL)g}{v}\,. \tag{3.32}$$

3.6.4 Momentum Pressure Drop

Since condensation takes place within the microchannel tubes and decreases the refrigerant velocity, there is a negative pressure drop that occurs due to momentum change. This pressure drop is so small as to be negligible, but it is included in this model for the sake of completeness. Momentum pressure drop is calculated for the microchannel tubes, but not the headers since there is no condensation in the headers, and thus no significant velocity change. The equations shown below are used to calculate momentum pressure drop.

Two-Phase

$$\left(\frac{dP}{dz}\right)_M = \left\{\left[\frac{x^2 v_g}{\alpha} + \frac{(1-x)^2 v_f}{(1-\alpha)}\right]_{out} - \left[\frac{x^2 v_g}{\alpha} + \frac{(1-x)^2 v_f}{(1-\alpha)}\right]_{in}\right\}\frac{G^2}{L_{seg}} \tag{3.33}$$

Single-Phase

$$\left(\frac{dP}{dz}\right)_M = \frac{G^2(v_{in} - v_{out})}{L_{seg}} \tag{3.34}$$

3.6.5 Header Pressure Drop

Header pressure drop is composed of several parts: frictional pressure drop for the header itself, frictional pressure drop for the inlet and outlet connecting tubes (when applicable), gravitational pressure drop, and minor loss pressure drops. Momentum pressure drop is not calculated for the header since no condensation, occurs. Frictional and gravitational pressure drops are calculated as shown in the previous sections. For each minor loss contribution, pressure drop is calculated using the following equations from Paliwoda (1992):

$$\Delta P = C_i \frac{G^2 v}{2} \beta_c, \qquad \text{and} \tag{3.35}$$

$$\beta_c = \left[\frac{v_f}{v_g} + C_j \left(1 - \frac{v_f}{v_g}\right) x\right] (1-x)^{0.333} + x^{2.276} \, . \tag{3.36}$$

where C_i and C_j are coefficients dependent upon the geometry of the minor loss element. The model takes into account minor losses due to elbows in the inlet and outlet connecting tubes, expansions and contractions when the fluid flows between connecting tubes and headers, and expansions and contractions when the fluid flows between the headers and microchannel tubes. The total pressure drop for a given header is the sum of all frictional, gravitational, and minor loss pressure drop contributions for the header.

3.7 Oil Retention

The oil retention portion of this model is designed to calculate the mass of oil that is present in the microchannel condenser for steady state operation at various oil mass fractions. The oil retention consists of two components: oil that is in circulation with the refrigerant and oil that is trapped within the condenser. The intent of the model presented here is to predict at least the amount of oil circulating with the refrigerant. By taking the difference between the amount of oil measured in experiments and the amount of oil circulating with the refrigerant, the oil that was trapped in the condenser was estimated and an analysis of the superheated regions of the condenser (including the inlet header) was performed to assess the feasibility of the resulting amount of oil trapped in the condenser.

There are also three different situations to consider when oil is in circulation with refrigerant: oil retention when the refrigerant is a superheated vapor, a two-phase liquid-vapor mixture, and a subcooled liquid. When the refrigerant is superheated, a liquid phase exists that is composed almost entirely of oil. This oil must be carried along by the refrigerant vapor. Since the oil has a much higher density than the vapor the vapor only carries it with difficulty, and a

relatively thick oil film forms, leading to high oil retention. When the refrigerant is a two-phase liquid-vapor mixture, some of the circulating oil is dissolved in the refrigerant and some is carried along by the vapor. The liquid helps to prevent an oil film from forming on the tube walls as well as carries the oil better than the vapor, so the oil moves through the tubes more quickly and oil retention is relatively small. Oil retention does increase, however, as condensation takes place and the liquid mass increases. Finally, when the refrigerant is a subcooled liquid, oil retention could be high. This is because liquid mass is much denser than vapor mass, leading to a higher refrigerant mass inventory even though mass flow rate is constant. Since oil mass is basically a percentage of total mass when the oil and refrigerant travel at similar velocities, when there is a large amount of total mass in a given segment then there is also a large amount of oil mass in the same segment, even if the lubricant is well mixed with the liquid refrigerant and it is transported well along the pipelines.

3.7.1 Oil Retention Mass Calculations

Despite the fact that there are three different flow situations as listed above, only one method is needed to calculate the oil retention mass. First, the mass of liquid in a segment is calculated using the volume of the segment and the void fraction. Volume of a tube segment is calculated as shown in Equation 3.36:

$$V_{seg} = a \cdot b \cdot L_{seg} \cdot N \tag{3.37}$$

where *a* and *b* are the height and width of a rectangular port, respectively, and *N* is the number of ports in the tube. Next the model calculates the void fraction for the segment. The void fraction correlation used for this portion of the model is the Mandrusiak and Carey (1988) correlation, which is shown below along with supporting equations.

$$\alpha = (1 + 0.25X_{tt})^{-2.0} \tag{3.38}$$

$$X_{tt} = \left[\frac{(dP/dz)_{liq}}{(dP/dz)_{vap}}\right]^{0.5} \tag{3.39}$$

$$(dP/dz)_{liq} = \frac{f_{liq} G^2 (1 - x_{mix})^2}{2 D_h \rho_{liq}} \tag{3.40}$$

$$(dP/dz)_{vap} = \frac{f_{vap} G^2 {x_{mix}}^2}{2 D_h \rho_{vap}} \tag{3.41}$$

$$f_{liq} = \begin{cases} \dfrac{16}{Re_{liq}} & Re_{liq} < 1500 \\ \dfrac{0.046}{Re_{liq}^2} & Re_{liq} \geq 1500 \end{cases} \tag{3.42}$$

$$f_{vap} = \begin{cases} \dfrac{16}{Re_{vap}} & Re_{vap} < 1500 \\ \dfrac{0.046}{Re_{vap}^2} & Re_{vap} \geq 1500 \end{cases} \tag{3.43}$$

$$Re_{liq} = \frac{G(1 - x_{mix}) D_h}{\mu_{liq}} \tag{3.44}$$

$$Re_{vap} = \frac{G x_{mix} D_h}{\mu_{vap}} \tag{3.45}$$

In the above equations, all vapor properties are for pure refrigerant vapor, while all liquid properties are for refrigerant-oil mixtures and are calculated as described in Section 3.4 of this thesis. x_{mix} is the mixture quality, and is calculated as shown in Equation 3.45,

$$x_{mix} = \frac{x}{1 - \omega} \tag{3.46}$$

where ω is the absolute oil mass fraction, which is defined as the mass flow rate of oil divided by the total mass flow rate. If there is oil in the system, x_{mix} is never equal to one, and thus the void fraction is also never equal to one. If the void fraction is never one, there is always some amount of liquid in the system. That amount of liquid is calculated as shown in below, where liquid properties are again equal to refrigerant-oil mixture properties.

$$m_{liq} = \frac{V_{seg}(1-\alpha)}{v_{liq}} \tag{3.47}$$

Finally, the mass of oil in a segment that is in circulation with the refrigerant is a percentage of the liquid mass in that segment. That percentage is the local oil mass fraction, which is calculated as shown in Equation (3.47).

$$\omega_{local} = \frac{\omega}{1 - x_{mix}} \tag{3.48}$$

As can be seen from the above equation, if x_{mix} is very small, the local oil mass fraction is almost equal to one and the liquid phase is composed almost entirely of oil. This is what happens in the superheated regions of the condenser. When the refrigerant is subcooled, however, the mixture quality is equal to zero and the local oil mass fraction is equal to the absolute oil mass fraction. Since the local oil mass fraction is the percentage of liquid mass that is oil, oil mass in circulation for a segment is calculated as follows:

$$m_{oil} = m_{liq}\omega_{local} \tag{3.49}$$

The total mass of oil in a tube is the sum of the oil masses in all the segments, and the total oil mass in the microchannel tubes for one pass is equal to the mass of oil in one tube multiplied by the number of tubes in that pass. Oil mass is calculated using the above equations for all portions of the condenser, whether superheated, subcooled, or two-phase. The total oil retention predicted by the model is the sum of the oil retention masses calculated for each element of the condenser.

3.7.2 Oil Retention in the Inlet Header

Oil retention mass in the inlet header is calculated the same way as for the rest of the condenser, but once mass is calculated, some additional analysis is needed. When there is liquid refrigerant, oil mass is dissolved in the liquid refrigerant and travels with it. When there is no liquid refrigerant, however, it is assumed that annular flow exists (an assumption that is checked in Chapter 5). For this flow, the core is primarily refrigerant vapor with a few entrained oil

droplets, and the film is the liquid phase which is composed almost entirely of oil. In order to make physical sense of the oil retention mass in the inlet header, it is converted into a dimensionless film thickness, δ/D_h, which is the oil film thickness divided by hydraulic diameter. Oil film thickness is calculated as

$$Vol_{oil} = \frac{m_{oil}}{\rho_{oil}}, \tag{3.50}$$

and additionally

$$Vol_{oil} = \frac{\pi}{4}\left[D_h^2 - (D_h - 2\delta)^2\right]L_{header}. \tag{3.51}$$

Rearranging Equation 3.50 results in Equation 3.51, which is the equation used to calculate the oil film thickness.

$$\delta = \frac{\sqrt{\pi}D_h L_{header} - \sqrt{L_{header}(\pi D_h^2 L_{header} - 4 \cdot Vol_{oil})}}{2\sqrt{\pi}L_{header}} \tag{3.52}$$

The dimensionless film thickness δ/D_h is used in Chapter 5 to analyze the results of the oil retention model. This same set of equations can also be used to estimate the resulting oil film thickness in the inlet tube and the superheated segments of the microchannels.

CHAPTER IV

MODEL VALIDATION: CAPACITY AND PRESSURE DROP

4.1 Refrigerant-Side Heat Transfer

The following sections describe the validation studies the author performed to check capacity predictions. Simulations to validate the heat transfer portion of the model were performed throughout this project in order to determine whether or not alterations to other parts of the model significantly degrade capacity predictions. They were also performed in order to test the heat transfer correlation in use so a decision could be made as to whether or not that correlation produces accurate enough predictions to be acceptable for this model.

4.1.1 Validation with Data from Hoehne and Hrnjak (2004)

One of the early validation studies the author performed uses experimental data gathered from Hoehne and Hrnjak (2014). The data set the author used consists of eight capacity measurements where propane (R290) is the working fluid. The condenser from which the measurements were taken is a two pass parallel microchannel condenser. It has a total of 23 tubes, each with 19 triangular ports with hydraulic diameters of 0.7747 mm. Unlike most of the papers presented in open literature, this report includes all geometry data and fluid property data (for both air and refrigerant) required as inputs to the model. The author performed simulations for the

data, and found that the model is able to predict capacity of this condenser very well, with all eight data points predicted within a +6%, -1% error. The results of this study are shown in Figure 4.1 below.

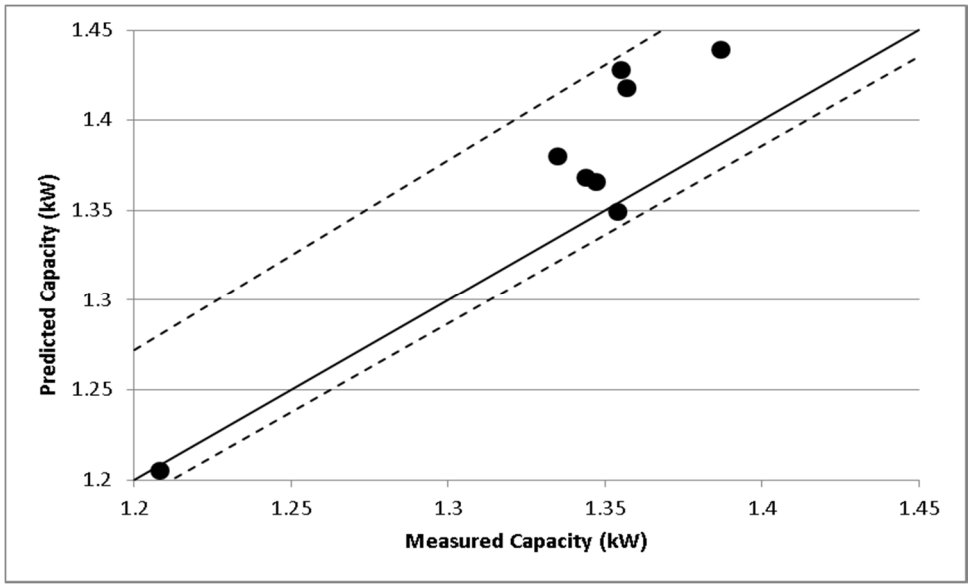

Figure 4.1 – Predicted capacity vs. measured capacity for propane data from Hoehne and Hrnjak (2004)

4.1.2 Validation with Data from Yatim et al. (2016)

The primary data used with the model for the current research was gathered by the author's colleagues and is presented in Yatim et al. (2016). The condenser used in their research is a two pass parallel microchannel condenser. It has 69 tubes in the first pass and 32 tubes in the second, each with four rectangular ports. Nominal size and operation information was not given to Yatim et al. (2016), so they had to estimate internal volume and port hydraulic diameter. Their initial estimates were 2.4 L and 1.4 mm, respectively. No estimates are provided by Yatim et al. (2016) for nominal capacity or pressure drop. The data set consists of capacity, pressure drop, and oil retention measurements for both R410A and R134a, with and without oil circulating through the system. The data set is summarized in Table 1 below.

Table 4.1 – Summary of experimental data from Yatim et. al. (2016)

R410A		
Series	Saturation Temperature (°F)	Refrigerant Flow Rate (lb/hr)
A	85	400
B	105	400
C	130	400
D	85	600
E	105	600
F	130	600

R134a		
Series	Saturation Temperature (°F)	Refrigerant Flow Rate (lb/hr)
A	95	250
B	105	250
C	130	250
D	95	450
E	105	450
F	130	450

Each series listed in Table 1 one contains four or five data points, with oil mass fraction for each ranging from 0 % to 5 %. The first data point in every series has an oil mass fraction of 0 %. There are twice the number of data points for R410A as for R134a; measurements were taken twice for R410A series A-F so as to include data points at both high and low superheat conditions.

Capacity predictions were checked against this data many times throughout the course of this research in order to gauge how the model was performing as alterations were made. The capacity predictions never changed more than a few percent throughout the research process, showing that changing other parts of the model, specifically pressure drop and mass inventory predictions, does not have a significant effect on the heat transfer calculations. Figures 4.2 and 4.3 show the validation results for the final version of the model for all R410A and R134a data points, respectively. As shown in these figures, most of the R410A data is predicted within a +29%, -7% error, and all of the R134a data except for one outlying series is predicted within a

+52%, -41% error. Separate validation plots were also generated for the cases with no oil in circulation to see how the model performs without the extra complexity of adding oil to the fluid properties. It was discovered that capacity trends are similar for both oil and no-oil cases, but the

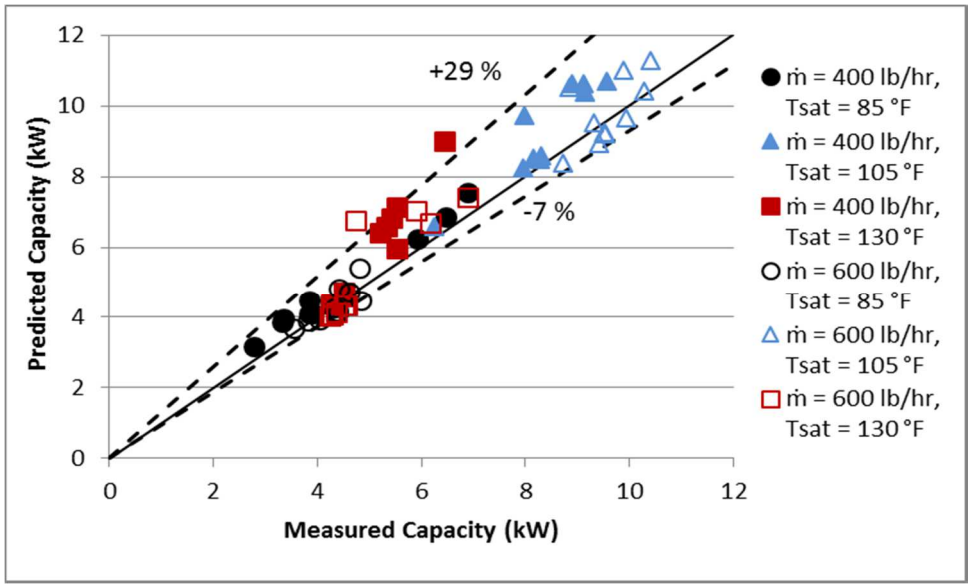

Figure 4.2 – Predicted vs. measured capacity for R410A data from Yatim et. al. (2016)

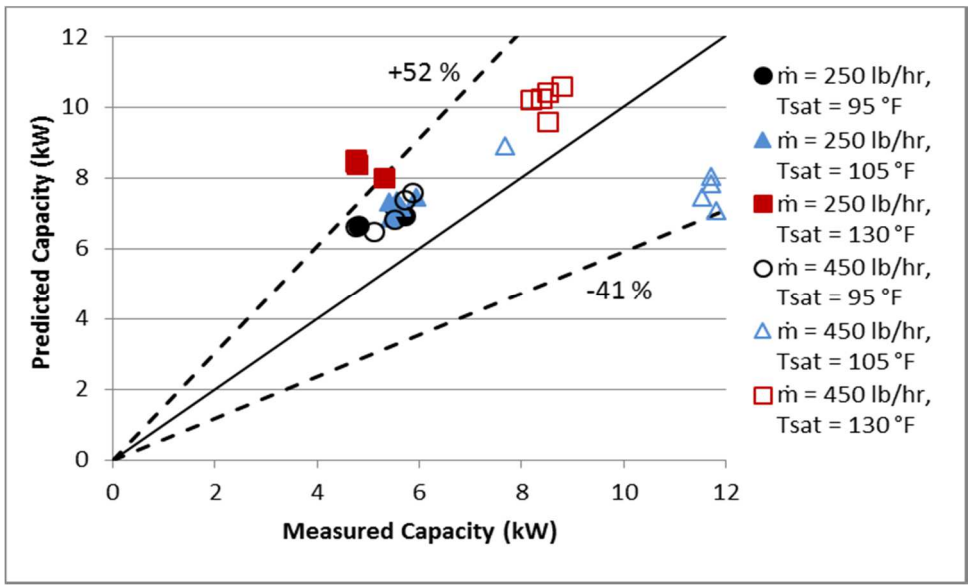

Figure 4.3 – Predicted vs. measured capacity for R134a data from Yatim et. al. (2016)

no-oil case is predicted slightly better than the overall case. These additional plots are Figures A.1 and A.2 on page 89 in the Appendix.

As seen from all the capacity validation plots, the current model gives acceptable predictions for the propane data from Hoehne and Hrnjak (2004) and the R410A data from Yatim et. al. (2016), but not for the R134a data from Yatim et. al. (2016). This leads to two possible conclusions. First, it could be that there is a problem with the way the model calculates R134a properties. This does not seem to be the case based on the pressure drop validation performed in the next section, but it is still a possibility. Second, the Huang et. al. (2010) correlation was developed for R410A-oil mixtures, and may not be applicable for R134a mixtures. It does not, however, appear to be solely applicable for R410A because the propane data was predicted very well. A solution to this problem to be addressed in future work could be to search for a more universally applicable correlation for heat transfer coefficient, implement it in the model, and do a more extensive capacity validation.

4.2 Refrigerant-Side Pressure Drop

4.2.1 Validation with Original Pressure Drop Correlation

Similarly to the heat transfer validation shown above, simulations were run in in order to test the pressure drop correlation in the model to determine whether it provided good predictions, or whether it needed to be replaced. The correlation in place when the author began to work with the model was that presented by Mishima and Hibiki (1996), and is given below. The authors use the Lockhart-Martinelli method, shown below,

$$\Phi_L^2 = 1 + \frac{C}{X} + \frac{1}{X^2} \tag{4.1}$$

but propose a new equation for the Chisholm parameter, C:

$$C = 21\left(1 - e^{-0.319 d_e}\right) \tag{4.2}$$

This correlation was developed using a database consisting of liquid-vapor flows through vertical and horizontal round tubes and thin horizontal ducts. All round tubes had diameters of 1-5 mm. The working fluid combinations were air-water, ammonia-vapor, and R113-N_2, though most of the data was for adiabatic air-water flows.

The author began the pressure drop validation with the data from Yatim et al. (2016). The results obtained for both the R410A and R134a cases without oil are shown in Figures 4.4 and 4.5 below. As can be seen, the results are good for R410A as all but one data point are within a +32 %, -36 % error. The predictions are very bad for R134a, however, as all points are underpredicted within a -75 % error. The author only shows the cases without oil here because these are the ones that are important to simulate accurately first since they are the "control" cases. After that, oil can be added and it can be determined if the code predicts less accurately when oil mixture properties are introduced. The author determined that the same possible explanations for the discrepancy that appeared for the capacity validations could also apply here: properties for

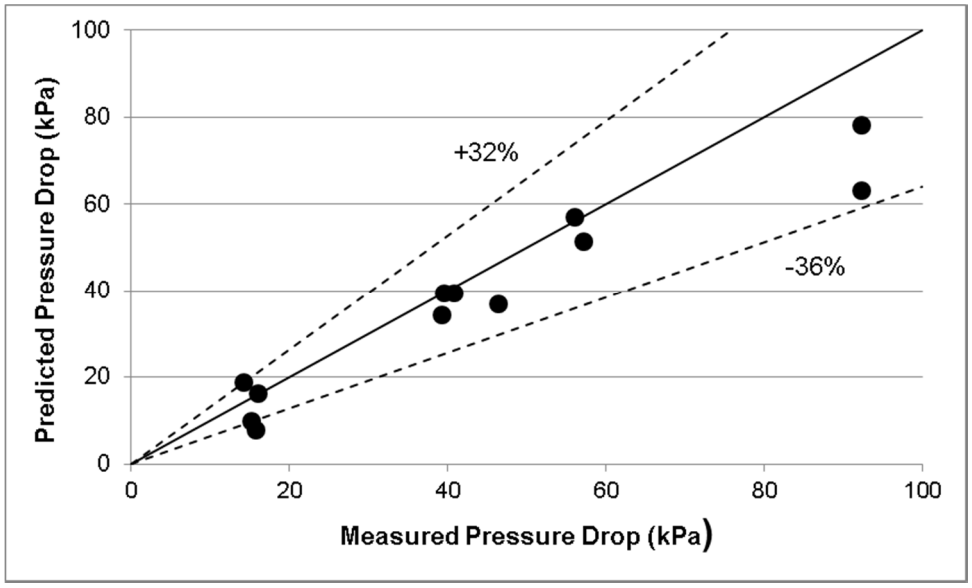

Figure 4.4 – Predicted pressure drop vs. measured pressure drop for R410A data without oil from Yatim et al. (2016)

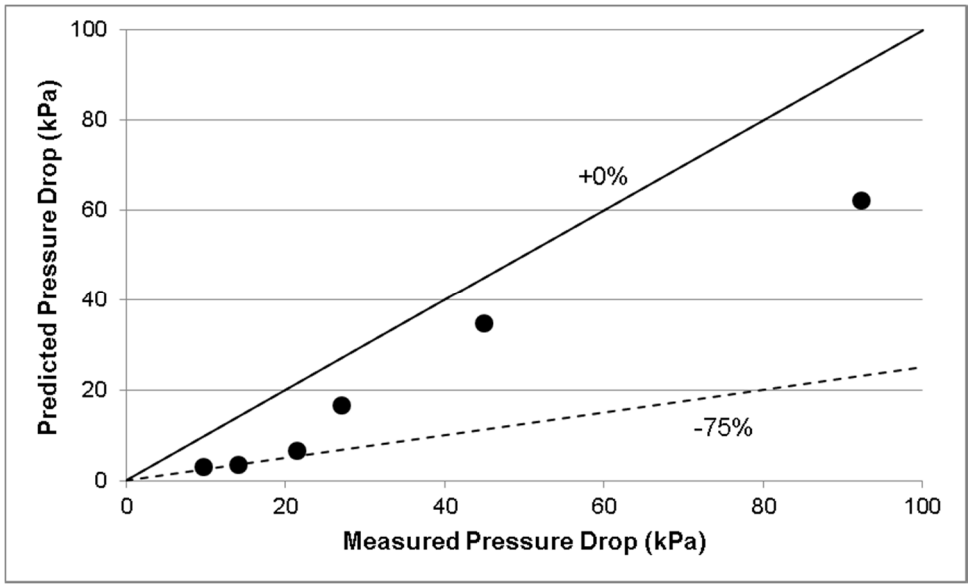

Figure 4.5 – Predicted pressure drop vs. measured pressure drop for R134a data without oil from Yatim et al. (2016)

R134a could be calculated incorrectly, or the Mishima and Hibiki (1996) correlation is not applicable for the R134a data.

More validation simulations were needed in order to decide which of the above explanations is most likely true, so the author also simulated the pressure drop data from Hoehne and Hrnjak (2004) as well. The results of this study are given in Figure 4.6 below. As can be seen, the prediction trend does not even follow the experimental trend for this data, and the model far underpredicts the experimental data with an error of -81 %.

From all the pressure drop validation plots presented here, it can be seen that the code at this point only gives good pressure drop predictions for the R410A data, and not for the R134a or propane data. Because of this, it did not seem likely to the author that the main issue with the model was a problem in calculating fluid properties for R134a. This could explain why it did not predict heat transfer or pressure drop well for R134a, but it could not explain why it was able to predict heat transfer and not pressure drop for the propane data.

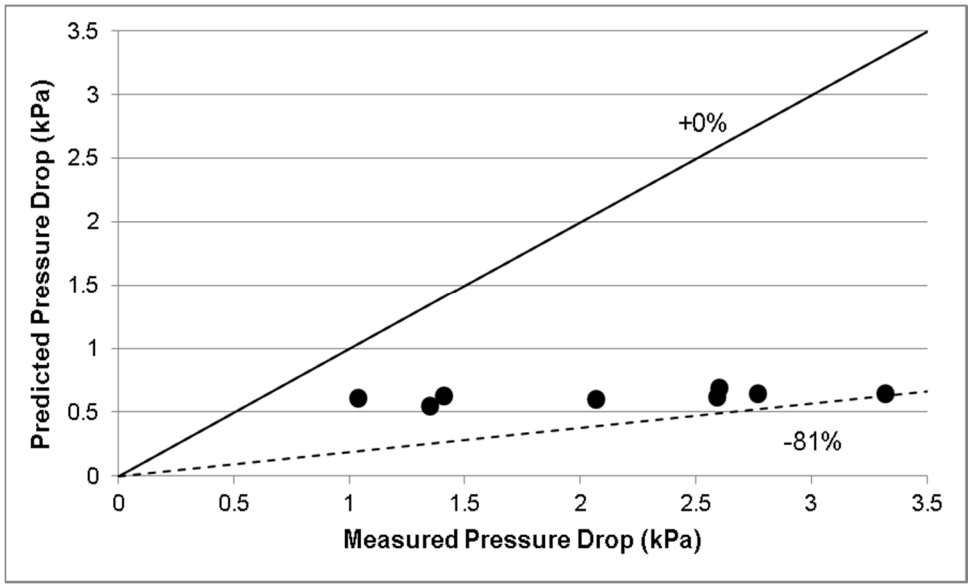

Figure 4.6 – Predicted pressure drop vs. measured pressure drop for propane data from Hoehne and Hrnjak (2004)

In order to be sure of this conclusion, however, a sensitivity analysis was performed with R410A and R134a fluid properties. Two properties were chosen, dynamic viscosity and specific volume, both of which are important to the calculation of frictional pressure drop. These properties were individually raised and lowered by 10 %, and frictional pressure drop gradient was calculated for each using the Mishima and Hibiki (1996) correlation. These pressure drop gradients were calculated apart from the model in order to have greater control over the refrigerant properties, but the same equations used in the model were used for these calculations. The results of these calculations are presented below in Table 4.2. From this table, it can be seen that as viscosity and specific volume are raised and lowered 10 %, the frictional pressure drop per unit length only increases or decreases by a maximum of 10 % for both refrigerants. Because of this, it can be concluded that an error in the calculation of fluid properties cannot account for the huge underpredictions seen for the R134a data. Changing properties like this would definitely affect other aspects of the model, such as heat transfer, but it is not necessary to know by how

much since this analysis shows that changing refrigerant properties does not fix the R134a pressure drop predictions.

Table 4.2 – Sensitivity analysis of frictional pressure drop to change in refrigerant properties

	R410A				
	Original	**Raise μ 10%**	**Lower μ 10%**	**Raise v 10%**	**Lower v 10%**
μ_f (N-s/m^2)	8.038×10^{-5}	8.842×10^{-5}	7.234×10^{-5}	8.038×10^{-5}	8.038×10^{-5}
μ_g (N-s/m^2)	1.775×10^{-5}	1.953×10^{-5}	1.598×10^{-5}	1.775×10^{-5}	1.775×10^{-5}
v_f (m^3/kg)	1.148×10^{-3}	1.148×10^{-3}	1.148×10^{-3}	1.263×10^{-3}	1.033×10^{-3}
v_g (m^3/kg)	6.122×10^{-3}	6.122×10^{-3}	6.122×10^{-3}	6.734×10^{-3}	5.510×10^{-5}
$(dP/dz)_F$ (Pa/m)	2920.3	3036.2	2798.6	3212.4	2628.3

	R134a				
	Original	**Raise μ 10%**	**Lower μ 10%**	**Raise v 10%**	**Lower v 10%**
μ_f (N-s/m^2)	1.364×10^{-4}	1.500×10^{-4}	1.228×10^{-4}	1.364×10^{-4}	1.364×10^{-4}
μ_g (N-s/m^2)	1.341×10^{-5}	1.475×10^{-5}	1.207×10^{-5}	1.341×10^{-5}	1.341×10^{-5}
v_f (m^3/kg)	9.184×10^{-4}	9.184×10^{-4}	9.184×10^{-4}	1.010×10^{-3}	8.266×10^{-4}
v_g (m^3/kg)	0.0139	0.0139	0.0139	0.0153	0.0125
$(dP/dz)_F$ (Pa/m)	5621.8	5831.3	5401.3	6184.0	5059.6

It then seemed likely to the author that the Mishima and Hibiki (1996) correlation for pressure drop that was implemented in the model was not a very good correlation to use for a wide variety of uses. This is not surprising based on the fact that it was developed primarily for adiabatic air-water flows. Because of this, the author decided to search for a new, more universal pressure drop correlation to implement in the model instead.

4.2.2 Literature Search for Frictional Pressure Drop Correlations

For this literature search, the author looked for papers that used large databases to compare several correlations for frictional pressure drop in small channels. Most of the review papers like this in open literature use adiabatic two-phase flow data because that is the data readily available, but some papers also include condensation data. For these purposes, the author

Table 4.3 – Summary of literature search for applicable pressure drop correlations

Paper	Size of Database	Working Fluids	D_h (mm)	Number of Correlations Compared	Top Correlations
Sun and Mishima (2009)	2092 data points	R123, R134a, R22, R236ea, R245fa, F404a, R407C, R410A, R507, CO2, water, air-water	0.506 - 12	11 existing 1 new	**Whole database:** Sun and Mishima (2009) Müller-Steinhagen and Heck (1986)* Homogeneous Model Mishima and Hibiki (1996) **Refrigerants only:** Sun and Mishima (2009) Müller-Steinhagen and Heck (1986)* Homogeneous Model Zhang and Webb (2001)
Cioncolini et al. (2009)	582 data points	R134a R245fa	0.517 0.803 1.03	24 existing 1 new	Cioncolini et al. (2009) Lombardi (1992) Müller-Steinhagen and Heck (1986) Cicchitti et al. (1960)
Zhang et al. (2010)	2201 data points	ammonia, R134a, R22, R404a, R410A, R236ea, R12, R113, water, R113-N_2, water-air, water-N_2, ethanol-air, oil-air	0.07 - 6.25	15 existing 1 new	**Liquid-gas data:** Mishima and Hibiki (1996) Zhang et al. (2010) Dukler et al. (1964) Lee and Lee (2001) **Liquid-vapor data:** Ackers et al. (1959) Beattie and Whalley (1982) Lee and Mudawar (2005) Zhang et al. (2010)
Li and Wu (2010)	769 data points	R245fa, R134a, R22, R410A, R12, R236ea, R32 R404a, R422d, ammonia, propane, liquid nitrogen	0.148 - 3.25	11 existing 1 new	Li and Wu (2010) Beattie and Whalley (1982) Awad and Muzychka (2008) McAdams et al. (1942)
Xu et al. (2012)	3480 data points	R134a, R410A, R22, R245fa, R404A, R407C, R125, R422D, R123, R507, CO_2, ammonia water-air, ethanol-air	0.0695 - 14	29 existing	**Whole database:** Müller-Steinhagen and Heck (1986) Sun and Mishima (2009) Beattie and Whalley (1982) McAdams et al. (1942) **Condensation data:** Müller-Steinhagen and Heck (1986) Souza and Pimenta (1995) Cicchitti et al. (1960) Sun and Mishima (2009) **Refrigerant data:** Müller-Steinhagen and Heck (1986) Sun and Mishima (2009) Souza and Pimenta (1995) Awad and Muzychka (2008)

Table 4.3 (continued)

Paper	Size of Database	Working Fluids	D_h (mm)	Number of Correlations Compared	Top Correlations
Xu and Fang (2013)	525 data points	R134a, R410A, R236ea, R32, R125, R290, R22, R600a, ammonia	0.1 - 10.07	29 existing 1 new	**Whole database:** Xu and Fang (2013) Müller-Steinhagen and Heck (1986) Friedel (1979) Cicchitti et al. (1960) **Microchannel data:** Xu and Fang (2013) Friedel (1979) Müller-Steinhagen and Heck (1986) Cicchitti et al. (1960)
Kim and Mudawar (2014)	7115 data points	R134a, R410A, R12, R245fa, R22, R236ea, R407C, R404A, CO_2, ammonia, water, methane, propane, air-water, N_2-water, N_2-ehtanol, CO_2-water	0.0695 - 6.22	18 existing 1 new	**Condensation data:** Kim and Mudawar (2012) Sun and Mishima (2009) Müller-Steinhagen and Heck (1986) Yang and Webb (1996) **Adiabatic liquid-vapor data:** Kim and Mudawar (2012) Müller-Steinhagen and Heck (1986) Akers et al. (1958) Beattie and Whalley (1982) **Adiabatic liquid-gas data:** Kim and Mudawar (2012) Dukler et al. (1964) Mishima and Hibiki (1996) Beattie and Whalley (1982)
López-Belchi et al. (2014)	318 data points	R1234yf, R134a, R32	1.16	8 existing 1 new	López-Belchi et al. (2014) Cavallini et al. (2009) Homogeneous Model Sun and Mishima (2009)
Ghajar and Bhagwat (2014)	514 data points	R134a	1.4 - 13.8	35 existing	Friedel (1979) Xu and Fang (2012) Davidson et al. (1943)

paid most attention to results for adiabatic and condensing flow of refrigerants (as opposed to other two-phase combinations) in microchannels. Table 4.3 gives a summary of the nine review papers the author considered in this search. As can be seen in the table, the top performing correlations for each paper or for the major categories of interest in the paper, if available, are listed. Also listed for each paper are the size of the database, working fluids, range of hydraulic diameters, and the number of correlations compared. These factors were all taken into account when the author determined the best correlations for the purposes of this research.

The author decided to choose three correlations that appeared from the literature search to be the best options for the current research. These three correlations would need to consistently perform well in the review papers, especially when tested using only condensation data. They would also need to perform well for refrigerant data specifically, with a special emphasis on R410A and R134a data, when possible. This is because the primary data used in this research is R134a-oil and R410A-oil mixtures from Yatim et al. (2016), and it is necessary to get good predictions for these refrigerants on their own before adding in oil properties. Lastly, they would need to perform well for channel sizes on the order of 1 mm, since that is about the size of the channels in the condenser used in the Yatim et al. (2016) experimental study. Based on this search, the Mishima and Hibiki (1996) correlation, formerly implemented in the code, is not a good option for this research. It does not appear often in the Top Correlations column of Table 4.3, and when it does, it is primarily for adiabatic flows of fluids other than refrigerants. This makes sense since it was originally developed for adiabatic air-water flows. The three correlations chosen from the literature search are Müller-Steinhagen and Heck (1986), Sun and Mishima (2009), and Kim and Mudawar (2012).

The Müller-Steinhagen and Heck (1986) correlation was chosen because it appears in the Top Correlations column of Table 4.3 more often than any other correlation, and seems to perform well especially for condensation and refrigerant data. This correlation was not developed for microchannel data; in fact, the smallest tube diameter in the database used to develop the correlation is 5 mm. It was also not developed with refrigerants specifically in mind; the database contains some measurements for R11, R12, and R22, but is primarily composed of gas-liquid combinations where the gas and liquid phases are different fluids. Regardless of the fact that it was not developed for use with the kind of data used in the current research, several authors have determined that it still performs very well for similar data, so it was chosen. The Müller-Steinhagen and Heck (1986) correlation is given below in Equations 4.3 and 4.4.

$$R = \left(\frac{dp}{dL}\right)_{F,l} + 2\left(\left(\frac{dp}{dL}\right)_{F,g} - \left(\frac{dp}{dL}\right)_{F,l}\right)x \tag{4.3}$$

$$\left(\frac{dp}{dL}\right)_{F,tp} = R(1-x)^{\frac{1}{3}} + x^3\left(\frac{dp}{dL}\right)_{F,g} \tag{4.4}$$

The Sun and Mishima (2009) correlation was chosen for a few reasons. For one, it was developed using a large database, and was tested for refrigerant data separately from the whole database. For both refrigerant data and overall data, it performed better than the Müller-Steinhagen and Heck (1986) correlation, which was second best. It also made the list of top correlations for the two review papers with the largest databases, performing particularly well for condensation and refrigerant data. This correlation uses the Lockhart-Martinelli method for calculating two-phase frictional pressure drop, with some alterations. It changes the power of the Martinelli parameter in the second term of the two-phase multiplier from 1 to 1.19, and proposes a new equation for the constant C in the Chisholm equation. These updated equations are given below as Equations 4.5 and 4.6.

$$\Phi_l^2 = 1 + \frac{C}{X^n} + \frac{1}{X^2} \tag{4.5}$$

where $n = 1.19$

$$C = 1.79\left(\frac{Re_g}{Re_l}\right)^{0.4}\left(\frac{1-x}{x}\right)^{0.5} \tag{4.6}$$

The final equation chosen from the literature search is the Kim and Mudawar (2012) correlation. This equation only appears in the Top Correlations column in Table 4.3 for one paper, Kim and Mudawar (2014). It was still chosen, however, because out of the nine papers, Kim and Mudawar (2014) has by far the largest database. It can be seen from this paper that not only does it predict the entire database best, but it also is best for condensation specifically and

for liquid-vapor specifically (which is mostly refrigerant data). It is also a new correlation, and so was not even available when the first five or six of the review papers in Table 4.3 were written. The Ghajar and Bhagwat (2014) paper does not even consider it, so it is unknown how it would perform with their database. López-Brcelchi et al. (2014) do consider it, but their database is about 20 times smaller than the Kim and Mudawar (2014) database, and it has a much more narrow range of operating conditions and working fluids. Only one hydraulic diameter is considered, and R410A data is not even part of this database. Because of these reasons, the Kim and Mudawar correlation was chosen for this analysis. The Kim and Mudawar (2012) correlation is given in detail in Chapter 3.

4.2.3 Validation with Top Three Frictional Pressure Drop Correlations from Literature

Once the author chose the three correlations from the literature search that seemed most likely to provide the best predictions for the Yatim et al. (2016) data, all three correlations were tested in the microchannel condenser model using data from several literature sources. This data is comprised of adiabatic frictional pressure drop measurements for single microchannel tubes where the working fluid is either R134a or R410A. In order to reduce potential error, only papers that reported frictional pressure drop itself were included as sources; papers that reported only total pressure drop were not considered because of the uncertainty associated with calculating minor losses due to the test section inlets and outlets. Only papers with data for single tubes were included (though multiple ports per tube was considered acceptable) for the same reason; with multiple tubes, there are minor losses due to the more complex geometry that are not yet fully understood. The goal of this validation study is to check the three correlations under very simple operating conditions. Unfortunately, no papers reporting condensation data could be found that included the necessary inlet conditions and met all the criteria for simplicity given above. It was seen from the literature search summary given above and from the analysis in Kim and Mudawar (2014), specifically, that the correlations which perform well for adiabatic refrigerant data tend to

also perform well for the condensation data. Because of this, even though only adiabatic refrigerant data is used, this validation study can still provide valuable information for the purposes of this research. It is especially helpful since all the data used is for either R134a or R410A; it could not be determined from the literature search which of these three correlations is most accurate for these refrigerants in particular, so this study should help determine that. Once all the data was gathered from the sources, the three correlations were added to the microchannel condenser model, correct geometry was implemented, and simulations were run to see how well each could predict frictional pressure drop when working as part of this model. The following sections show the results of this validation study for each source, and overall for each refrigerant. The results in each section are compared using the Mean Absolute Error (MAE) as defined in Equations 4.7 and 4.8:

$$Absolute\ Error = \text{Abs}\left(\frac{\Delta P_{simulated} - \Delta P_{experimental}}{\Delta P_{experimental}}\right) \tag{4.7}$$

$$MAE = \frac{1}{N}\left[\sum_{i=1}^{N}(Absolute\ Error)_i\right] \cdot 100\% \tag{4.8}$$

where N is the number of data points in a set

The results are also compared using bias, which is the average of the errors for all the predicted values.

ZHANG AND WEBB (2001) – R134A

The data gathered from Zhang and Webb (2001) that is used in this study is for R134a flowing through a horizontal round copper tube with hydraulic diameter of 3.25 mm at a mass flux of 600 kg/m^2-s. Measurements were taken at two saturation temperatures, 40 °C and 65 °C, and quality of the fluid ranges from 0.20 to 0.86 for the data set. Pressure taps were placed

directly on the tube itself, so no entrance or exit losses need to be taken into account; the pressure drop reported is only frictional pressure drop. Figure 4.7 shows predicted vs. experimental pressure drop for this data set using all three correlations. From this figure, it can be seen that all three correlations perform well, but the Müller-Steinhagen and Heck (1986) correlation appears to have the smallest deviation. This is confirmed by the comparison of the MAE values for each correlation given in Table 4.4; the MAE for the Müller-Steinhagen and Heck (1986) correlation is just over half that for either of the other two correlations.

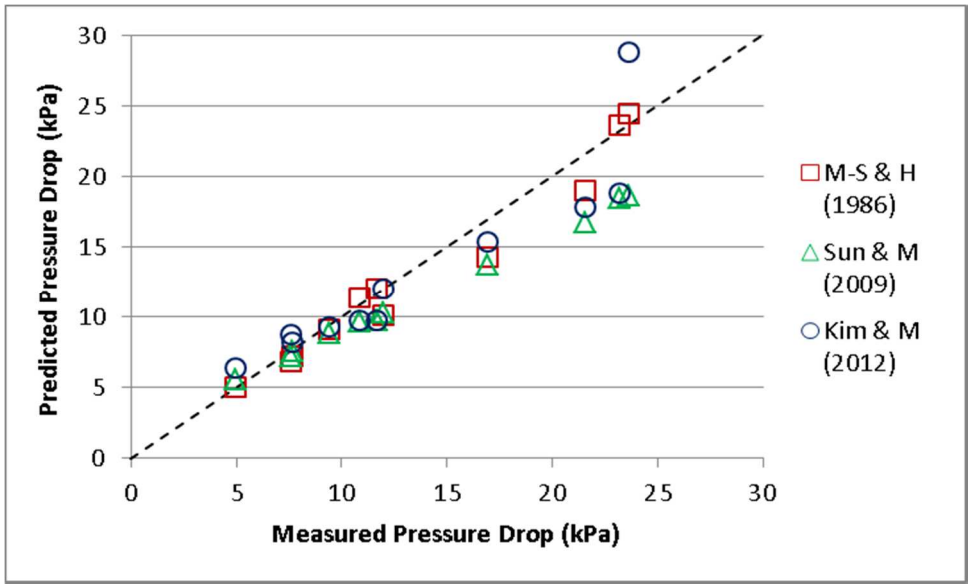

Figure 4.7 – Comparison of the three chosen frictional pressure drop correlations with R134a data from Zhang and Webb (2001)

Table 4.4 – Values of MAE and bias for R134a data from Zhang and Webb (2001)

Correlation	MAE (%)	Bias (%)
Müller-Steinhagen and Heck	6.9	-4.4
Sun and Mishima	13.7	-11.3
Kim and Mudawar	13.3	-0.1

CAVALLINI ET AL. (2005) – R134A

The R134a data gathered from Cavallini et al. (2005) for this study is for fluid flowing through a horizontal multiport tube with a port hydraulic diameter of 1.4 mm. Measurements are taken at mass fluxes of 400, 600, 800, and 1000 kg/m^2-s and inlet qualities of 0.25, 0.51, and 0.75. Pressure drop for the test section was calculated using the saturation temperature drop, measured by thermocouples placed on the tube itself. This was done in order to avoid the losses associated with the fluid entering and exiting the multiport tube. Figure 4.8 shows the experimental vs. predicted pressure drop for all three correlations. It appears from the figure that this time, the Sun and Mishima (2009) correlation predicts the data best; this is confirmed by Table 4.5, which reports that this correlation has the lowest MAE of the three.

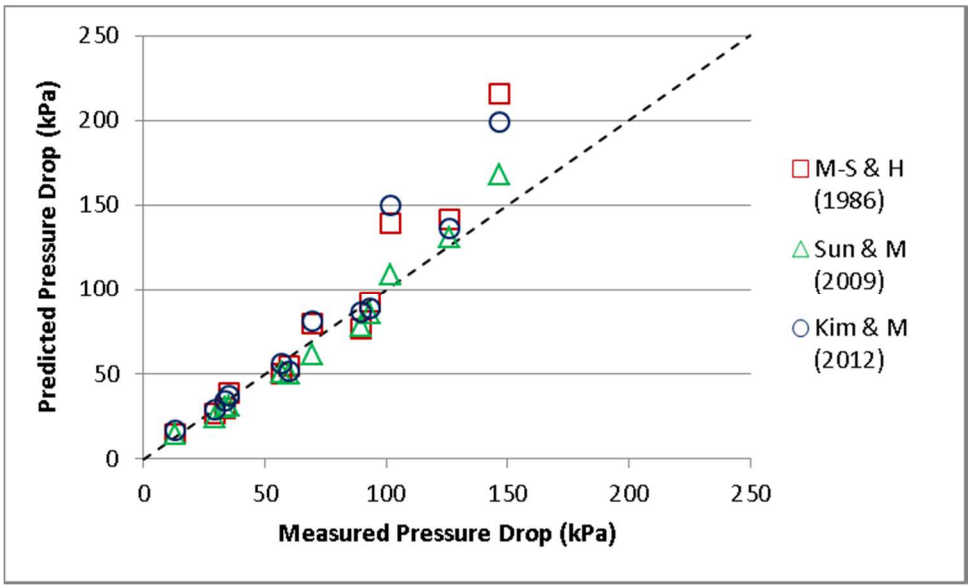

Figure 4.8 – Comparison of the three chosen frictional pressure drop correlations with R134a data from Cavallini et al. (2005)

Table 4.5 – Values of MAE for R134a data from Cavallini et al. (2005)

Correlation	MAE (%)	Bias (%)
Müller-Steinhagen and Heck	15.7	6.0
Sun and Mishima	11.4	-5.5
Kim and Mudawar	13.9	9.4

REVELLIN AND THOME (2007) – R134A

The data gathered from Revellin and Thome (2007) is for R134a flowing through a horizontal tube with hydraulic diameter of 0.509 mm. Saturation temperature is 30 °C, and fluid quality for all data tested in the current study ranges from 0.01 to 0.92. As in Cavallini et al. (2005), the authors calculated pressure drop of the test section using saturation temperature drop data gathered from thermocouples attached to the tube wall so as not to disturb the flow. The authors presented data for eight different series, each with a different mass flux but the same saturation temperature. The different mass flux series had varying pressure drop trends, so the author of this work decided to choose two of them to see how the correlations would respond. The series chosen had mass fluxes of 350 kg/m^2-s and 1000 kg/m^2-s. Predicted vs. experimental pressure drop for all three correlations for the 350 kg/m^2-s series is shown in Figure 4.9 below. Table 4.6 gives the MAE values for each correlation using this data series, and indicates that the Kim and Mudawar (2012) correlation, with the lowest MAE, is best for this case.

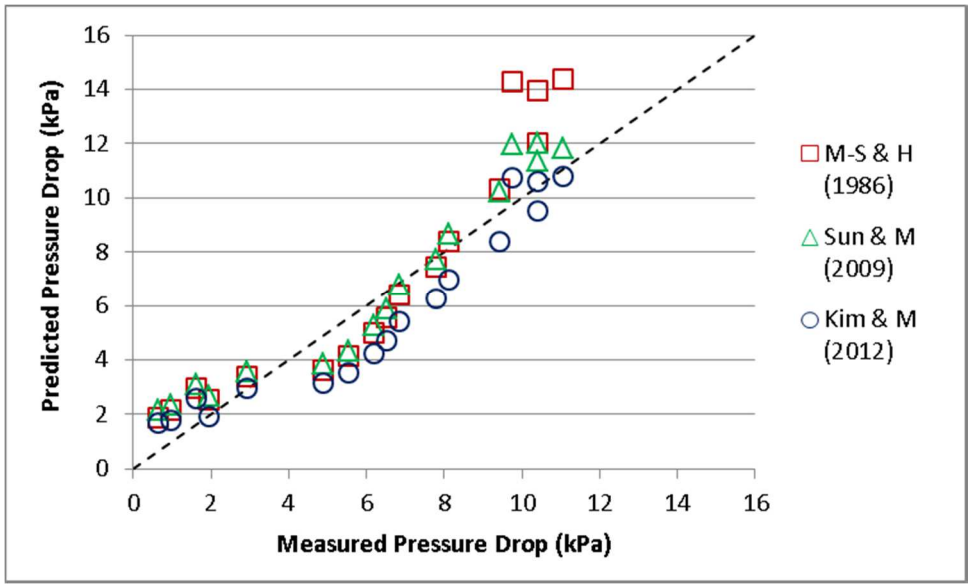

Figure 4.9 – Comparison of the three chosen frictional pressure drop correlations with R134a, 350 kg/m^2-s data from Revellin and Thome (2007)

Table 4.6 – Values of MAE for R134a, 350 kg/m^2-s data from Revellin and Thome (2007)

Correlation	MAE (%)	Bias (%)
Müller-Steinhagen and Heck	39.8	28.6
Sun and Mishima	38.9	30.9
Kim and Mudawar	30.7	6.1

Predicted vs. experimental pressure drop values for the 1000 kg/m^2-s series are given below in Figure 4.10. As can be seen, this series has a very distinct pressure drop trend that none of the three correlations are able to accurately capture. According to Revellin and Thome (2007), the break that can be seen in the trend of measured pressure drop vs. flow quality is due to a transition in flow type from wavy annular to smooth annular. None of the trends of the three correlations tested here can reflect this break, and that is why a break also appears in the predicted vs. measured pressure drop values presented in Figure 10. It appears, however, that the Kim and Mudawar (2012) correlation gives the best predictions, especially at lower values of pressure

drop. This is confirmed by Table 4.7, which shows that this correlation has the lowest MAE for this data series.

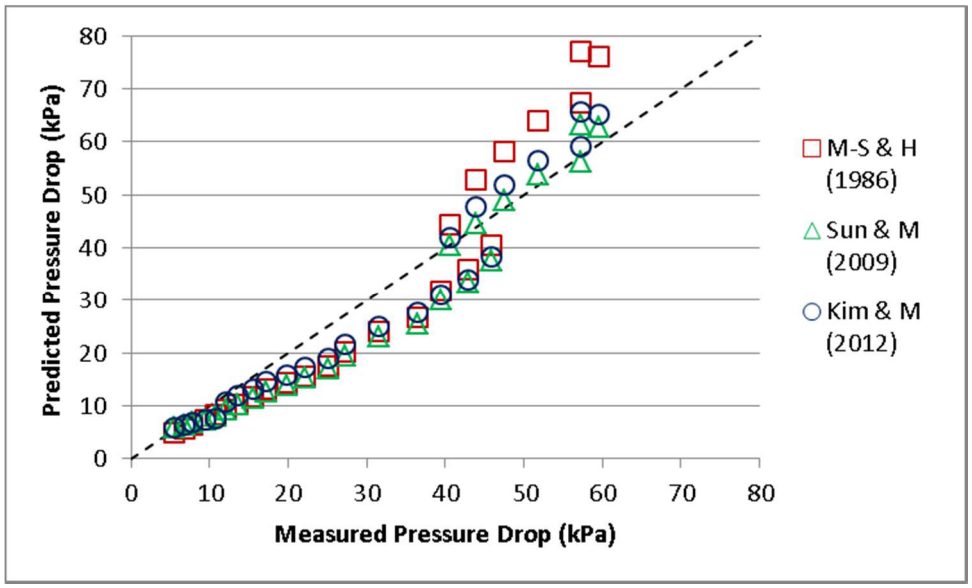

Figure 4.10 – Comparison of the three chosen frictional pressure drop correlations with R134a, 1000 kg/m^2-s data from Revellin and Thome (2007)

Table 4.7 – Values of MAE for R134a, 1000 kg/m^2-s data from Revellin and Thome (2007)

Correlation	MAE (%)	Bias (%)
Müller-Steinhagen and Heck	22.4	-10.0
Sun and Mishima	17.8	-15.5
Kim and Mudawar	15.4	-10.4

R134A OVERALL

For the three validation studies performed above, it was found that a different correlation performed best for each of the three sources considered. Based solely on this fact, a decision as to which correlation would be best for the R134a data in Yatim et al. (2016) could not be made. The

author then decided to calculate the overall MAE for each correlation for all the R134a data considered above for validation. The overall MAE values for each correlation are given below in Table 4.8. From the table, it was determined that, to the author's best knowledge, the Kim and Mudawar (2012) correlation is best to use for the R134a predictions in the current research, though any of the three would likely be satisfactory.

Table 4.8 – Values of MAE for all R134a literature data

Correlation	MAE (%)	Bias (%)
Müller-Steinhagen and Heck	23.1	4.0
Sun and Mishima	21.5	-0.8
Kim and Mudawar	18.8	-0.7

CAVALLINI ET AL. (2005) – R410A

The R410A data gathered from Cavallini et al. (2005) for this study is for fluid flowing through a horizontal multiport tube with port hydraulic diameter of 1.4 mm. Measurements are taken at mass fluxes of 600, 1000, and 1400 kg/m^2-s and inlet qualities of 0.26, 0.50, and 0.74. As for the R134a data, pressure drop for the test section was calculated using the saturation temperature drop, measured by thermocouples placed on the tube itself. Predicted vs. experimental pressure drop for all three correlations is shown below in Figure 4.11. Surprisingly, none of these correlations predicts the R410A data very well. Regardless, MAE values for each correlation were calculated and tabulated in Table 4.9. Of the three, the Sun and Mishima (2009) correlation has the smallest MAE and so is considered best for this data set.

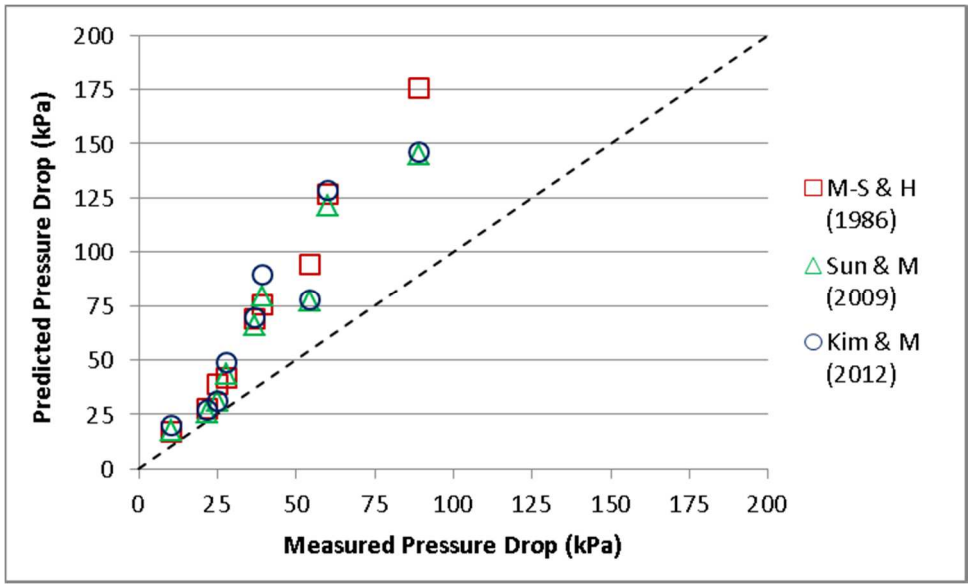

Figure 4.11 – Comparison of the three chosen frictional pressure drop correlations with R410A data from Cavallini et al. (2005)

Table 4.9 – Values of MAE and bias for R410A data from Cavallini et al. (2005)

Correlation	MAE (%)	Bias (%)
Müller-Steinhagen and Heck	72.7	72.7
Sun and Mishima	61.5	61.5
Kim and Mudawar	72.4	72.4

WANG ET AL. (2001) – R410A

The data gathered from Wang et al. (2001) is for R410 flowing through a horizontal round tube with hydraulic diameter of 3 mm. Measurements are taken at a mass flux of 400 kg/m^2-s and at saturation temperatures of 5 °C and 25 °C, while fluid quality for the data set ranges from 0.12 to 0.89. The pressure drop measurements reported in this paper are stated by the authors to be frictional pressure drop values. Predicted vs. experimental pressure drop for the three correlations is shown for this data set in Figure 4.12 below. The calculated MAE values for

each correlation are given in Table 4.10, which indicates that the Kim and Mudawar (2012) correlation is best for use with this data set.

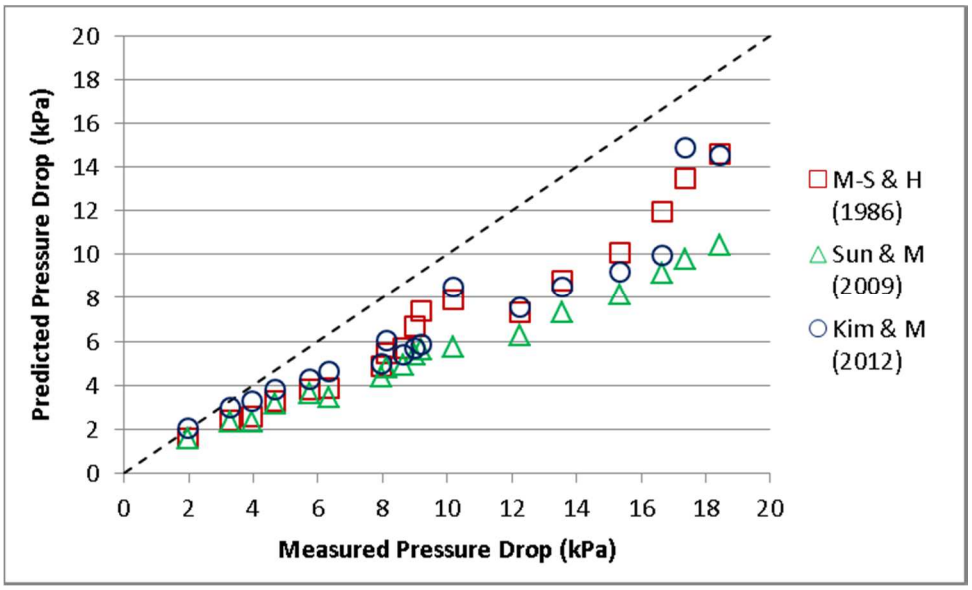

Figure 4.12 – Comparison of the three chosen frictional pressure drop correlations with R410A data from Wang et al. (2001)

Table 4.10 – Values of MAE and bias for R410A data from Wang et al. (2005)

Correlation	MAE (%)	Bias (%)
Müller-Steinhagen and Heck	30.0	30.0
Sun and Mishima	40.5	40.5
Kim and Mudawar	26.8	26.5

R410A OVERALL

From the two previous sections dealing with R410A validation, it should be noticed that all three correlations over predict one data set, while all three under predict the other. This indicates that the predictability of R410 pressure drop data is most likely highly dependent on the flow conditions, especially mass flux. In order to really understand the reasons for this difference,

more validation should be performed. Additional validation was not performed for this research, however, because of the difficulty in finding frictional pressure drop data for R410A where all necessary inlet conditions are supplied. A choice of correlation for R410A data was therefore made based on the validation using the two sources above. As for the R134a, overall MAE values were calculated and tabulated, and they are presented in Table 4.8 below. The lowest overall MAE is for the Kim and Mudawar (2012) correlation, so it was selected for use with R410A data. Since the Kim and Mudawar (2012) correlation was determined through the author's validation to be best for both R134a and R410A data, it is used for all the remainder of the simulations studies presented in this thesis.

Table 4.11 – Values of MAE and bias for all R410A literature data

Correlation	MAE (%)	Bias (%)
Müller-Steinhagen and Heck	44.2	4.2
Sun and Mishima	47.5	-6.5
Kim and Mudawar	42.0	6.5

DATA FOR OVERALL MICROCHANNEL CONDENSERS

The next step the author wanted to take was to validate each of these three pressure drop correlations using R410A or R134a data from open literature for overall microchannel condensers. The author was having difficulty finding any usable data, so decided to perform a very detailed literature search for applicable papers. The author performed four searches in Engineering Village; the first two were broad, with the first only specifying "microchannel" and "condensation" as key words, and the second using the original two and adding "refrigerant". The first search received 669 hits, but the second only 149. The third and fourth searches used the three words from the second but added "R410A" and "R134a", respectively. The third search received a mere thirteen hits, while the fourth received 48. For each search, papers that looked

like they may have usable data were chosen and saved (though for the first search, the author only looked at the first 100 hits or so). From this search, no data was found that could be used for this research, so the author was not able to validate the model with overall condenser data from the literature. The author compiled a list of key papers that were a result of the search as well as notes explaining why each was not used in this research; this list can be found in Table A.1 of the Appendix.

4.2.4 Hydraulic Diameter Sensitivity Analysis

The next step to take after determining which frictional pressure drop correlation should perform well for the data in Yatim et al. (2016) was to rerun simulations for that data with the new correlation, Kim and Mudawar (2012), and see if the pressure drop predictions were improved. Once again, simulations were run only for the cases without oil circulating in the system. It was seen from the literature search that this correlation performs well for R410A and R134a but there is no information given on how it would perform for refrigerant-oil mixtures. Thus it is important to make sure it is working properly for pure refrigerant before adding in oil properties. Figures 4.13 and 4.14 below give predicted pressure drop vs. experimental pressure drop for the pure refrigerant data for R134a and R410A, respectively. As can be seen from these plots, pressure drop predictions become worse after implementing the new correlation. It is certain based on the literature search, however, that the previous correlation in the code performs worse for refrigerants than the new one does. This means that there is some aspect of pressure drop that is not captured correctly in the model for the data in Yatim et al. (2016). Since both refrigerants are now under predicted, it is possible that the original assumption of channel hydraulic diameter of 1.4 mm for the condenser used in their study is incorrect. The author therefore decided to perform a hydraulic diameter sensitivity analysis to find out how much the hydraulic diameter would need to be reduced in order to get good pressure drop predictions for both refrigerants.

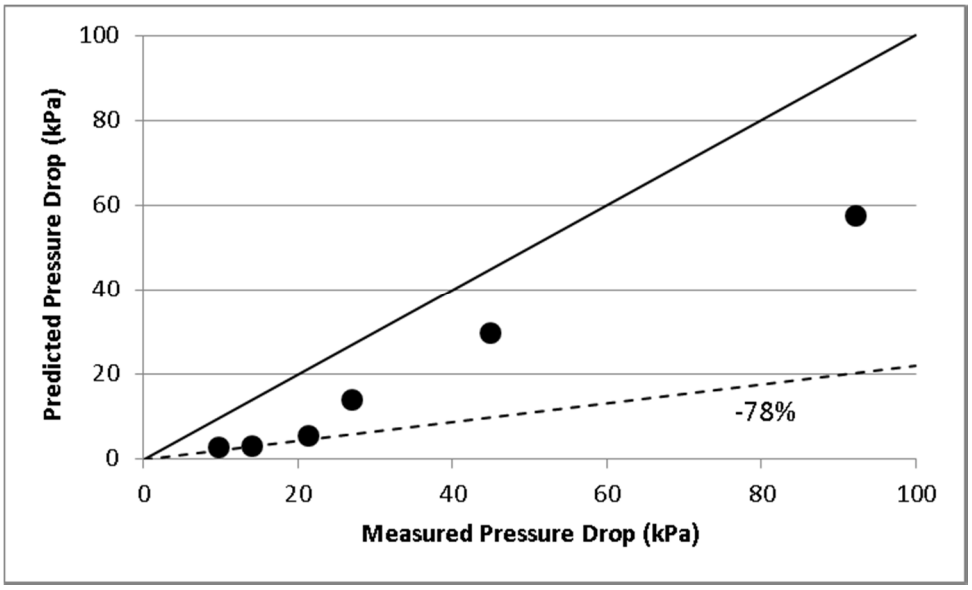

Figure 4.13 – Predicted vs. measured pressure drop for R134a data without oil using the Kim and Mudawar (2012) correlation

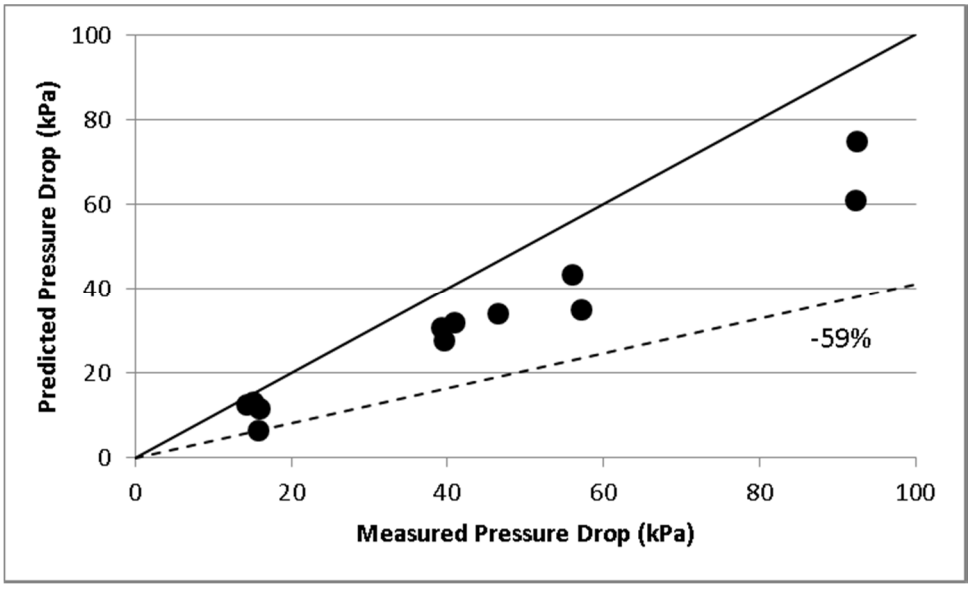

Figure 4.14 – Predicted vs. measured pressure drop for R410A data without oil using the Kim and Mudawar (2012) correlation

In order to see how pressure drop predictions would respond to a decrease in hydraulic diameter, simulations for all cases of both refrigerants without oil were run for various values of

this parameter. Hydraulic diameters were chosen in decreasing increments of 0.1 mm; 1.4 mm is the first assumption, and 1.3 mm, 1.2 mm, and 1.1 mm were also tested. Figures 4.15 and 4.16 below show predicted vs. experimental pressure drop for all four diameters for R134a and R410A, respectively. In order to evaluate which hydraulic diameter fits the data best, the MAE values were calculated for each hydraulic diameter for both refrigerants. These are given in Tables 4.9 and 4.10. For R134a, the lowest MAE occurs for the hydraulic diameter of 1.2 mm, and it increases by at least 10% as hydraulic diameter increases to 1.3 mm or decreases to 1.1 mm. For R410A, however, MAE is lowest for the hydraulic diameter of 1.3 mm. It is much higher for 1.4 mm and higher still for 1.1 mm, but it only increases slightly for 1.2 mm. Based on the two tables together, it seems that 1.2 mm is the mostly likely value of actual channel hydraulic diameter for the condenser in the Yatim et al. (2016) study. Therefore, this value will be used for all further simulations involving this data.

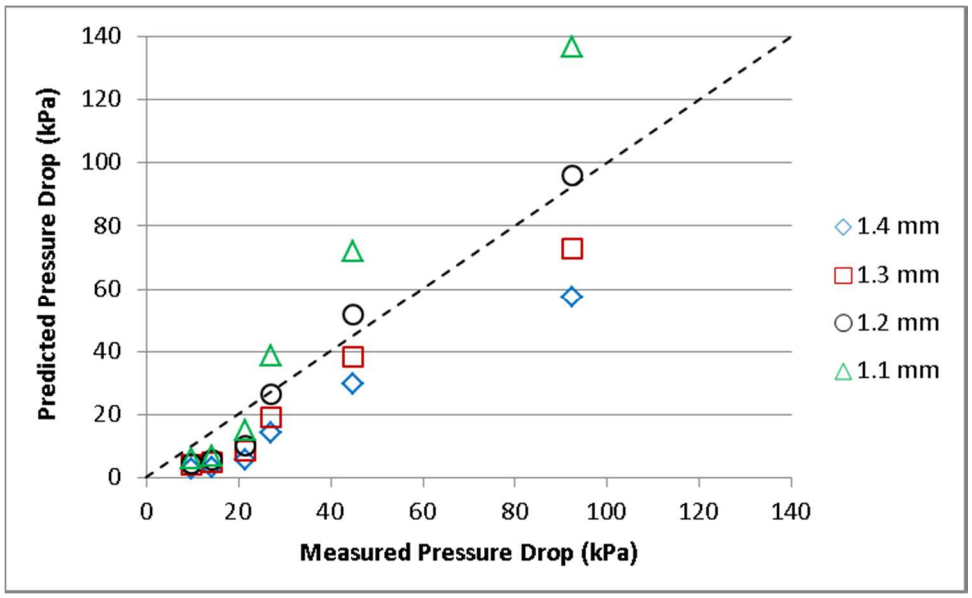

Figure 4.15 – Predicted vs. measured pressure drop for R134a data without oil at various values of hydraulic diameter

Table 4.12 – Values of MAE for R134a data at various hydraulic diameters

D_h (mm)	MAE (%)
1.4	57.314
1.3	41.819
1.2	31.522
1.1	44.956

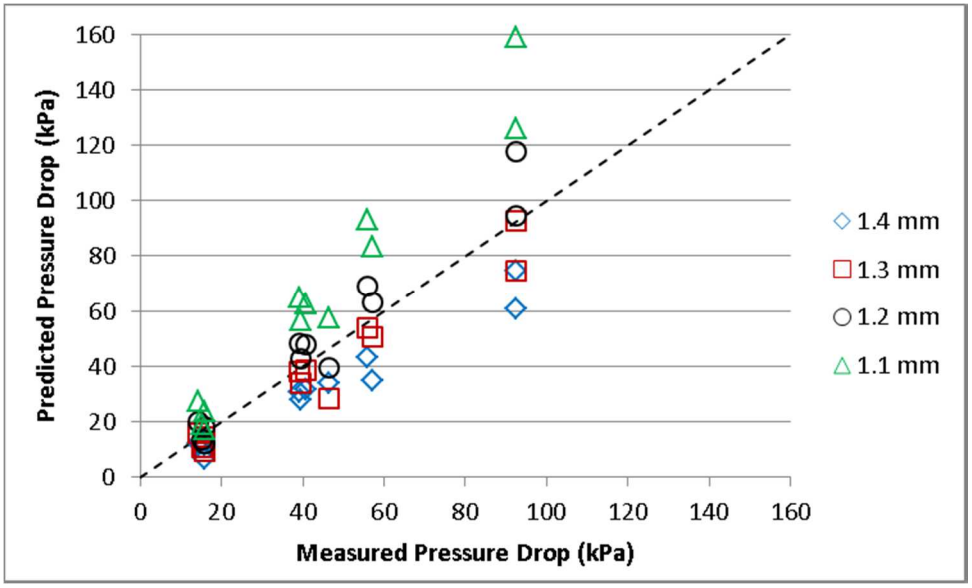

Figure 4.16 – Predicted vs. measured pressure drop for R410A data without oil at various values of hydraulic diameter

Table 4.13 – Values of MAE for R410A data at various hydraulic diameters

D_h (mm)	MAE (%)
1.4	27.658
1.3	15.733
1.2	17.894
1.1	48.338

4.2.5 Pressure Drop Predictions for the Final Version of the Model

The major changes to the pressure drop model are those detailed above: the pressure drop correlation was changed from Mishima and Hibiki (1996) to Kim and Mudawar (2012), and hydraulic diameter used with the data from Yatim et al. (2016) was changed from 1.4 mm to 1.2 mm. Other minor changes were made along the way, such as adding components to header pressure drop; these changes did not significantly improve or degrade pressure drop predictions, however, so they were not given space in the chapter for model validation. The pressure drop predictions for the Yatim et al. (2016) data using the final version of the model are given in Figures 4.17 and 4.18 for R134a and R410A, respectively. From these two figures, it can be seen that the pressure drop is improved for both refrigerants, though most significantly for the R134a data, and that the model can capture the overall trends of both. It can also be seen, however, that there are still some sizeable errors in the predictions for both refrigerants. This must be due to the fact that instead of a single tube, an entire condenser is being modeled. The geometry is complex, and the internal geometry of the headers in the microchannel condenser used in this study is unknown. Because of the validation studies performed above, there is now confidence in the pressure drop correlations used in the model, and confidence that it performs correctly for these two refrigerants flowing through single tubes, but there is still work to be done. Future work should focus on modeling the minor losses associated with pressure drop for an entire condenser to see if improving this aspect of the model would enable it to provide more improved predictions for overall pressure drop.

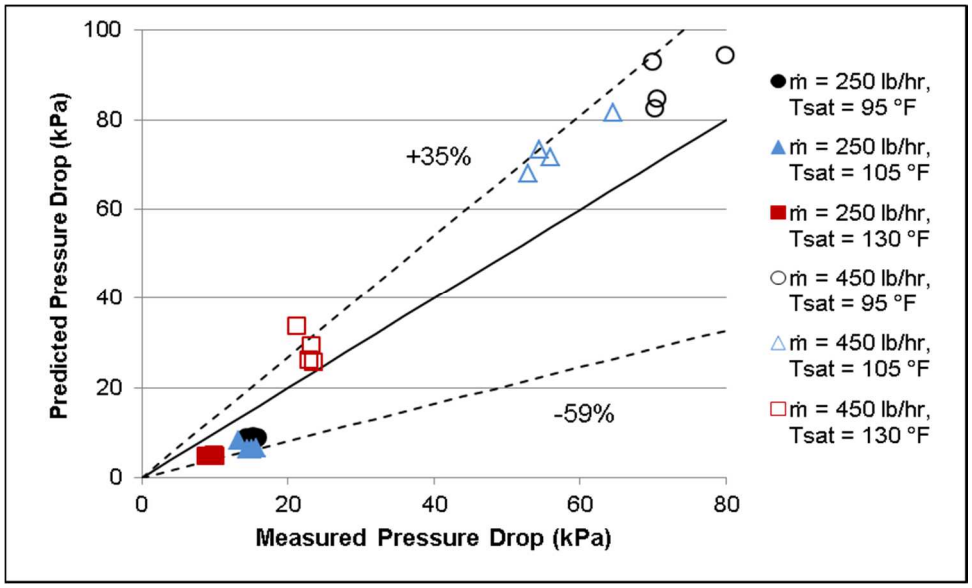

Figure 4.17 – Predicted vs. measured pressure drop for all R134a data using the final version of the model

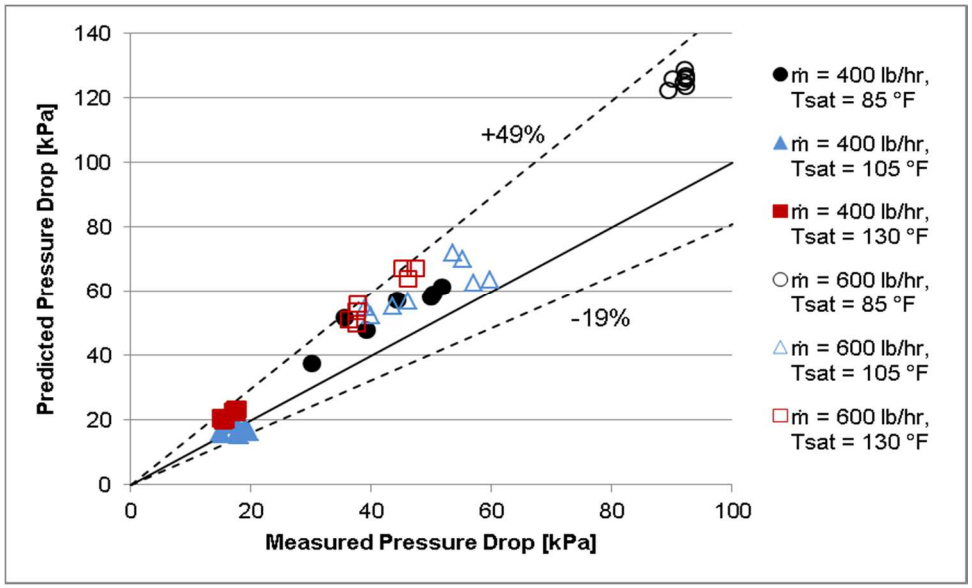

Figure 4.18 – Predicted vs. measured pressure drop for all R410a data using the final version of the model

CHAPTER V

RESULTS AND DISCUSSION FOR THE OIL RETENTION MODEL

This chapter will discuss the results of the oil retention portion of the microchannel condenser model when used with the data from Yatim et al (2016). It will identify where the model excels and where it performs poorly, and what can be learned from it about the behavior of refrigerant-oil mixtures in microchannel condensers. It will discuss the model's predictive ability and what can be learned about the system based on the model's predictions.

5.1 Oil Retention Model Predictions

The first step the author took when investigating oil retention in the microchannel condenser was to use the model to predict the data from Yatim et al. (2016). In this model, it is assumed that the lubricant is completely miscible with the liquid refrigerant and thus, it is well mixed and carried along with the liquid refrigerant through the condenser. The amount of oil is obtained from the mass of the liquid phase multiplied by the local oil mass fraction. Oil retention is calculated for all portions of the condenser, including the inlet and outlet tubes, the inlet, outlet, and intermediate headers, and the microchannels. This model does not compute the oil in the condenser that may be held up in internal traps of the refrigerant circuitry and not in circulation during steady state conditions. An example of these traps are the regions formed by the microchannel tube protrusions inside he header as well as the bottom side of the inlet vertical header of the microchannel type condenser, where the internal baffles are located. Figures 5.1,

5.2, and 5.3 show predicted vs. measured mass of oil retained in the condenser for R410A with low degree of superheat, R410A with high degree of superheat, and R134a, respectively

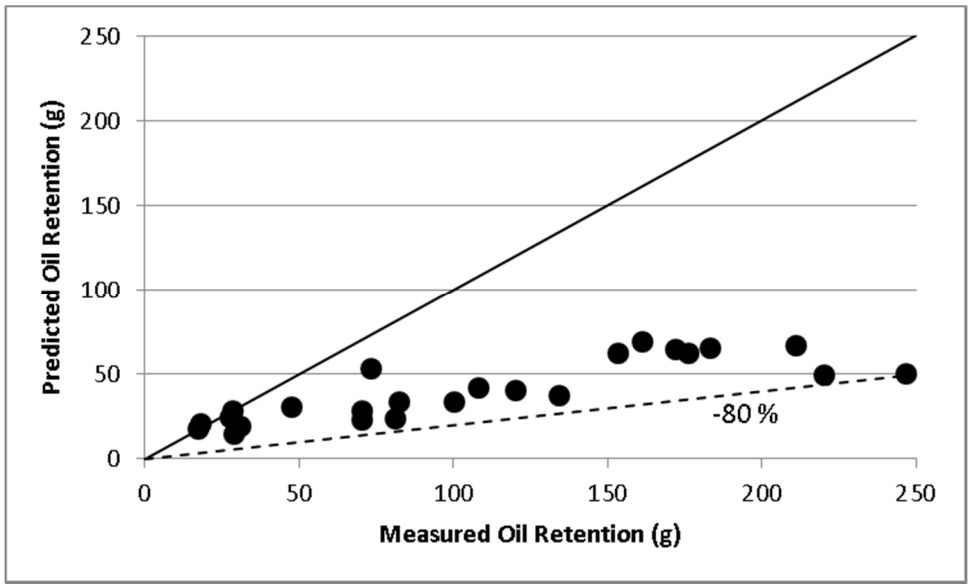

Figure 5.1 – Predicted vs. measured oil retention for R410A with low degree of superheat

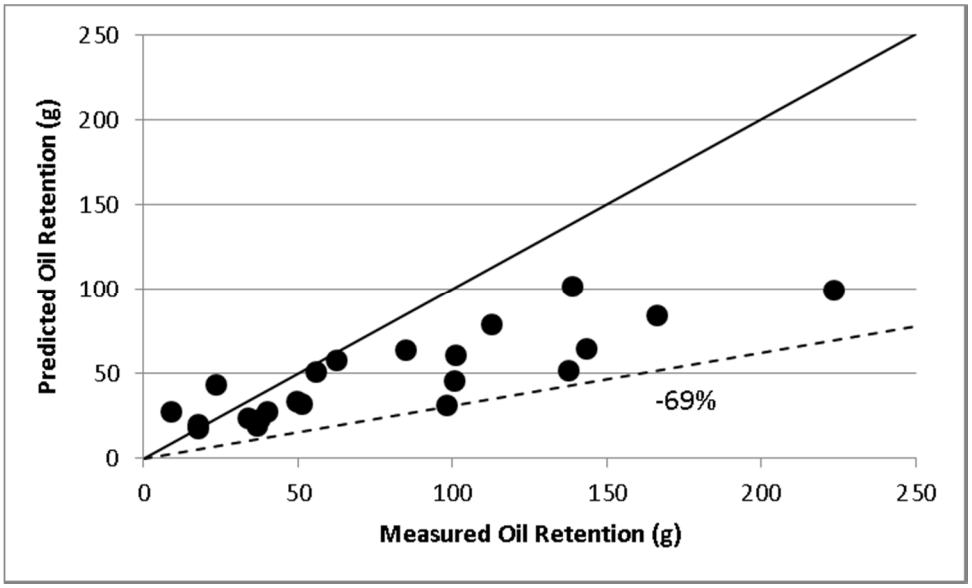

Figure 5.2 – Predicted vs. measured oil retention for R410A with high degree of superheat

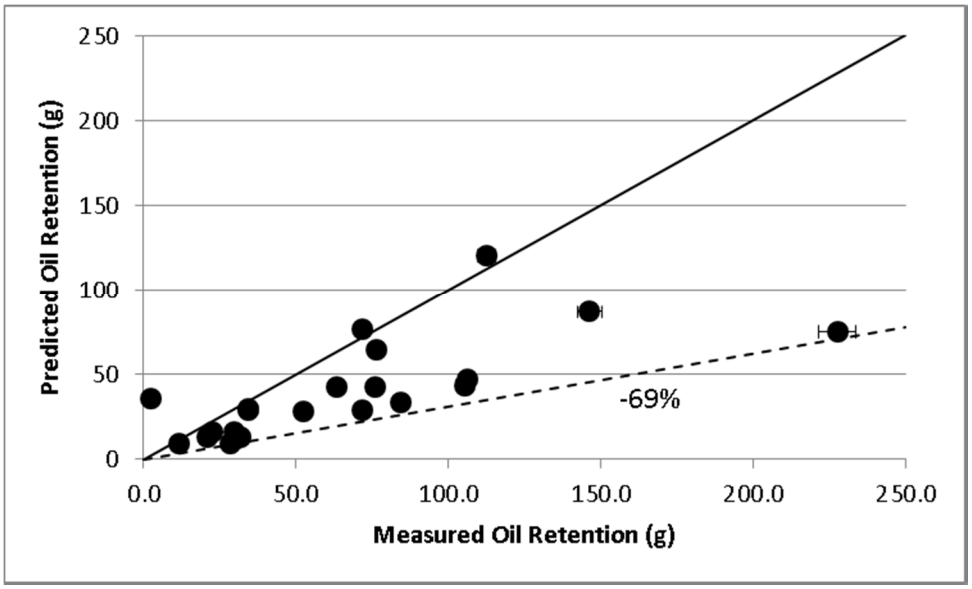

Figure 5.3 – Predicted vs. measured oil retention for R134a

As can be seen from Figures 5.1, 5.2, and 5.3, the experimental data is mostly underpredicted for all three cases, though it is worst for R410A with low degree of superheat and slightly better for R410A with high degree of superheat and R134a. There are three possible reasons for why the predicted values are lower than the experimental values. First, it is possible that something is missing in the calculation of refrigerant mass, and that there should be more liquid (and therefore more oil) than is currently being predicted. Second, there may be oil trapped somewhere within the condenser due to fluid flow conditions or condenser geometry; a model that only calculates mass of oil carried by the refrigerant through the condenser cannot predict the presence of trapped oil. Third, it is possible that there is a large enough uncertainty in the measurement of the oil retention to cause an improvement in the predictions. This third reason was investigated, and it was found to not significantly alter the results. According to Yatim et al. (2016), the uncertainty on the measurement of oil retention volume is only 2.7%. Error bars are present in Figure 5.3 to reflect this uncertainty. Error bars were omitted in Figures 5.1 and 5.2 because they would yield very similar results. As can be seen, the error is small as to not even be visible for most of the data points, which shows that experimental uncertainty is not a significant cause of the model's

underpredictions. The following sections investigate the first and second reasons for the difference between predicted and measured oil retention mass.

5.2 Oil Difference Fills Inlet Header

A first assumption made by the author is that all oil in the condenser that is not dissolved in the liquid refrigerant is trapped in the inlet header. This assumption is made because in the tests performed by Yatim et al. (2016), the refrigerant is always superheated when it enters the condenser. Superheated refrigerant vapor cannot dissolve any oil, and thus has difficulty carrying it through the condenser, especially through complex geometry such as contractions for the channel inlets. It is expected that in the superheated regions of the condenser oil may form a film around the inside wall, sink to the bottom of the header because of gravitational effects coupled with downward fluid flow, and become trapped within pockets in the condenser, primarily in the inlet header. It is a possibility that oil completely fills some of the tubes at the bottom of the first pass, but this is not likely since there is no serious degradation of pressure drop with the addition of oil, which is what would be expected if the available flow area was reduced in this way.

For these reasons, the author decided to calculate how much of the inlet header would need to be filled with oil in order to make up the difference between the predicted and experimental oil retention masses for the data points where the model underpredicts the measured oil retention, and decide if this is a reasonable assumption. Figures 5.4, 5.5, and 5.6 show the volume percentage of the inlet header that must be filled with oil for R410A with low degree of superheat, R410A with high degree of superheat, and R134a, respectively. The mass of oil used to calculate these percentages includes the oil predicted to be in the header as well as the mass of oil required to make up the difference between the predicted and measured oil retention values.

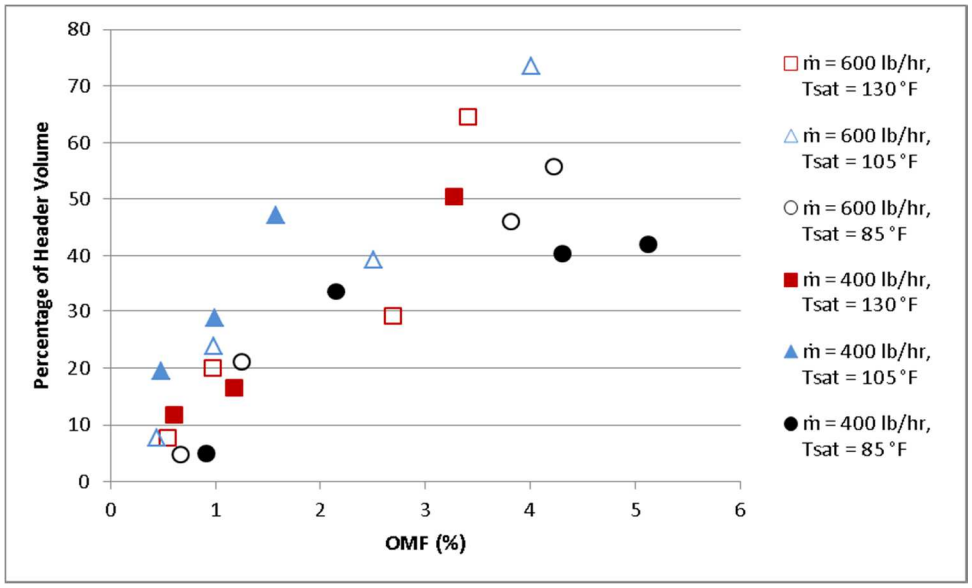

Figure 5.4 – Percentage of inlet header that must be filled with oil for R410A with low degree of superheat

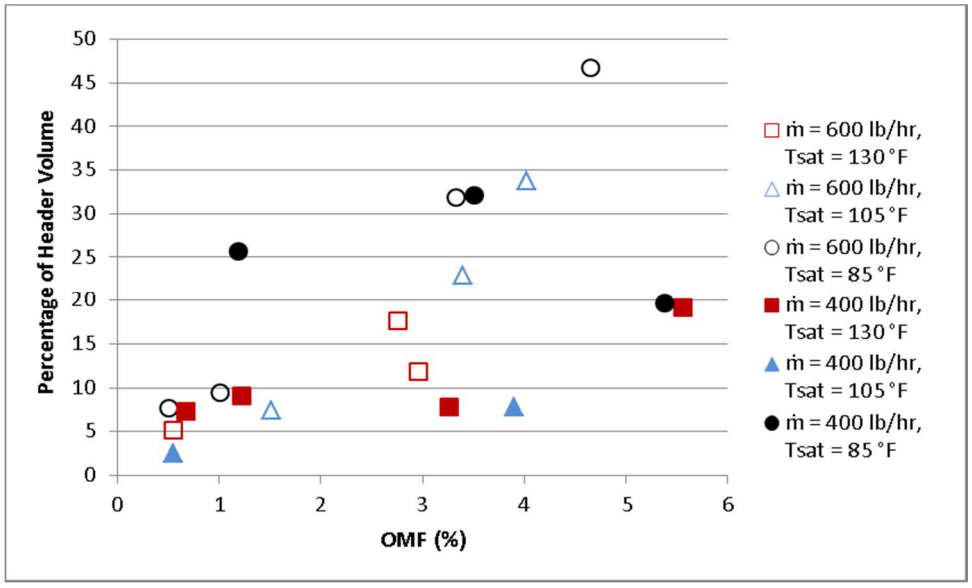

Figure 5.5 – Percentage of inlet header that must be filled with oil for R410A with high degree of superheat

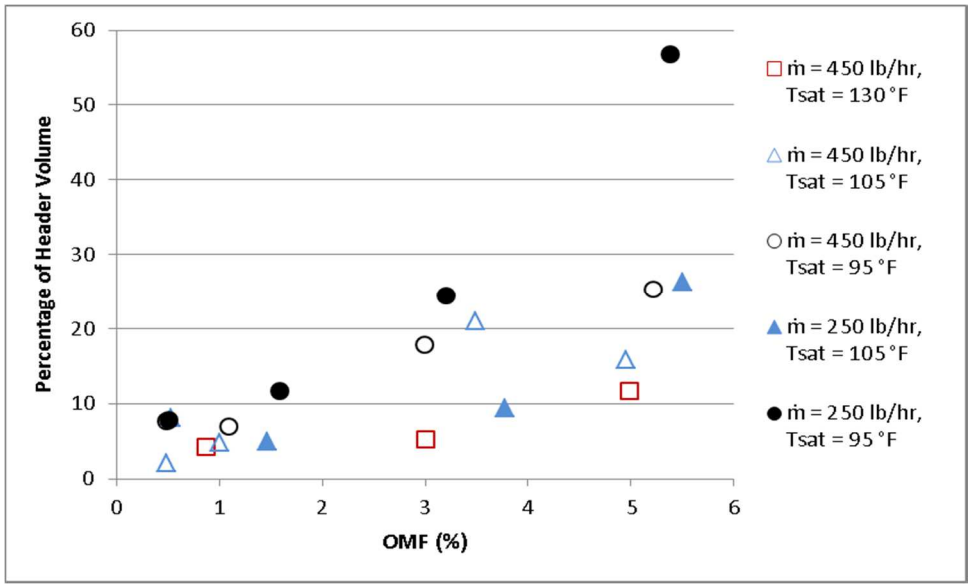

Figure 5.6 – Percentage of inlet header that must be filled with oil for R134a

In the figures above, it can be seen that R410A with high degree of superheat requires the largest inlet header volume to be filled with oil, and R134a requires the smallest (except for the one point above 30%). For the R410A with low degree of superheat, the maximum percentage is between 70 % and 80 %; it does not seem possible that this much of the header could be filled with oil since then there would not be room for the refrigerant that passes through the condenser. Because of the results shown in these figures, the author decided to investigate other places for oil to be trapped in the condenser as well as possible sources of error in the calculations of oil retention.

5.3 Oil Film in Inlet Header and Tubes

This portion of the chapter investigates the possibility that some of the extra oil which appears in the experimental data but not the simulation results could exist as an extra oil film on the inner walls of the condenser. Two methods are considered. First, it is assumed that there is an oil film on the inner wall of the inlet header whose thickness is dependent on the oil mass fraction, and a different maximum allowed thickness is selected to best fit R410A with low

degree of superheat, R410A with high degree of superheat, and R134a. Second, a data point where pressure drop is under predicted by the model is considered, and channel hydraulic diameter is decreased until the predicted pressure drop matches the experimental pressure drop. It is then assumed that the difference in hydraulic diameter is the thickness of an oil film covering the inside walls of the ports. The following sections provide an analysis of these two methods and their results.

5.3.1 Constant Oil Film around Inlet Header and Superheated Tube Segments

For this analysis, the author assumed that an oil film exists on the inner wall of the inlet header that accounts for the predicted oil retention in the header as well as the oil needed to make up the difference between predicted and measured values. Furthermore, it is assumed that this oil film has a certain maximum thickness when oil mass fraction is equal to 5%, and that this thickness varies linearly with oil mass fraction as it increases from 0% to 5%. It is not expected that this same oil film exists in the two-phase or subcooled tube segments because the presence of liquid refrigerant will help to wash away the oil film. There will probably some oil film in the two-phase segments with small amounts of liquid, but it should not be as thick as for the superheated portions. For this analysis, the ratio of film thickness to hydraulic diameter, δ/D, was kept constant. A maximum value of δ/D was chosen by minimizing the root mean squared error of the sum of the differences in oil retention volume between the predicted and measured values. For this analysis, δ is calculated using the method outlined in Section 3.7.2 of this thesis. A different maximum value of δ/D was selected for R410A with low degree of superheat, R410A with high degree of superheat, and R134a. This was done because it can be seen from Figures 5.1, 5.2, and 5.3 that oil retention behaves differently for these three fluid conditions, so it cannot be assumed that they would all need the same maximum oil thickness. It was determined that the best values of maximum δ/D are 0.163 for R410A with low degree of superheat, 0.069 for R410A with high degree of superheat, and 0.053 for R134a. Figures 5.7, 5.8, and 5.9 show predicted vs.

measured oil retention when these values of δ/D are used to calculate oil mass in the film on the wall of the inlet header.

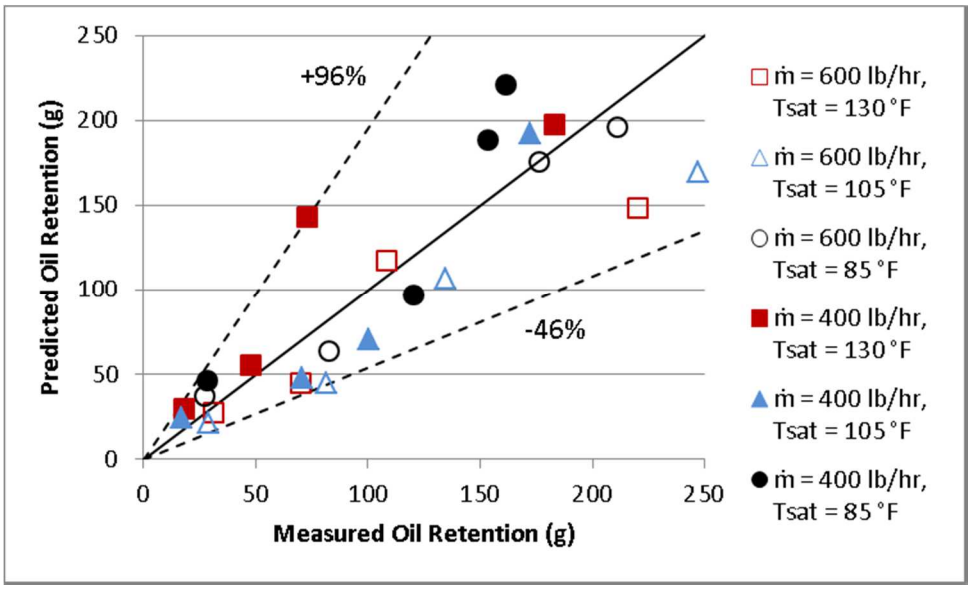

Figure 5.7 – Predicted vs. measured oil retention for R410A with low degree of superheat, δ/D = 0.163

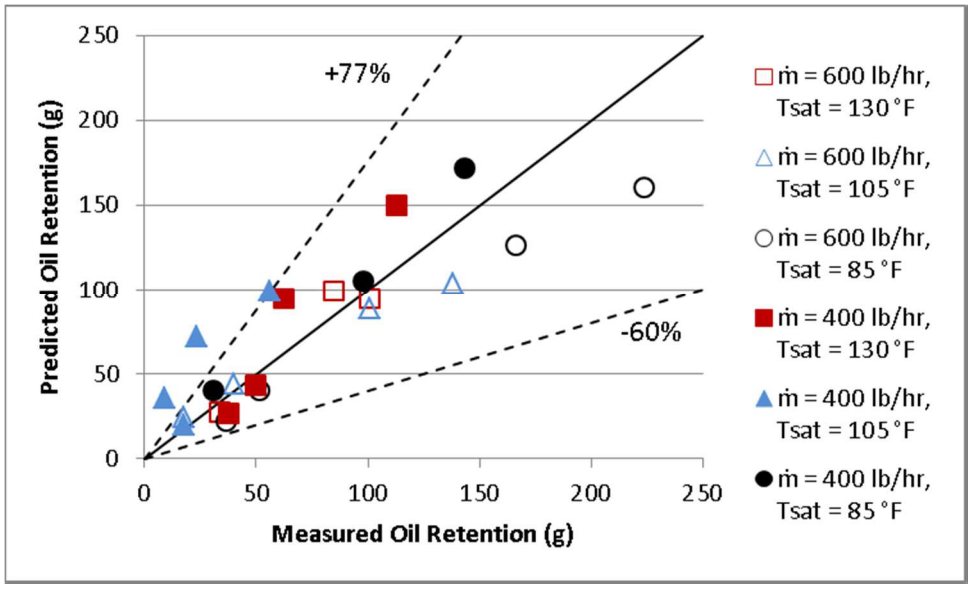

Figure 5.8 – Predicted vs. measured oil retention for R410A with high degree of superheat,

δ/D = 0.069

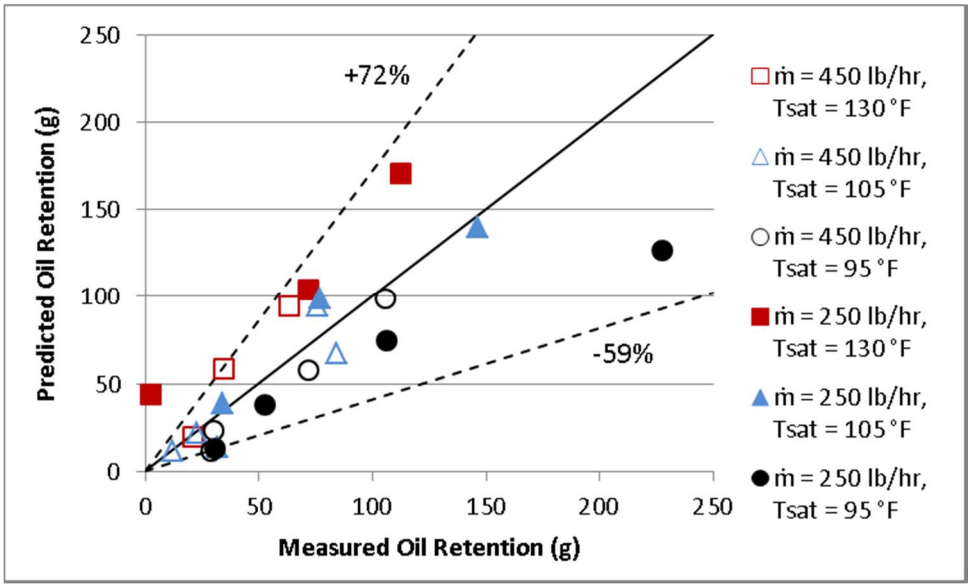

Figure 5.9 – Predicted vs. measured oil retention for R134a, δ/D = 0.053

As can be seen from the above figures, δ/D is highest for R410A with low degree of superheat, less for R410A with high degree of superheat, and least for R134. This may be due in part to the velocities of the different refrigerants in the inlet tube and header, and therefore the ability of each to carry oil through the superheated portions of the condenser. In general, R410A density is larger than R134a density, so vapor velocity of R134a should be higher, resulting in a greater ability to carry oil and thus a smaller required δ/D. Similarly, vapor density is lower for R410A with high degree of superheat than for R410A with low degree of superheat, so it should also have greater velocity and smaller δ/D. Therefore, the relative values of δ/D obtained for this analysis are physically reasonable with regard to vapor velocity.

Based on Figures 5.7, 5.8, and 5.9, assuming an oil film as outlined above is not a very good way to estimate oil retention in microchannels. For all three cases, this method over predicts oil retention by 72% to 96%, and under predicts it by 46 % to 60 %. It does not predict oil

retention with enough consistency for the author to assume that this is what is going on in the condenser, so this method is not included as part of the oil retention model.

5.3.2 Oil Film Added to Match Pressure Drop

As a further investigation, the author decided to determine how thick an oil film on the walls of the microchannels would need to be in order to match predicted pressure drop with measured pressure drop. In order to do this, two R134a data points where predicted pressure drop is much less than measured pressure drop were chosen, one for low oil mass fraction and one for high oil mass fraction. For each data point, hydraulic diameter was decreased incrementally and simulations were run for each value until the pressure drop predicted by the model increased enough to equal the measured pressure drop. It was then assumed that the necessary decrease in hydraulic diameter was due to an oil film covering the superheated portions of the microchannels; thus volume and the resulting mass of this assumed oil film could be calculated. This oil film is in addition to the oil mass already predicted by the model for these segments of the microchannels. The author calculated the mass of this new film, added it to the calculated mass of oil dissolved in the liquid refrigerant, and calculated the new percentage of header volume that must be filled with oil to match experimental values for each of these two points. The results of this analysis are presented in Table 5.1.

Table 5.1 – Results of hydraulic diameter reduction analysis

Oil Mass Fraction (%)	Predicted ΔP (kPa)	Measured ΔP (kPa)	New D_h (mm)	Original Header Volume to be Filled (%)	New Header Volume to be Filled (%)
1.6	9.25	15.17	1.057	11.7	10.9
5.4	8.68	15.74	1.025	56.8	56.8

As shown in the table above, when hydraulic diameter is reduced so that predicted pressure drop matches experimental pressure drop, the percentage of header volume that must be filled with oil to make up the difference between predicted and experimental oil retention only

decreases by about 1% for the first data point, and does not decrease at all for the second data point. It does not decrease for the second point because the mass of oil calculated for this portion of the microchannels is already sufficient to form a thick enough oil film to make up for the difference in predicted and measured pressure drop. Based on this analysis, it can be determined that assuming a value for oil film thickness that makes sense with the pressure drop data does not result in a significant change in oil retention predictions, or header filling requirements. Assuming a thicker oil film would help reduce the required header volume to a more reasonable amount, but then pressure drop would be very much over predicted.

5.3.3 Sensitivity of Oil Retention Predictions to Changing Refrigerant Mass

As concluded in the previous sections, assuming oil films on the microchannels cannot account for much of the difference between predicted and experimental oil mass. Because of this, the author decided there was a possibility that the model incorrectly calculates liquid mass, and as a result incorrectly predicts oil retention. The author decided to investigate the sensitivity of oil retention predictions to varying liquid mass to see if this could be a legitimate source of error. This was done using three different methods of analysis: a "mass factor" analysis, a mass approximation analysis, and a void fraction sensitivity analysis. These three methods and their results are all presented below.

REFRIGERANT SOLUBILITY: CHANGE OF REFRIGERANT MASS

With this analysis, the author simply wanted to determine if increasing the amount of total mass in the condenser by up to 50 % would significantly improve the oil retention predictions. If so, it would mean that there is most likely an error in the way the model calculates total mass. For this analysis, the author implemented a factor in the code simply referred to as the "mass factor." The mass factor is a number multiplied by both the calculated refrigerant vapor

and liquid masses. If the factor is equal to one, the values of both masses are the regular values the program calculates. Changing this factor only changes the amount of total mass in a segment; it does not change the ratio of liquid to vapor mass, so it does not affect flow quality. The data point that was chosen for use in this analysis is the point in the R410A with low degree of superheat set that requires the highest percentage of header volume to be filled with oil. It has an oil mass fraction of 4.0%. Table 5.2 below gives the results of this analysis when the mass factor is equal to 1, 1.25, and 1.5.

Table 5.2 – Results of the Mass Factor Analysis when Oil Mass Fraction is 4.0 %

Mass Factor	Predicted Oil Mass (g)	Measured Oil Mass (g)	Header Volume to be Filled (%)
1	50.264	246.9	73.6
1.25	63.066	246.9	71.8
1.5	75.901	246.9	70.1

From Table 5.2 above, it can be seen that even when refrigerant mass is increased by 50 %, oil retention does not increase much and the percentage of the inlet header volume that must be filled with oil only decreases by three and one-half percent. Because of this, it can be concluded that even if the total mass calculations are off by up to 50 %, it should not affect the oil retention results enough to bring the required header volume down to a more reasonable value.

MASS APPROXIMATION ANALYSIS

The next step the author took was to perform another check to see if the model calculates liquid refrigerant and oil masses correctly. For this analysis, the condenser was broken into segments, and the volume was calculated for each, along with the percentage of the total volume that each occupies. Then, using the calculated volume for each segment as well as the corresponding specific volumes and quality that are outputs of the simulations, liquid refrigerant

masses for each segment were found by solving the system of equations given in Equations 5.1 and 5.2 below.

$$m_{liq} = \frac{m_{vap}}{x} - m_{vap} \tag{5.1}$$

$$Volume = m_{liq} v_{liq} + m_{vap} v_{vap} \tag{5.2}$$

Note that the average quality used for the microchannel tubes is a weighted average based on the inlet and outlet qualities of both passes; this quality is an approximation, not an exact value. Once the liquid refrigerant mass is found, it can be multiplied by the oil mass fraction to get an approximate value of oil dissolved in the liquid refrigerant. The oil mass found using this method should not be taken as an exact value, but as an order of magnitude analysis to double-check that there is no serious error in the model's mass calculations. The results of this analysis for two different data points, with oil mass fractions of 0.98 % and 4.0 %, are given below in Tables 5.3 and 5.4.

As can be seen from the tables, the approximate values of oil dissolved in refrigerant are on the same order of magnitude as the values predicted by the model, so it is concluded that there are no major errors in the way that the model calculates mass. It can also be seen, however, that the approximate values are almost twice the predicted values. This could be due to the fact that the flow quality used for the microchannel tubes is an approximation and not exact. It could also be due to that fact that void fraction is used to calculate vapor and liquid masses in the model but is not considered in this approximation, or that the void fraction correlation implemented in the model for mass calculations is not a good fit for these conditions. The following section investigates void fraction and its effect on oil retention predictions.

Table 5.3 – Results of the mass approximation analysis for R410A with low degree of superheat and an oil mass fraction of 0.98 %

Segment	Volume (dm^3)	Volume (%)	Liquid Mass (g)	Dissolved Oil Mass (g)
Inlet Line	0.0528	1.82	0	0
Inlet Header (x = 1)	0.3438	11.82	0	0
Intermediate Header (x = 0.502)	0.5027	17.29	49.9	0.49
Outlet Header (x = 0.276)	0.1594	5.48	36.0	0.35
Microchannel Tubes	1.8381	63.21	112.6	1.10
Outlet Line	0.0109	0.37	2.5	0.02
Total	**2.9077**	**100**	**201.0**	**1.97**

Predicted Dissolved Oil Mass (g)	1.03

Experimental Oil Mass (g)	81.2

Table 5.4 – Results of the mass approximation analysis for R410A with low degree of superheat and an oil mass fraction of 4.0 %

Segment	Volume (dm^3)	Volume (%)	Liquid Mass (g)	Dissolved Oil Mass (g)
Inlet Line	0.0528	1.82	0	0
Inlet Header (x = 1)	0.3438	11.82	0	0
Intermediate Header (x = 0.495)	0.5027	17.29	50.2	2.01
Outlet Header (x = 0.265)	0.1594	5.48	37.6	1.50
Microchannel Tubes	1.8381	63.21	114.9	4.60
Outlet Line	0.0109	0.37	2.6	0.10
Total	**2.9077**	**100**	**205.3**	**8.21**

Predicted Dissolved Oil Mass (g)	3.96

Experimental Oil Mass (g)	246.9

VOID FRACTION SENSITIVITY ANALYSIS

In the mass approximation analysis, liquid and vapor masses are calculated using flow quality. In the model these masses are calculated using void fraction, which is a function of flow quality, but the relationship is not linear. The void fraction method of calculating mass is more correct because it takes into account the fact that the liquid and vapor phases have different velocities; simply using quality to calculate the masses is assuming that both phases travel at the same velocity. Different void fraction correlations calculate the ratio between the velocities differently, which can lead to vastly different values of void fraction, and thus total mass, for the same flow conditions. This void fraction sensitivity analysis was performed in order to see how much the oil retention predictions change as void fraction is altered. The void fraction correlations used in this investigation are those by Mandrusiak and Carey (1988), Premoli et al. (1971), and Smith (1969). The correlation by Mandrusiak and Carey was implemented in the refrigerant mass calculations portion of the model by a previous contributor, and is the one primarily used in this thesis. For this analysis, the two data points used in the mass approximation analysis above are both simulated using the three void fractions. Tables 5.5 and 5.6 presents the results of this void fraction sensitivity analysis.

Table 5.5 – Results of the void fraction sensitivity analysis for R410A with low degree of superheat and an oil mass fraction of 0.98 %

Void Fraction Correlation	Mass of Liquid Mixture (g)	Mass of Vapor Refrigerant (g)	Total Mass (g)	Mass of Oil (g)
Mandrusiak and Carey (1988)	72.7	300.0	372.7	23.5
Premoli et al. (1971)	439.4	387.7	827.1	23.5
Smith (1961)	519	371.9	891.9	13.4

Table 5.6 – Results of the void fraction sensitivity analysis for R410A with low degree of superheat and an oil mass fraction of 4.0 %

Void Fraction Correlation	Mass of Liquid Mixture (g)	Mass of Vapor Refrigerant (g)	Total Mass (g)	Mass of Oil (g)
Mandrusiak and Carey (1988)	122.5	298.1	420.6	50.3
Premoli et al. (1971)	508.3	379.7	888.0	87.4
Smith (1961)	559.9	373.4	933.3	54.1

As can be seen from the tables, the chosen void fraction does in fact have a relatively large effect on the mass of oil retained in the condenser. For the data point analyzed in Table 5.5, measured oil retention is 81.2 g; thus for this point, the void fraction correlation chosen does have a significant effect on oil retention predictions. For the point presented in Table 5.6, however, the measured oil retention is 246.9 g. Changing the void fraction correlation can change the predicted oil retention by over 30 g, but since the measured oil retention is so much higher this does not significantly alter the relative results; a very large percentage of the inlet header would still need to be filled with oil to make up the difference between predicted and measured oil retention. Some future work could focus on choosing the best void fraction for these flow conditions, but even a good void fraction model cannot fix the oil retention problem. Based on all the mass analyses performed above, it is clear that the discrepancy between predicted and experimental oil retention is not primarily due to errors in the calculation of refrigerant mass.

5.4 Oil Difference Fills Inlet Header and Inlet Tube

From the results of the studies performed so far in this chapter, three conclusions can be made. First, there is oil measured in the experiments from Yatim et al. (2016) that is not accounted for by the model, which calculates the amount of oil that is carried through the

condenser with the refrigerant. Second, since there is not generally a large increase in pressure drop from cases without oil to cases with oil, and since the model predicts the cases with oil well using the same hydraulic diameter as for the cases without oil, it does not make physical sense for there to be a large reduction of flow area in the microchannel tubes due to a thick oil film in the superheated portions of the tubes. This was further confirmed by the fact that the reduction in flow area necessary to account for difference between predicted and experimental pressure drop, when it is assumed that this reduction is due to an oil film, is not enough to significantly increase oil retention predictions. Third, through several different analyses it was determined that there are no major errors in fluid mass calculations in the model, and even if there were, they would not affect oil retention predictions enough to make a significant improvement in the difference between predicted and experimental masses.

From the conclusions above, the author determined that the rest of the oil measured by Yatim et al. (2016) that is not predicted by the model must be in a part of the condenser where it would not significantly impede heat transfer or increase pressure drop. This leaves the headers and the inlet and outlet tubes as likely places for oil to reside. But refrigerant always begins to condense in the top pass of the condenser, so there is liquid refrigerant in the flow by the time it reaches the intermediate header. Liquid refrigerant will mix with the oil and carry it through the condenser, essentially removing the majority of oil films on the walls of the rest of the condenser. Thus, only the inlet header and the inlet tube are left as likely to contain the bulk of the oil. Out of these two, vapor velocity will be slower in the inlet header because its diameter is larger than that of the inlet tube. Because of this, the vapor will have the most difficulty transporting the oil in the inlet header, so this is assumed to be the portion of the condenser where the extra oil resides. Figures 5.10, 5.11, and 5.12 again show the percentage of the inlet header that would need to be filled with oil in order to make up the difference between predicted and measured values. These

figures, unlike the ones before, contain solid and dashed lines to emphasize 20% and 30% of the header volume, respectively.

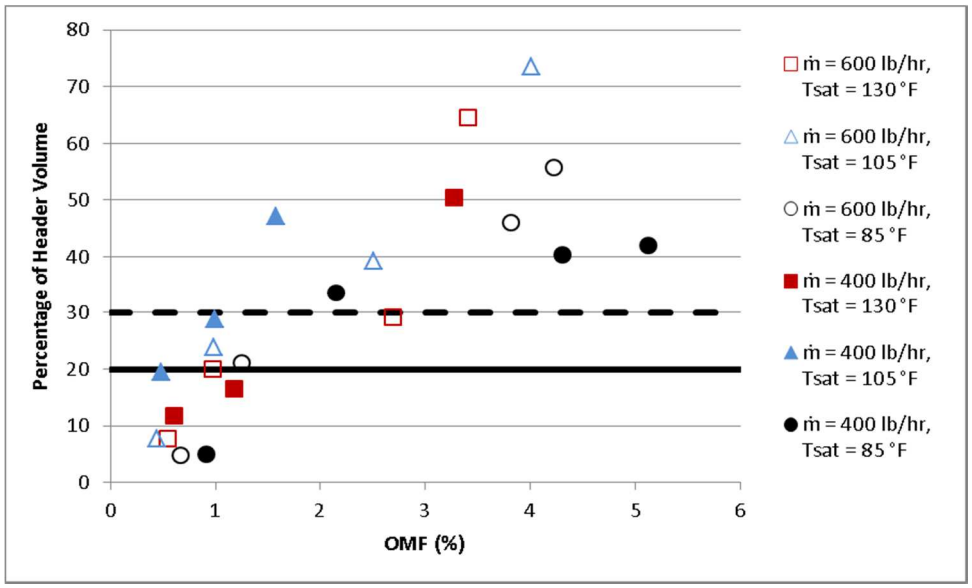

Figure 5.10 – Percentage of inlet header that must be filled with oil for R410A with low degree of superheat

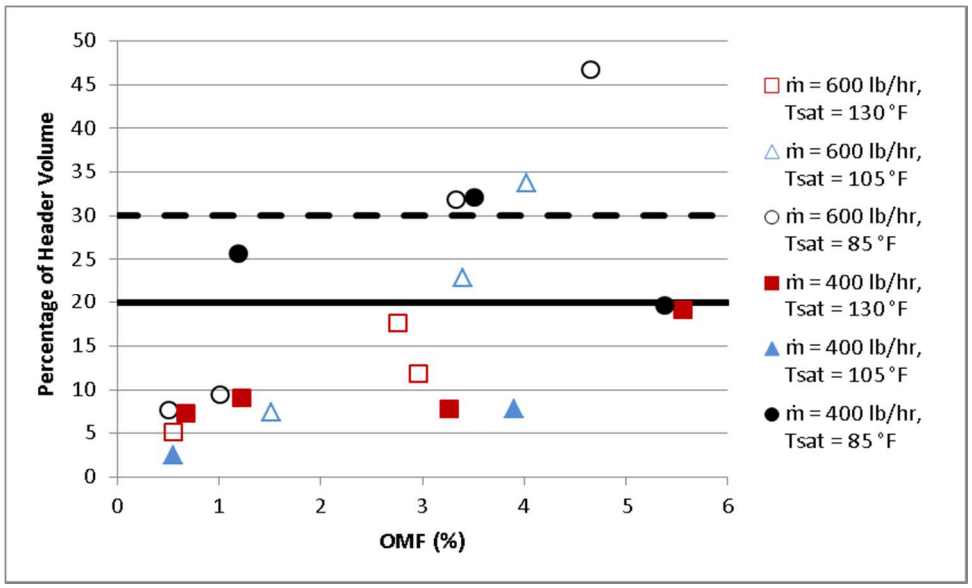

Figure 5.11 – Percentage of inlet header and that must be filled with oil for R410A with high degree of superheat

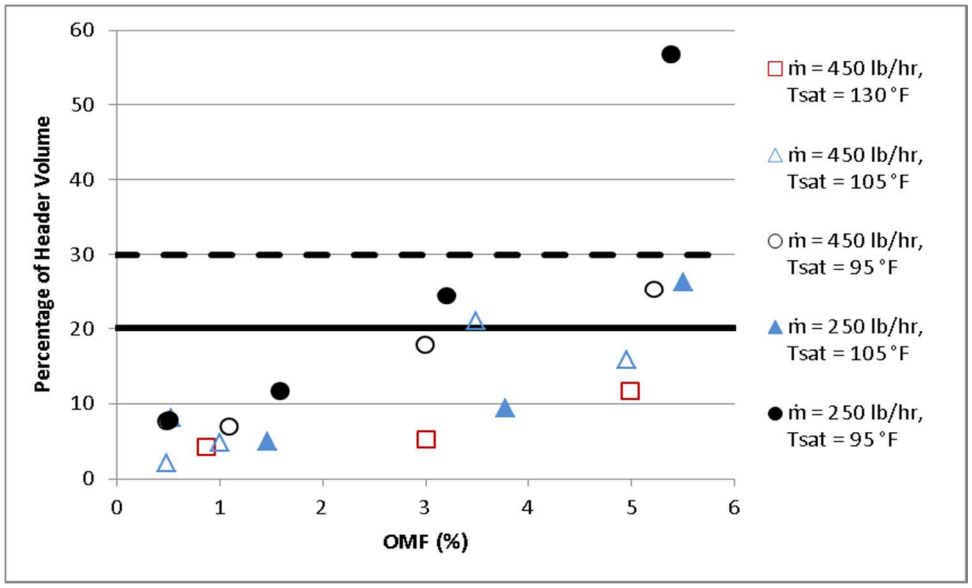

Figure 5.12 – Percentage of inlet header that must be filled with oil for R134a

In the figures above, the points under the 20% line are considered well within the realm of physical possibility, as filling the header only up to 20% full of oil would not interfere significantly with the operation of the condenser, especially if this oil exists as a film on the header wall. Points under the 30% line are also acceptable, though not as much as those under the 20% line. Those above 30% are not good, as filling the header so much with oil would definitely degrade condenser performance. Therefore, from these plots, it can be seen that the assumption that all extra oil resides in the inlet header is good for R134a, slightly worse for R410A with low degree of superheat, and not good for R410A. Thus there is still something that the model misses in the calculation of oil retention mass, especially for R410A data.

Since it can be seen from the figures that for many tests oil fills up more than 5% of the inlet header, it is logical to assume that this oil exists in the header as an oil film on the wall of the header. If it did not, and all the oil sinks to the bottom of the header, oil would block the lowest tubes in the first pass which would cause a reduction in total flow area and thus a potentially large increase in pressure drop. This phenomenon is not present in the measured oil

retention data, however, so it is a good assumption that very few tubes, if any, are blocked and that the oil exists as a film. This assumption is checked using the modified Baker's flow map utilized in Cremaschi (2004). According to this flow map the flow is annular in the inlet header, as expected. Since the flow was determined to be annular, it is helpful to present the information in Figures 5.10, 5.11, and 5.12 in the form of a dimensionless film thickness, δ/D, where δ is calculated as described in Section 3.7.2 of this thesis. This will relate the information to what is physically happening inside the header, giving more meaning to the results. The information is presented in this form in Figures 5.13, 5.14, and 5.15 below.

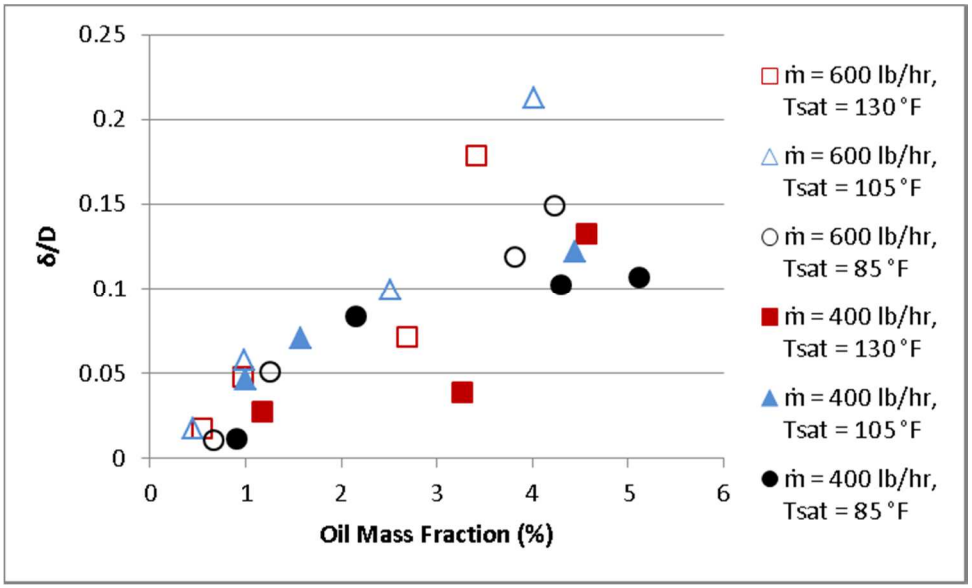

Figure 5.13 – δ/D vs. oil mass fraction for R410A with low degree of superheat

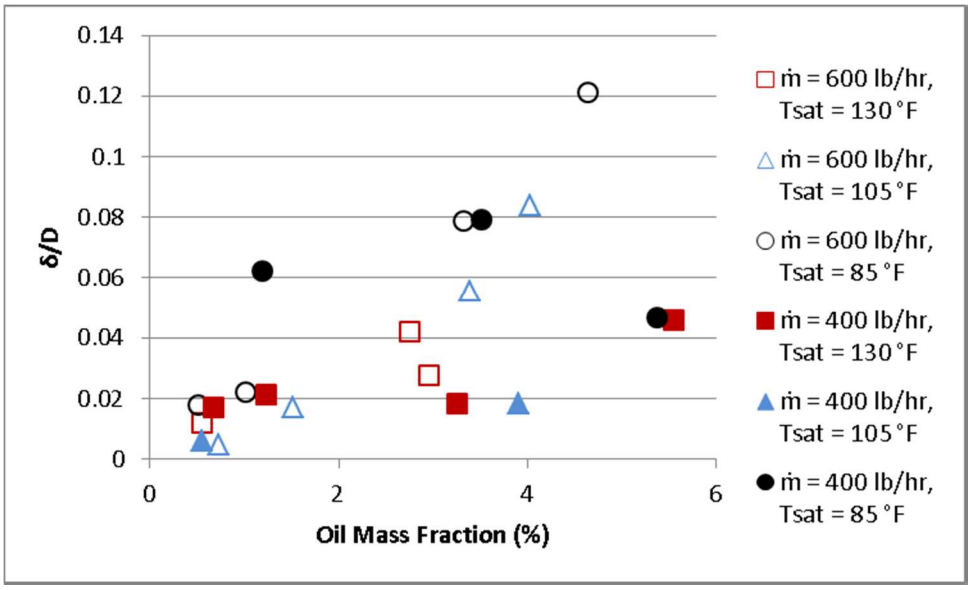

Figure 5.14 – δ/D vs. oil mass fraction for R410A with high degree of superheat

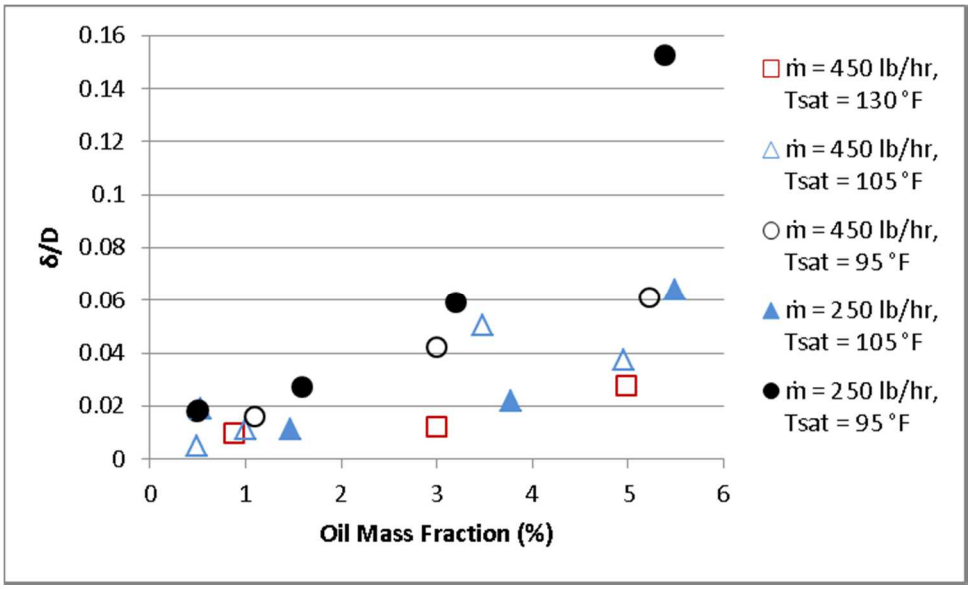

Figure 5.15 – δ/D vs. oil mass fraction for R134a

There are two primary reasons why this assumption of all extra oil residing in the inlet header works well for R134a and not as well for R410A. First, the experimental oil retained for the R134a data with high mass flow rate is much less than that retained for any of the R410A data. The predicted oil retention for these cases does not differ much from the R410A cases, but

since there is less measured oil mass the difference that needs to be made up is also less. The other reason is that for the R134a data with low mass flow rate, the refrigerant exits the condenser as a subcooled liquid; for almost all of the R410A data, the refrigerant exits as a two-phase mixture. Since the refrigerant is subcooled for a significant portion of the condenser for this R134a data, there is a high liquid mass and thus a high mass of dissolved oil. Therefore, even though measured oil mass is as high for these cases as for some of the R410A cases, the difference that needs to be made up is less. As can also be seen from the figures above, the assumption that leftover oil fills the inlet header is better for R410A with high degree of superheat than for R410A with low degree of superheat. Predicted oil mass is very similar for both cases, so this difference is simply due to the fact that experimental oil retention is higher for R410A with low degree of superheat than for R410A with high degree of superheat.

According to Yatim et al. (2016), the amount of oil retained for the R410A cases is highly dependent on mass flux, saturation temperature, miscibility, and degree of superheat. For example, if there is a high degree of superheat superficial gas velocity is high and thus the refrigerant can move oil through the condenser more easily, resulting in smaller oil retention and thus a smaller dimensionless film thickness. The oil retention model presented in this thesis is calculated using only oil mass fraction and mass of the liquid mixture, so oil retention is only dependent on mass flux, saturation temperature, miscibility, and degree of superheat insofar as they affect the void fraction correlation and the fluid mixture properties when oil is in circulation. It is uncertain how these parameters affect the oil that is trapped in the condenser.

Even though the oil retention model presented in this thesis was not able to predict the mass of oil retained in the microchannel condenser for all the operating conditions and refrigerants tested, the present study identified some key points for continuing oil retention model development in future research. The work in this thesis highlighted what the method of calculating the mass of oil in circulation is capable of, and showed that it seems to be lacking in

its inability to calculate the mass of trapped oil. With this knowledge and with additional experimental studies that specifically investigate the effects of mass flux, saturation temperature, miscibility, and degree of superheat on oil retention, future researchers should be able to craft more accurate models for oil retention in microchannel condensers.

CHAPTER VI

CONCLUSIONS AND RECOMMENDATIONS

6.1 Summary and Conclusions

This research was conducted in order to fill the gap, as demonstrated in a literature review, for a microchannel condenser model that is capable of accurately predicting heat transfer, pressure drop, and oil retention.

The first objective of the research was to improve the pressure drop predictions of the previous version of the model. This was done by conducting a literature search for papers which reviewed and compared several frictional pressure drop correlations using large databases in their analysis. Based on this search, three correlations were chosen and tested against pressure drop data from open literature for R134a and R410A, since those refrigerants are the ones used in this research. The best correlation from this analysis was chosen to use for the remainder of the research.

The second objective was to perform model validation for the heat transfer and pressure drop portions of the model, with specific emphasis on pressure drop. The pressure drop validation was performed as a part of the process of choosing a new and better frictional pressure drop correlation for the purposes of this research.

Finally, the last objective was to present a model that is able to predict the mass of oil in circulation with the refrigerant, compare it to the measured oil retention mass, and determine where extra oil may be trapped if there is any. A model was created based on void fraction and oil mass fraction which underpredicts the measured data, leading to the conclusion that oil is trapped in the condenser, most likely in the inlet header where the refrigerant is superheated.

Although the model presented in this thesis was not able to accurately predict the mass of oil retained in the microchannel type condenser for all the operating conditions and refrigerants tested, it was, for the first time according to author's best knowledge, experimentally verified against a large set of oil retention data for two refrigerants (i.e., R410A and R134a) and for a broad range of refrigerant mass flux, oil circulation ratios, saturation pressures, and degrees of inlet superheat of the refrigerant vapor. The comparison between the simulation results and the measured data of oil retention identified unique oil retention characteristics of microchannel type condensers. In addition, it was pointed out the limitations of the current models in the literature that more or less consider only the mass of oil miscible with and in circulation with the liquid refrigerant. And it was highlighted the need to consider the mass of trapped oil in the headers and in the superheated region of the microchannel tube in order to predict a realistic range of oil retention volumes in the condenser. With this knowledge and with additional experimental studies that specifically investigate the effects of mass flux, saturation temperature, miscibility, and degree of superheat on oil retention, future researchers should be able to craft more accurate models for oil retention in microchannel condensers.

6.1.1 Heat Transfer Model

The heat transfer correlation used in this model is that presented in Huang et al. (2010), and was developed for R410A-oil mixtures flowing through small diameter tubes. The heat transfer portion of the model was validated using two different data sources, both of which

provide overall capacity measurements for microchannel condensers. The source Yatim et al. (2016), which is the primary data source for this research, provides data for pure refrigerant and refrigerant-oil mixtures for R410A and R134a, while the source Hoehne and Hrnjak (2004) provides data for pure propane. It was found that the model predicts the propane data within a +6%, -1% error, the R410A data within a +29%, -7% error, and the R134a data within a +52%, -41% error. It was theorized that the large error associated with the R134a data arises from errors in the calculation of R134a properties, but this idea was discarded based on the subsequent satisfactory pressure drop validation with R134a data from other sources. Therefore, it is assumed that while the Huang et al. (2010) correlation is acceptable for R410A and propane data, it is not adequate for R134a data, and research should be done to find a correlation that is more universally applicable to condensation in microchannels.

6.1.2 Pressure drop Model

The frictional pressure drop correlation in place when the author began working with the model was that set forth in Mishima and Hibiki (1996). This correlation was developed for adiabatic liquid-vapor flows, and primarily for combinations of air and water. When this correlation was used to predict the data from Yatim et al. (2016), it was found that it predicted the R410A data within an error of +32%, -36%, and underpredicted the R134a data by as much as 75%. Since the model was not able to acceptably predict the R134a data using this correlation, the author began a search for a new correlation that would work for both R410A and R134a, since those are the refrigerants used in the refrigerant-oil mixtures from Yatim et al. (2016). To begin with, the author found nine papers from the open literature that use large databases to compare frictional pressure drop correlations. From the correlations reviewed in these papers, the author

chose three that were top performers for the largest databases and for condensation and refrigerant data, specifically. Then these three correlations were used to predict R410A and R134a adiabatic frictional pressure drop data from five different sources. No data for entire microchannel condensers was used in this validation study because the author was unable to find papers that report R410A or R134a pressure drop measurements along with all the conditions needed as inputs to the model. The correlation that performed best in this analysis, the Kim and Mudawar (2012) correlation, was then implemented in the model and used for all subsequent simulations. It was then found that when using this correlation, which should be best for both R410A and R134a, the predictions became worse for both refrigerants in the data from Yatim et al. (2016). This led to the conclusion that the hydraulic diameter that had been in use for the data from Yatim et al. (2016), which was an assumed value since it could not be directly measured, was incorrect. Because of this, a hydraulic diameter sensitivity analysis was performed and it was determined that 1.2 mm is the most likely value of the hydraulic diameter for that condenser. This value was therefore used for all subsequent simulations. After these improvements were made to the model, it predicts R134a pressure drop within a +35%, - 59% error, and R410A pressure drop within a +49%, -19% error. The pressure drop portion of the model is now more correct and applicable to the refrigerants used in this study, but it still needs some improvement, primarily in the calculation of minor losses due to the complex geometry within the condenser.

When validating the pressure drop model for this work, it is best to use data from the literature that is as close as possible to the data used for this research along with the primary data. There was enough data available for validation of adiabatic flow of R134a and R410A in single tubes, which is excellent data for use in choosing a frictional pressure drop model. Validation with literature data should be done for the entire condenser as well. Unfortunately, this data is very difficult to find. The author performed an extensive literature search, becoming narrower with the search parameters for each iteration. All papers of interest were documented and checked

for useable data. No useable data was found for R134a or R410A pressure drop in entire microchannel condensers, so this portion of the validation cannot yet be performed. A table with a list of the papers investigated as well as the author's notes as to why each is not useful is provided in the Appendix.

6.1.3 Oil Retention Model

This model calculates oil retention as the local oil mass fraction multiplied by the mass in the liquid phase, only taking into account the mass of oil in circulation with the refrigerant. When this model was used to predict the data from Yatim et al. (2016), it was found that it underpredicts the data. The author's first assumption after seeing this result was that the oil which makes up the difference between the predicted and experimental mass values must be caught in the inlet header, since refrigerant vapor cannot transport oil nearly as well as liquid refrigerant. Calculations were made for how much of the inlet header volume would need to be filled with oil in order to make up the difference between the predicted and experimental values of oil mass, and it was discovered that for some data points with high oil mass fractions, the header would need to be 50% – 75% full of oil, which is not plausible since this would seriously inhibit the operation of the condenser. Since oil could not possibly be taking up that much of the inlet header because the condenser still operates as expected, the author investigated the possibility of an oil film existing on the inner walls of the superheated portions of the microchannel tubes. It was discovered that an oil film thick enough to significantly improve oil retention predictions would be so thick that it would greatly increase pressure drop in the microchannels. The model predicts pressure drop well with the same hydraulic diameter used for the cases without oil, and the data does not show a huge increase in pressure drop as oil mass fraction increases, so it was concluded that there cannot be a large enough amount of oil residing as a film in the microchannels to significantly decrease the required volume of oil in the inlet header.

The author then thought that perhaps there was an error in how the model calculates liquid mass, which would lead to errors in the predicted oil mass. A few studies were then performed that investigated the sensitivity of oil retention predictions to changing mass. From these studies it was determined that the method the model uses to calculate liquid mass is correct. There was a significant variation in oil retention predictions as different void fraction correlations were used to calculate the liquid mass, so further investigation is needed to determine which of the available correlations is best for refrigerant-oil mixtures. It was found, however, that all the void fraction models still underpredicted measured data by a larger amount, so it did not make a large difference in the results when the void fraction correlation was changed. Therefore, choosing the best correlation for void fraction would still not be enough to fix the oil retention model.

Based on all these analyses, the author determined that the only logical places for the extra oil to be located are in the inlet header and the inlet tube, both of which contain refrigerant as a superheated vapor. From these two, the most likely place for oil to be retained is in the inlet header since vapor velocity is slower here than in the inlet tube, making it more difficult for the vapor to carry the oil. It was determined using a flow map that the fluid flow is annular in the inlet header, so a dimensionless oil film thickness, δ/D, was calculated for each data point. From these calculations, it was determined that the assumption that all trapped oil is located as a film on the inner walls of the inlet header is logical for R134a as only one data point requires the inlet header and tube to be filled more than 30% with oil. It is not a good assumption for R410A with high degree of superheat, and an even worse assumption for R410A with low degree of superheat; both of these cases have several points above 30%, with a couple points even above 60%. This assumption works for R134a because experimental oil retention is low for half of the points, and for the other half the refrigerant reaches a subcooled state early so there is a large amount of liquid, and thus a lot of predicted oil in circulation. According to Yatim et al. (2016), oil retention

is highly dependent on mass flux, saturation temperature, miscibility, and degree of superheat. This oil retention model is primarily dependent on oil mass fraction and void fraction, so these other parameters only affect predicted oil retention insofar they affect the calculations of liquid mass in circulation. From this project, it appears that these parameters must influence the amount of oil trapped in the condenser in a way the model cannot capture. With data from future studies that target sensitivity to these parameters and trapped oil specifically, more accurate models for oil retention in microchannel condensers can be developed.

6.2 Recommendations for Future Work

Some recommendations for future research in this area are summarized as follows:

- Investigate heat transfer correlations in the same way that pressure drop correlations were investigated for this work. Choose one that is applicable for both R410A and R134a, or find one applicable for R134a and use different correlations for different fluids. Perform more validation with overall microchannel condensers if data can be found.
- Investigate more fully minor losses associated with entire microchannel condensers, specifically within the headers. Cut open the header under investigation to see exactly what is inside and to measure the precise hydraulic diameter for the microchannel tubes.
- Investigate void fraction correlations in the same way that pressure drop correlations were investigated. Choose one that is very accurate for condensing flow of refrigerants in microchannels.
- Perform more experimental tests for oil retention in microchannel condensers using R410A and R134a. In these tests, place special emphasis on determining the sensitivity of oil retention to mass flux, saturation temperature, miscibility, and degree of superheat.

Also place emphasis on attempting to determine exactly where and how oil is trapped in the condenser.

- Use the data gathered from these new experimental tests as well as the data from Yatim et al. (2016) to develop a model for oil retention that incorporates all of these parameters.

REFERENCES

Awad, M., Dalkiliç, A. S., Wongwises, S. (2015). A critical review on condensation pressure drop in microchannels and minichannels. *Heat Transfer Studies and Applications*. InTech, 2015.

Bigi, A., Cremaschi, L., Fisher, D. (2014). Modeling of lubricant effects in a microchannel type condenser. *International Refrigeration and Air Conditioning Conference at Purdue*. July 2014. Paper 1429.

Bullard, C., Proctor, J., Brezner, J., Mercer, K., Davis, R., 2006. Modeling and testing of a utility peak reducing residential hot/dry air conditioner (HDAC) using microchannel heat exchangers. *ASHRAE transactions*, *112(1)*.

Cavallini, A., Del Col, D., Doretti, L., Matkovic, M., Rossetto, L., Zilio, C., 2005. Two-phase frictional pressure gradient of R236ea, R134a and R410A inside multi-port mini-channels. *Experimental Thermal and Fluid Science 29*, 861-870.

Chang, Y.-J., Hsu, K.-C., Lin, Y.-T., Wang, C.-C., 2000. A generalized friction correlation for louver fin geometry. *International Journal of Heat and Mass Transfer 43*, 2237-2243.

Chang, Y.-J., Wang, C.-C., 1997. A generalized heat transfer correlation for louver fin geometry. *International Journal of Heat and Mass Transfer 40(3)*, 533-544.

Cioncolini, A., Thome, J., Lombardi, C., 2009. Unified macro-to-microscale method to predict two-phase frictional pressure drops of annular flows. *International Journal of Multiphase Flow 35*, 1138-1148.

Coleman, J., 2004. An experimentally validated model for two-phase sudden contraction pressure drop in microchannel tube headers. *Heat transfer engineering*, *25(3)*, 69-77.

Cremaschi, L., 2004. Experimental and theoretical investigation of oil retention in vapor compression systems. Ph.D. Thesis, Department of Mechanical Engineering, University of Maryland, College Park, MD.

Crompton, J. A., Newell, T. A., Chato, J. C., 2004. Experimental measurement and modeling of oil holdup. Air Conditioning and Refrigeration Center, University of Illinois, Mechanical and Industrial Engineering Department, Urbana, IL. ACRC TR-226.

García-Cascales, J. R., Vera-García, F., Gonzálvez-Maciá, J., Corberán-Salvador, J. M., Johnson, M. W., Kohler, G. T., 2008. A model for the analysis of compact heat exchangers. International Refrigeration and Air Conditioning Conference at Purdue. July 2008. Paper 866.

García-Cascales, J. R., Vera-García, F., Gonzálvez-Maciá, J., Corberán-Salvador, J. M., Johnson, M. W., Kohler, G. T., 2010. Compact heat exchangers modeling: Condensation. *International Journal of Refrigeration 33*, 135-147.

Ghajar, A., Bhagwat, S., 2014. Flow patterns, void fraction and pressure drop in gas-liquid two phase flow at different pipe orientations. L. Cheng (ed.), *Frontiers and Progress in Multiphase Flow I*, Springer International Publishing, Switzerland.

Harms, T., Kazmierczak, M., Gerner, F., 1999. Developing convective heat transfer in deep rectangular microchannels. *International Journal of Heat and Fluid Flow 20*, 149-157.

He, X.-D., Cheng, T., Asada, H., Kasahara, S., 2004. An oil circulation observer for estimating oil concentration and oil amount in refrigerant compressors. *ASHRAE Transactions 110.2*, 489-497.

Heun, M., Dunn, W., 1996. Principles of refrigerant circuiting with application to microchannel condenser. Part 1: Problem formulation and the effects of port diameter and port shape. No. CONF-960606--. American Society of Heating, Refrigerating and Air-Conditioning Engineers, Inc., Atlanta, GA.

Heun, M., Dunn, W., 1996. Principles of refrigerant circuiting with application to microchannel condenser. Part 2: The pressure-drop effect and the cross-flow heat exchanger effect. No. CONF-960606--. American Society of Heating, Refrigerating and Air-Conditioning Engineers, Inc., Atlanta, GA.

Hoehne, M., Hrnjak, P., 2004. Charge minimization in systems and components using hydrocarbons as a refrigerant. Air Conditioning and Refrigeration Center, University of Illinois, Mechanical and Industrial Engineering Department, Urbana, IL. ACRC TR-224.

Hrnjak, P., 2012. Low refrigerant charge: With a focus on microchannel heat exchangers. *ASHRAE/NIST Refrigerants Conference: Moving Towards Sustainability*, 272-283.

Huang, L., 2014. Development of advanced numerical models for variable geometry microchannel heat exchangers. Ph.D. Thesis, Department of Mechanical Engineering, University of Maryland, College Park, MD.

Huang, L., Aute, V., Radermacher, R., 2012. A generalized effectiveness-NTU based variable geometry microchannel heat exchanger model. *International Refrigeration and Air Conditioning Conference at Purdue*. July 2012. Paper 1206.

Huang, L., Aute, V., Radermacher, R., 2014. A model for air-to-refrigerant microchannel condensers with variable tube and fin geometries. *International Journal of Refrigeration 40*, 269-281.

Huang, X., Ding, G., Hu, H., Zhu, Y., Peng, H., Gao, Y., Deng, B., 2010. Influence of oil on flow condensation heat transfer of R410A inside 4.18 mm and 1.6 mm diameter horizontal smooth tubes. *International Journal of Refrigeration 33*, 158-169.

Iu, I. S. (2007). Development of air-to-air heat pump simulation program with advanced heat exchanger circuitry algorithm. Ph.D. Dissertation, Department of Mechanical Engineering, Oklahoma State University, Stillwater, OK.

Ison, J., Madadnia, J., and Vakiloroaya, V., 2012. Experimental investigation on influence of integrated heat pump in performance of domestic water heaters. *ASME 2012 Heat Transfer Summer Conference collocated with the ASME 2012 Fluids Engineering Division Summer Meeting and the ASME 2012 10th International Conference on Nanochannels, Microchannels, and Minichannels*, 151-155. American Society of Mechanical Engineers.

Jiang, Y., Garimella, S., 2001. Compact air-coupled and hydronically coupled microchannel heat pumps. *International Mechanical Engineering Conference and Exposition, New York, NY,* 1-13. American Society of Mechanical Engineers.

Jin, S. (2012). Distribution of refrigerant and lubricant in automotive air conditioning systems. Master's Thesis, Department of Mechanical Engineering, University of Illinois, Urbana, IL.

Jin, S., Hrnjak, P., 2014. An experimentally validated model for predicting refrigerant and lubricant inventory in MAC heat exchangers. *SAE International Journal of Passenger Cars – Mechanical Systems 7(2)*, 769-780.

Jin, S., Hrnjak, P., 2016. Refrigerant and lubricant charge in air condition heat exchangers: Experimentally validated model. *International Journal of Refrigeration 67*, 395-407.

Kim, M., Bullard, C., 2002. Performance evaluation of a window room air conditioner with microchannel condensers. *Journal of Energy Resources Technology*, *124(1)*, 47-55.

Kim, S.-M., Mudawar, I., 2012. Universal approach to predicting two-phase frictional pressure drop for adiabatic and condensing mini/micro-channel flows. *International Journal of Heat and Mass Transfer 55*, 3246-3261.

Kim, S.-M., Mudawar, I., 2014a. Review of databases and predictive methods for pressure drop in adiabatic, condensing and boiling mini/micro-channel flows. *International Journal of Heat and Mass Transfer 77*, 74-97.

Kim, S.-M., Mudawar, I., 2014b. Review of databases and predictive methods for heat transfer in condensing and boiling mini/micro-channel flows. *International Journal of Heat and Mass Transfer 77*, 627-652.

Lee, J.-P., 2003. Experimental and theoretical investigation of oil retention in a carbon dioxide air-conditioning system. Ph.D. Thesis, Department of Mechanical Engineering, University of Maryland, College Park, MD.

Lemmon, E.W., Huber, M.L., McLinden, M.O. *NIST Standard Reference Database 23: Reference Fluid Thermodynamic and Transport Properties-REFPROP, Version 8.0*, National Institute of Standards and Technology, Standard Reference Data Program: Gaithersburg, MD, 2007.

Li, H., Hrnjak, P., 2013. Effect of lubricant on two-phase refrigerant distribution in microchannel evaporator. *SAE International Journal of Materials and Manufacturing 6(3)*, 567-575.

Li, H., Hrnjak, P., 2013. An experimentally validated model for microchannel heat exchanger incorporating lubricant effect. *International Journal of Refrigeration 59*, 259-268.

Li, H., Hrnjak, P., 2015. Quantification of liquid refrigerant distribution in parallel flow microchannel heat exchanger using infrared thermography. *Applied Thermal Engineering 78*, 410-418.

Li, W., Wu, Z., 2010. A general correlation for adiabatic two-phase pressure drop in miro/mini-channels. *International Journal of Heat and Mass Transfer 53*, 2732-2739.

Liu, X., 2015. Effect of oil in circulation on automotive A/C component and system performance. Master's Thesis, Department of Mechanical Engineering, University of Illinois, Urbana, IL.

López-Belchi, A., Illán-Gómez, F., Vera-García, F., García-Cascales, J., 2014. Experimental condensing two-phase frictional pressure drop inside mini-channels. Comparisons and new model development. *International Journal of Heat and Mass Transfer 75*, 581-591.

Lottin, O., Guillemet, P., Lebreton, J.-M., 2003a. Effects of synthetic oil in a compression refrigeration system using R410A. Part I: modelling of the whole system and analysis of its response to an increase in the amount of circulating oil. *International Journal of Refrigeration 26*, 772-782.

Lottin, O., Guillemet, P., Lebreton, J.-M., 2003b. Effects of synthetic oil in a compression refrigeration system using R410A. Part II: quality of heat transfer and pressure losses within the heat exchangers. *International Journal of Refrigeration 26*, 783-794.

Mandrusiak, G., Carey, V., 1988. Pressure drop characteristics of two-phase flow in a vertical channel with offset strip fins. *Experimental Thermal and Fluid Science 1(1)*, 41-50.

Martínez-Ballester, S., Corberán, J.-M., Gonzálvez-Maciá, J., Domanski, P. A., 2011. Impact of classical assumptions in modelling a microchannel gas cooler. *International Journal of Refrigeration 34*, 1898-1910.

Martínez-Ballester, S., Corberán, J.-M., Gonzálvez-Maciá, J., 2013a. Numerical model for microchannel condensers and gas coolers: Part I – Model description and validation. *International Journal of Refrigeration 36*, 173-190.

Martínez-Ballester, S., Corberán, J.-M., Gonzálvez-Maciá, J., 2013b. Numerical model for microchannel condensers and gas coolers: Part II – Simulation studies and model comparison. *International Journal of Refrigeration 36*, 191-202.

McQuiston, F., Parker, J., Spitler, J., 2005. *Heating, Ventilating, and Air Conditioning.* John Wiley & Sons, Inc., Danvers, MA.

Meng, J., Liu, M., Zhang, W., Cao, R., Li, Y., Zhang, H., Gu, X., Du, Y., Geng, Y., 2015. Experimental investigation on cooling performance of multi-split variable refrigerant flow system with microchannel condenser under part load conditions. *Applied Thermal Engineering 81*, 232-241.

Müller-Steinhagen, H., Heck, K., 1986. A simple friction pressure drop correlation for two-phase flow in pipes. *Chemical Engineering and Processing: Process Intensification 20*, 297-308.

Nelson, S., Hrnjak, P., 2003. Effect of internal heat exchanger on performance of R134a systems. *Vehicle Thermal Management Systems 6*, 17-27.

Park, C. Y., Hrnjak, P. (2008). Experimental and numerical study on microchannel and round-tube condeners in a R410A residential air-conditioning system. *International Journal of Refrigeration 31*, 822-831.

Qi, Z., Zhao, Y., Chen, J., 2010. Performance enhancement study of mobile air conditioning system using microchannel heat exchangers. *International Journal of refrigeration*, *33(2)*, 301-312.

Ragazzi, F., Pedersen, C. O. (1991). Modular-based computer simulation of an air-cooled condenser. *Air Conditioning and Refrigeration Center*, Mechanical and Industial Engineering Department at the University of Illinois, Urbana, IL.

Ren, T., Ding, G., Wang, T., Hu, H., 2013. A general three-dimensional simulation approach for micro-channel heat exchanger based on graph theory. *Applied Thermal Engineering 59*, 660-674.

Revellin, R., Thome, J., 2007. Adiabatic two-phase frictional pressure drops in microchannels. *Experimental Thermal and Fluid Science 31*, 673-685.

Schwentker, R., 2005. Advances to a computer model used in the simulation and optimization of heat exchangers. Master's Thesis, Department of Mechanical Engineering, University of Maryland, College Park, MD.

Shao, L.-L., Yang, L., Zhang, C.-L., Gu, B., 2009. Numerical modeling of serpentine microchannel condensers. *International Journal of Refrigeration 32*, 1162-1172.

Subramaniam, V., Garimella, S., 2005. Design of air-cooled R-410A microchannel condensers. *ASHRAE Transactions 111(1).*

Sun, L., Mishima, K., 2009. Evaluation analysis of prediction methods for two-phase flow pressure drop in mini-channels. *International Journal of Multiphase Flow 35*, 47-54.

Wang, C.-C., Chiang, S.-K., Chang, Y.-J., Chung, T.-W., 2001. Two-phase flow resistance of refrigerants R-22, R-410A and R-407C in small diameter tubes. *Chemical Engineering Research and Design 79*, 553-560.

Wu, J., Wang, S., Ge, Y., 2009. Experimental research on microchannel heat exchanger performance for residential air conditioner applications. *ASME 2009 Second International Conference on Micro/Nanoscale Heat and Mass Transfer*, 653-657. American Society of Mechanical Engineers.

Xu, Y., Fang, X., 2013. A new correlation of two-phase frictional pressure drop for condensing flow in pipes. *Nuclear Engineering and Design 263*, 87-96.

Xu, Y., Fang, X., Su, X., Zhou, Z., Chen, W., 2012. Evaluation of frictional pressure drop correlations for two-phase flow in pipes. *Nuclear Engineering and Design 253*, 86-97.

Ye, L., Tong, M., Zeng, X., 2009. Design and analysis of multiple parallel-pass condensers. *International Journal of Refrigeration*, *32(6)*, 1153-1161.

Yin, J. M., Bullard, C. W., Hrnjak, P. S. (2001). R-744 gas cooler model development and validation. *International Journal of Refrigeration*, 692-701.

Yin, X.-W., Wang, W., Patnaik, V., Zhou, J.-S., Huang, X.-C., 2015. Evaluation of microchannel condenser characteristics by numerical simulation. *International Journal of Refrigeration 54*, 126-141.

Zhang, W., Hibiki, T., Mishima, K., 2010. Correlations of two-phase frictional pressure drop and void fraction in mini-channel. *International Journal of Heat and Mass Transfer 53*, 453-465.

Zhang, M., Webb, R. 2001. Correlation of two-phase friction for refrigerants in small-diameter tubes. *Experimental Thermal and Fluid Sciences 25*, 131-139.

Zhao, Y., Qi, Z., Chen, J., Xu, B., He, B., 2012. Experimental analysis of the low-GWP refrigerant R1234yf as a drop-in replacement for R134a in a typical mobile air conditioning system. *Proceedings of the Institution of Mechanical Engineers, Part C: Journal of Mechanical Engineering Science 226 (11)*, 2713-2725.

Zhong, T., Chen, Y., Zheng, W., Hua, N., Luo, X., Yang, Q., Mo, S., Jia, L., 2014. Experimental investigation on microchannel condensers with and without liquid–vapor separation headers. *Applied Thermal Engineering*, *73(2)*, 1510-1518.

Zou, Y., Li, H., Hrnjak, P., 2014. Lubricant impact on R134a distribution and microchannel heat exchanger performance. SAE Technical Paper.

APPENDIX

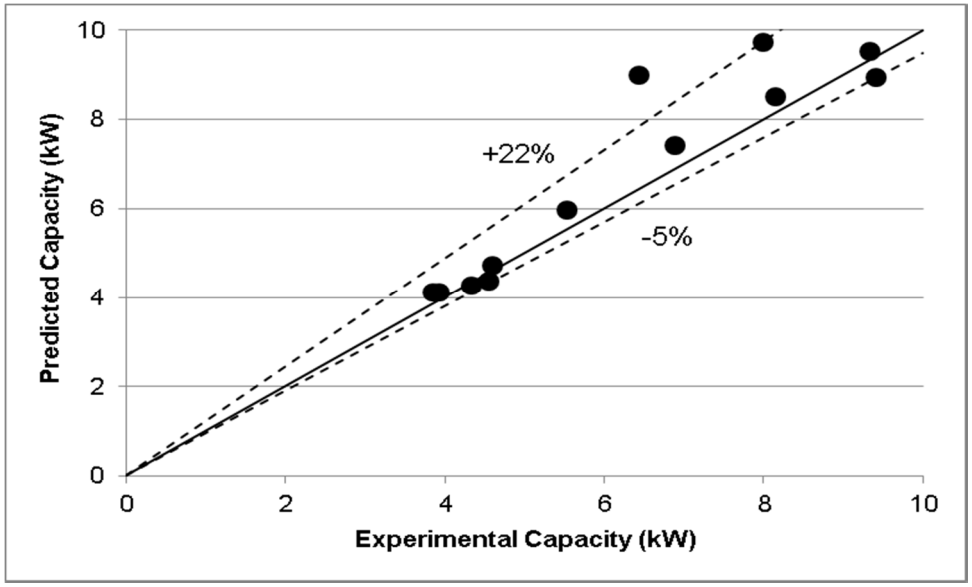

Figure A.1 – Predicted vs. experimental capacity for R410A data without oil from Yatim et al. (2016)

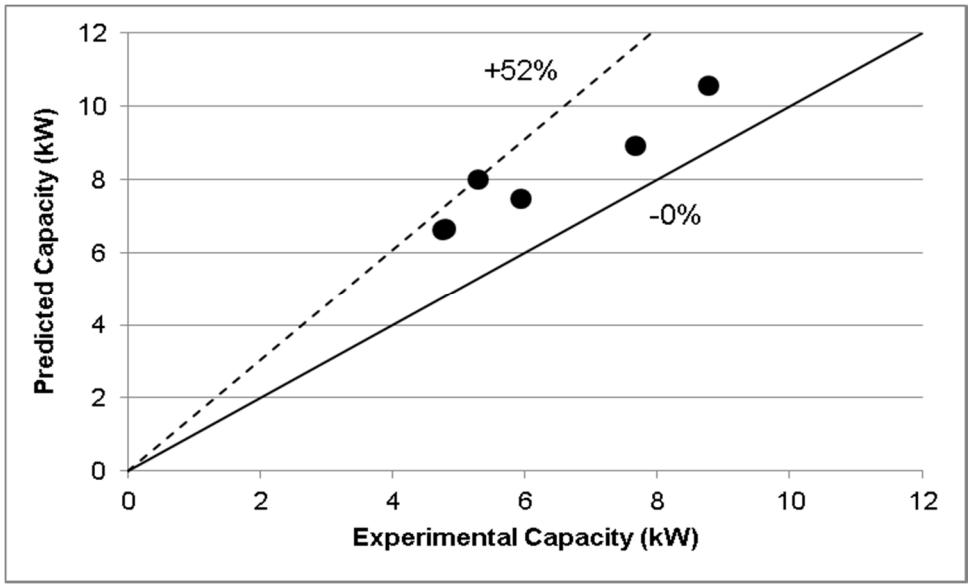

Figure A.2 – Predicted vs. experimental capacity for R134a data without oil from Yatim et al. (2016)

Table 4.9 – Papers of interest from search for overall microchannel condenser data for R134a or R410A

Papers of Interest	Notes
Zhao et. al., 2012 - Experimental Analysis of the Low-GWP Refrigerant R1234yf as a Drop-In Replacement for R134a in a Typical Mobile Air Conditioning System	Note: This paper is concerned more with whole system performance than component performance. There is no heat transfer or pressure drop data for the microchannel condenser.
Nelson and Hrnjak, 2003 - Effect of Internal Heat Exchanger on Performance of R134a Systems	Note: This paper is concerned more with whole system performance than component performance. There is no heat transfer or pressure drop data for the microchannel condenser.
Garcia-Cascales et. al., 2010 - Compact Heat Exchangers Modeling: Condensation	Note: This paper seems to be perfect, but the data seems untrustworthy. Some of the pressure drop measurements seem far too small to make physical sense. The authors never model this pressure drop data like they do the other data.
Park and Hrnjak, 2007 - Experimental and Numerical Study on Microchannel and Round-Tube Condensers in a R410A Residential Air-Conditioning System	Note: Has only one data point. The condenser is a different shape than ours (it is curved), so the model would have to be significantly altered to use this data.
Awad et. al., 2014 - A Critical Review on Condensation Heat Transfer in Microchannels and Minichannels	Note: This paper only deals with single tubes, not entire microchannel condensers, so no good for this analysis.
Ison et. al., 2012 - Experimental Investigation on Influence of Integrated Heat Pump in Performance of Domestic Water	Note: This paper is only for an overal heat pump system and does not have data on individual component heat transfer
Heun and Dunn, 1996 - Principles of Refrigerant Circuiting with Application to Microchannel Condensers: Part II - the Pressure-Drop Effect and the Cross-Flow Heat Exchanger Effect	Note: No experimental data; analysis was performed using correlations from the literature.
Heun and Dunn, 1996 - Principles of Refrigerant Circuiting with Application to Microchannel Condensers: Part I - Problem Formulation and the Effects of Port Diameter and Port Shape	Note: No experimental data; analysis was performed using correlations from the literature.
Meng et. al., 2015 - Experimental Investigation on Cooling Performance of Multi-Split Variable Refrigerant Flow System with Microchannel Condenser Under Part Load Conditions	Note: No good data for this research here and the microchannels are a different shape.
Li and Hrnjak, 2015 - Quantification of Liquid Refrigerant Distribution in Parallel Flow Microchannel Heat Exchanger Using Infrared Thermography	Note: The only data given is for an evaporator.
Pega Hrnjak, 2012 - Low Refrigerant Charge: With a Focus on Microchannel Heat Exchangers	Note: This paper focuses on refrigerant charge, not pressure drop.
Shao et. al., 2009 - Numerical Modeling of Serpentine Microchannel Condensers	Note: There is some data, but the geometry is quite different from a standard microchannel condenser, so the model would have to be significantly altered to use this data.
Huang et. al., 2014 - A Model for Air-to-Refrigerant Microchannel Condensers with Variable Tube and Fin Geometries	Note: This paper only uses data from other sources, mostly with refrigerants other than R134a and R410A.
Subramaniam and Garimella, 2005 - Design of Air-Cooled R410A Microchannel Condensers	Note: This paper does not contain experimental data; it rather contains the results of a simulation analysis.
Kim and Bullard, 2002 - Performance Evaluation of a Window Room Air Conditioner with Microchannel Condensers	Note: This paper only has data for R22.

Table 4.9 (continued)

Wu et. al., 2009 - Experimental Research on Microchannel Heat Exchanger Performance for Residential Air Conditioner Applications	Note: No R134a or R410A data.
Martinez-Ballester et. al., 2013 - Numerical Model for Microchannel Condensers and Gas Coolers: Part II - Simulation Studies and Model Comparison	Note: This paper only deals with simulation studies; there is no experimental data involved.
Qi et. al., 2010 - Performance Enhancement Study of Mobile Air Conditioning System Using Microchannel Heat Exchangers	Note: This paper has good data for R134a, but at least one condenser has a receiver/dryer insterted between condenser passes that would greatly increase the pressure drop. The other condenser has one, but I am unclear on whether it in included in the measured pressure drop.
Yin et. al., 2015 - Evaluation of Microchannel Condenser Characteristics by Numerical Simulation	Note: This paper has R410A data for one slab and two slab microchannel condensers. The test conditions are just ranges of values, however, so predictions could not be exact. Also, no mass flow rate of refrigerant is given.
Coleman, 2003 - An Experimentally Validated Model for Two-Phase Sudden Contraction Pressure Drop in Microchannel Tube Headers	Note: This may be helpful for the model later, but not for validation. It does not have data for an entire microchannel condenser.
Martinez-Ballester et. al., 2013 - Numerical Model for Microchannel Condensers and Gas Coolers: Part I - Model Description and Validation	Note: Only contains capacity data; no pressure drop data. The data it does use comes from Garcia-Cascales et. al., 2010.
Zhong et. al., 2014 - Experimental Investigation on Microchannel Condensers with and without Liquid-Vapor Separation Headers	Note: This paper has good data for R134a pressure drop, but mass flow rate is not given. Inlet mass flux is given, but it could not be determined (after much investigation) to what area this applied.
Jiang and Garimella, 2001 - Compact Air-Coupled and Hydronically Coupled Microchannel Heat Pumps	Note: No pressure drop data.
Ye et. al., 2009 - Design and Analysis of Multiple Parallel-Pass Condensers	Note: No pressure drop data.
Bullard et. al., 2006 - Modeling and Testing of a Utility Peak Reducing Residential Hot/Dry Air Conditioner (HDAC) Using Microchannel Heat Exchangers	Note: There is no separate condenser data in this paper. There is only evaporator data and overall system data.

VITA

Ellyn Harges

Candidate for the Degree of

Master of Science

Thesis: MODELLING OILRETENTION, PRESSURE DROP, AND HEAT TRANSFER OF REFRIGERANT-OIL MIXTURES IN A MICROCHANNEL CONDENSER

Major Field: Mechanical Engineering

Biographical:

Education:

Completed the requirements for the Master of Science in Mechanical Engineering at Oklahoma State University, Stillwater, Oklahoma in December, 2016.

Completed the requirements for the Bachelor of Science in Mechanical Engineering at Oklahoma State University, Stillwater, Oklahoma, 2014.

Experience: Research/Teaching Assistant at Oklahoma State University